UNIVERSIDADE FEDERAL DO PARANÁ

STEPHANE JANAINA DE MOURA ESCOBAR

EFEITOS CITOTÓXICOS DA 4’-HIDROXICHALCONA E DA ISOLIQUIRITIGENINA EM CÉLULAS DE NEUROBLASTOMA HUMANO

CURITIBA

2018

STEPHANE JANAINA DE MOURA ESCOBAR

EFEITOS CITOTÓXICOS DA 4'-HIDROXICHALCONA E DA ISOLIQUIRITIGENINA EM CÉLULAS DE NEUROBLASTOMA HUMANO

Tese apresentada ao Programa de Pós-Graduação em Ciências – Bioquímica, Setor de Ciências Biológicas, da Universidade Federal do Paraná, como requisito parcial à obtenção do grau de Doutor em Ciências – Bioquímica.

Orientadora: Profª. Drª. Maria Eliane Merlin Rocha

Coorientadora: Profª. Dra. Sheila M. B. Winnischofer

Supervisor no Exterior: Dr. Paul Keneth Witting - University of Sydney

CURITIBA

2018

Universidade Federal do Paraná. Sistema de Bibliotecas.
Biblioteca de Ciências Biológicas.
(Rosilei Vilas Boas – CRB/9-939).

Escobar, Stephane Janaina de Moura
Efeitos citotóxicos da 4 - hidroxichalcona e da isoliquiritigenina em células de neuroblastoma humano. / Stephane Janaina de Moura Escobar. – Curitiba, 2018.
86 f. : il. ; 30cm.

Orientador: Maria Eliane Merlin Rocha.
Coorientadora: Sheila M. B. Winnischofer.
Supervisor no exterior: Paul Keneth Witting.
Tese (Doutorado) – Universidade Federal do Paraná, Setor de Ciências Biológicas. Programa de Pós-Graduação em Ciências – Bioquímica.

1. Neuroblastoma. 2. Necrose. 3. Apoptose. 4. Toxicidade. 5. Câncer – Pesquisa. 6. Mitocôndria. 7. Células cancerosas. I. Título. II. Rocha, Maria Eliane Merlin. III. Winnischofer, Sheila M. B. IV. Witting, Paul Keneth. V. Universidade Federal do Paraná. Setor de Ciências Biológicas. Programa de Pós-Graduação em Ciências – Bioquímica.

CDD (20. ed.) 618.92994

MINISTÉRIO DA EDUCAÇÃO
SETOR CIÊNCIAS BIOLÓGICAS
UNIVERSIDADE FEDERAL DO PARANÁ
PRÓ-REITORIA DE PESQUISA E PÓS-GRADUAÇÃO
PROGRAMA DE PÓS-GRADUAÇÃO CIÊNCIAS (BIOQUÍMICA)

TERMO DE APROVAÇÃO

Os membros da Banca Examinadora designada pelo Colegiado do Programa de Pós-Graduação em CIÊNCIAS (BIOQUÍMICA) da Universidade Federal do Paraná foram convocados para realizar a arguição da tese de Doutorado de **STEPHANE JANAINA DE MOURA ESCOBAR** intitulada: **Efeitos citotóxicos da 4- hidroxichalcona e da isoliquiritigenina em células de neuroblastoma humano**, após terem inquirido a aluna e realizado a avaliação do trabalho, são de parecer pela sua aprovação no rito de defesa.

A outorga do título de doutor está sujeita à homologação pelo colegiado, ao atendimento de todas as indicações e correções solicitadas pela banca e ao pleno atendimento das demandas regimentais do Programa de Pós-Graduação.

CURITIBA, 27 de Junho de 2016.

MARIA ELIANE MERLIN ROCHA
Presidente da Banca Examinadora

SILVIA MARIA SUJEIR CORREIA CADENA
Avaliador Interno

CLAUDIA REGINA MARTINEZ
Avaliador Interno

SILVIO MARQUES ZANATA
Avaliador Externo

EMY LUIZA ISHII IWAMOTO
Avaliador Externo

Dedico essa tese à minha família e amigos;
Ao meu grande amor Pedro e meu filho amado Lucas;
Meus pais Margareth e Reinaldo
Meus avós Moura e Gina
Meus irmãos Ariadne, Guilherme e Eduardo.

AGRADECIMENTOS

Ao meu grande amor e companheiro, Pedro, que esteve ao meu lado em todos os momentos felizes e difíceis que vivemos durante esses 15 anos. Desse amor nasceu nosso filho, Lucas, que veio para agregar e tornar essa fase da minha vida ainda mais especial.

Aos meus pais, Margareth e Reinaldo, por todo o amor que me deram, além da educação, ensinamentos e apoio. Aos meus irmãos, Ariadne, Guilherme e Eduardo, por deixarem minha vida mais alegre. Aos meus avós, Moura e Gina, pelo amor incondicional que sempre me deram.

À minha querida orientadora, Dra. Maria Eliane Merlin Rocha, pela paciência, dedicação e ensinamentos que possibilitaram que eu realizasse esta tese. Obrigada por ter acreditado em mim e no meu trabalho durante todos esses anos!

A minha coorientadora, Dra. Sheila Maria Brochado Winnischofer, por toda orientação, incentivo e ajuda que me foram dados.

Ao grupo de Patologia da Universidade de Sydney que me recebeu de braços abertos e me ajudou dentro e fora do laboratório para que eu tivesse uma experiencia maravilhosa na Austrália. Em especial ao Dr. Paul Witting que me orientou e não mediu esforços para que tudo fosse realizado da melhor maneira possível.

Aos colegas e amigos do laboratório de oxidações biológicas que alegraram os meus dias e me deram força nos momentos difíceis. Os nossos “cafés” tornaram meus dias muito mais felizes!

À banca avaliadora, em especial a banca interna, Dra. Glaucia Regina Martinez e Dr. Sílvio Zanata, por todas as correções e sugestões que deram ao meu trabalho durante todo esse período.

Ao professor Ciro Alberto de Oliveira Ribeiro pelos experimentos de microscopia eletrônica de transmissão e ajuda na análise dos dados.

Ao Programa de Pós-Graduação em Ciências-Bioquímica por ter proporcionado a realização desta minha formação acadêmica e científica.

Ao CNPq, Programa Ciências sem Fronteiras, Capes e Fundação Araucária pelo suporte financeiro.

A todos os que contribuíram direta ou indiretamente para que eu alcançasse este objetivo.

“Tenho a impressão de ter sido uma criança brincando à beira-mar, divertindo-me em descobrir uma pedrinha mais lisa ou uma concha mais bonita que as outras, enquanto o imenso oceano da verdade continua misterioso diante de meus olhos”.

Isaac Newton

RESUMO

O neuroblastoma é um câncer infantil com alta mortalidade. As hidroxichalconas têm recebido atenção considerável devido às suas atividades citotóxicas em células tumorais. Deste modo, o objetivo do presente estudo foi caracterizar a citotoxicidade das hidroxichalconas, 4'-hidroxichalcona e isoliquiritigenina (4,2',4'-trihidroxi-chalcona; ISL) em neuroblastoma utilizando um modelo in vitro de células SH-SY5Y. A incubação das células SHSY5Y cultivadas com 4HC (10-60 μM) por 24 h diminuiu a confluência, a atividade metabólica e os níveis de ATP intracelulares em relação ao controle. Com base nos resultados, a toxicidade celular induzida por 4HC provavelmente está relacionado com as disfunções mitocondriais, como: inibição da respiração mitocondrial, despolarização do potencial de membrana mitocondrial e alterações morfológicas. Além disso, a perda de viabilidade celular foi acompanhada principalmente pelo aumento da exposição de fosfatidilserina na superfície das células, sugerindo que a 4HC poderia induzir a via intrínseca da apoptose em células SH-SY5Y. Além disso, o tratamento com 4HC inibiu a migração/proliferação celular de SH-SY5Y e induziu mudanças significativas na progressão do ciclo celular. A incubação das células SH-SY5Y com 10-100 μM de ISL (24 h) diminuiu a confluência e os níveis de ATP intracelular em relação ao controle; o inibidor da necroptose necrostatina-1 restaurou os níveis de ATP. A citotoxicidade mediada por ISL não envolveu ativação das caspases 3/7 ou aumento da exposição de fosfatidilserina na superfície das células, indicando que a morte celular foi independente da via clássica da apoptose. O tratamento com ISL inibiu a proliferação/migração celular e modificou a progressão do ciclo celular SH-SY5Y. Nossos resultados mostram que ambas as hidroxichalconas, 4HC e ISL, têm efeitos citotóxicos contra a linhagem celular de neuroblastoma humano SH-SY5Y apresentando valores de EC_{50} de 21,5 ± 3,4 μM para 4HC e 25,4 ± 1,4 μM para ISL. No entanto, os efeitos do 4HC nas células do neuroblastoma estão associados com a disfunção mitocondrial e sugerem morte celular por apoptose enquanto que a atividade de ISL em células de neuroblastoma envolve a morte celular possivelmente por necroptose.

Palavras-chave: hidroxichalcona; neuroblastoma; SH-SY5Y; necroptose; apoptose; disfunção mitocondrial.

ABSTRACT

Neuroblastoma is a childhood cancer with high mortality. Hydroxychalcones have received considerable attention because of their cytotoxic activities on cancer cells. Thus, the aim of the present study was to characterize the cytotoxicity of the hydroxychalcones, 4'-hydroxychalcone and isoliquiritigenin (4,2',4'-trihydroxychalcone; ISL) to neuroblastoma using an in vitro model of SH-SY5Y cells. Incubation of cultured SHSY5Y cells with 4HC (10-60 μM) for 24 h decreased cell confluency, cellular metabolic activity and depleted intracellular ATP relative to the vehicle-treated control. The mechanism of 4HC-induced cell toxicity likely involves mitochondria dysfunctional as judged by inhibition of mitochondrial respiration, depolarization of mitochondria membrane potential and morphological alterations. Furthermore, loss of cell viability was accompanied mainly by increase of phosphatidylserine exposure on the surface of cells, suggesting that the 4HC may induce the intrinsic pathway of apoptosis in SH-SY5Y cells. In addition, 4HC treatment inhibited SH-SY5Y cell migration/proliferation in a scratch assay and induced significant changes in the cell cycle progression. Incubation of SH-SY5Y cells with 10-100 μM ISL (24 h) decreased confluency and intracellular ATP relative to control; the necroptosis inhibitor necrostatin-1 restored ATP levels. ISL-mediated cytoxicity did not involve caspase 3/7 activation or increase of phosphatidylserine exposure on the surface of cells, indicating that cell death was apoptosis independent. ISL treatment inhibited cell proliferation/migration and arrested SH-SY5Y cell cycle transition. Our results showed that both of hydroxychalcones, 4HC and ISL, have cytotoxic effects against human neuroblastoma cell line SH-SY5Y with EC_{50} values of 21.5 ± 3,4 μM for 4HC and 25.4 ± 1,4 μM for ISL. However, 4HC effects on neuroblastoma cells are associated with mitochondrial dysfunctional and it suggest cell death by apoptosis. Whilst, activity of ISL on neuroblastoma cells involves cell death possibly via a necroptotic pathwayx.

Keywords: hydroxychalcona; neuroblastoma; SH-SY5Y; necroptosis; apoptosis; mitochondrial dysfunction.

LISTA DE ABREVIATURAS E SÍMBOLOS

Revisão Bibliográfica

AIF - fator indutor de apoptose

DCF - 2', 7'-diclorofluoresceína

DCFH - 2', 7'-diclorofluorescina

DCFH-DA - 2´,7´diclorofluorescina diacetato

DMSO - dimetilsulfóxido

EndoG - endonuclease G

ERO - espécies reativas de oxigênio

MTT - Brometo de 3-(4,5-demitiltiazol-2-il)-2,5-difenil tetrazólio

TNF - fator de necrose tumoral

TNFR1 - receptor do fator de necrose tumoral 1

TRAIL - ligante indutor de apoptose relacionado ao TNF

ΔΨm – potencial de membrana mitocondrial

$\Delta\mu H^+$ – gradiente eletroquímico de prótons

Artigos Científicos

Akt - Protein kinase B

BSA – bovine serum albumin

DCF - 2', 7'- dichlorofluorescein

DCFH – 2', 7'-dichlorodihydrofluorescein

DCFH-DA - 2', 7'- dichloro-dihydro-fluorescein diacetate

DMSO - dimethyl sulfoxide

EGTA - ethylene glycol tetraacetic acid

ERK - extracellular signal–regulated kinase

HEPES - 4-(2-hydroxyethyl)-1-piperazine ethanesulfonic acid

IDO - indolamine-2,3-dioxygenase

MAPK - Mitogen-activated protein kinases

MMP – mitochondria membrane potential

MTT - 3-(4,5-dimethylthiazol-2-yl)-2,5-diphenyltetrazolium bromide

PI - propidium iodide

RIPK - receptor-interacting serine/threonine protein kinases

ROS - reactive oxygen species

TRIS - tri(hydroxymethyl)-aminomethane

SUMÁRIO

1 INTRODUÇÃO

Neuroblastoma (NB) é um tipo de câncer do sistema nervoso simpático que apresenta maior incidência durante a infância (Park, Eggert et al. 2010). NB afeta até 800 crianças por ano nos Estados Unidos e representa aproximadamente 10% de todos os cânceres malignos em crianças <5 anos (ACS 2018). Assim como em países desenvolvidos, no Brasil, o câncer já representa a primeira causa de morte (8% do total) entre crianças e adolescentes de 1 a 19 anos (INCA 2018). Mais de 60% dos tumores de neuroblastoma são agressivos (Cheung and Dyer 2013) e as abordagens terapêuticas atuais, incluindo cirurgia, radioterapia e quimioterapia, não são completamente efetivas (Louis and Shohet 2015). Apesar do tratamento padrão para NB ser baseado na combinação de drogas quimioterápicas, como doxorrubicina, temozolomida e cisplatina; esses compostos não são completamente eficientes e possuem diversos efeitos colaterais (Cheung and Dyer 2013, Tibullo, Giallongo et al. 2017). Muitos fatores podem afetar a taxa de sobrevida dos pacientes, como a idade, a localização do tumor e sua responsividade ao tratamento. Para pacientes com neuroblastoma de baixo, intermediário e alto risco, a taxa de sobrevida em 5 anos é superior a 95%, entre 90% e 95% e cerca de 40% a 50%, respectivamente (ACS 2018). Por isso, novas terapias que melhorem as taxas de sobrevivência e apresentem menos efeitos colaterais são necessárias.

Entre os tipos de abordagem terapêutica tem se tornado de particular interesse o uso de compostos capazes de ativar vias de morte celular. A morte celular programada é importante em muitos processos fisiológicos, e alterações em componentes destas vias de morte estão implicadas no desenvolvimento do tumor (Nikoletopoulou, Markaki et al. 2013). A capacidade de induzir as vias de morte celular tornou-se uma vantagem terapêutica e estimulou o rastreio e o desenvolvimento de compostos com atividade pró-apoptótica (Curti, Di Lorenzo et al. 2017) e necroptótica (Gali-Muhtasib, Hmadi et al. 2015). Em algumas destas vias de indução de morte, em especial a apoptose por via intrínseca, participam moléculas de origem mitocondrial (ex.: citocromo *c*) (Lopez and Tait 2015), fato que torna esta organela um interessante alvo para quimioterápicos. Além disso, as mitocôndrias têm como funções a geração de ATP e homeostase de cálcio. A cadeia respiratória mitocondrial é geradora de espécies reativas de oxigênio (ERO) (Berry, Trewin et al. 2018) e a geração destas ERO também podem colaborar para indução de morte celular por apoptose via intrínseca (Wen, Zhu et al. 2013).

Dentre os compostos com potencial terapêutico para o tratamento de alguns tipos de canceres, entre eles o NB, destacam-se os flavonoides. Os flavonoides possuem diversos efeitos biológicos, dentre eles a atividade antitumoral (George, Dellaire et al. 2017). As chalconas, subclasse dos flavonoides, são biologicamente ativas e já demostraram propriedades anti-inflamatórias (Chiaradia, dos Santos et al. 2008), antioxidantes (Sikander, Malik et al. 2011), antifúngica (Gupta and Jain 2015) e anticâncer (Ramirez-Tagle, Escobar et al. 2016) *in vitro* e *in vivo*. Além disso, Sabzevari cols. demostraram que chalconas hidroxiladas são mais tóxicas para células de hepatocarcinoma (HepG2) do que para hepatócitos de ratos isolados (Sabzevari, Galati et al. 2004). Além disso, o presença de hidroxilas na estrutura dos flavonoides, entre eles as chalconas, podem alterar significativamente seus efeitos biológicos (Echeverria, Santibañez et al. 2009).

Neste trabalho foram utilizadas duas chalconas hidroxiladas: uma monohidroxilada a 4'-hidroxichalcona (4HC) e outra trihidroxilada, a isoliquiritigenina (4,2',4'-trihidroxichalcona; ISL). A 4HC é uma chalcona sintética e possui algumas propriedades biológicas conhecidas, incluindo potencial atividade antitumoral. A 4HC promove a inibição da ativação de NF-kβ induzida pelo TNFα em células de leucemia humana (K562 e Jurkat) (Orlikova, Tasdemir et al. 2011). Além disso, 4HC (100 μM) mostrou atividade desacopladora da fosforilação oxidativa em mitocôndrias isoladas de fígado de rato (Martineau 2012).

A ISL possui várias atividades biológicas, incluindo anti-inflamatória, antioxidante, antidiabética e efeitos cardioprotetores (Zhang, Zhu et al. 2013, Gaur, Yadav et al. 2014, Peng, Du et al. 2015). Estudos em camundongos mostram que a ISL é metabolizada no fígado, e pode atravessar a barreira hematoencefálica (BHE) (Han, Chin et al. 2013). A ISL também apresenta atividades antitumorais significativas, incluindo inibição da proliferação de células de glioma (U87MG), células de câncer de próstata (DU145 e MLL) e de endométrio (Ishikawa, HEC-1A, e RL95-2) (Lee, Lim et al. 2009, Zhou, Song et al. 2013, Wu, Chen et al. 2016). Além disso, ISL (10-100 μM) inibe seletivamente a proliferação de células de câncer de próstata (C4-2 e LNCaP) em comparação com células epiteliais não tumorais (IEC-¨6) (Zhang, Yeung et al. 2010) sugerindo que ela pode ser citotóxica para uma variedade de células tumorais, e não afetar significativamente as células normais; uma característica desejável em quimioterápicos.

Apesar de serem conhecidos alguns efeitos da 4HC e da ISL em diferentes modelos tumorais, não são descritos seus efeitos em células de neuroblastoma humano (SH-SY5Y).

Neste trabalho pode-se verificar os possíveis processos de indução de morte celular promovidos por estas chalconas. sobre as células de neuroblastoma humano SH-SY5Y.

2 JUSTIFICATIVA E OBJETIVOS

Apesar do tratamento padrão para NB ser baseado na combinação de drogas quimioterápicas, ele não é eficaz (Cheung and Dyer 2013, Tibullo, Giallongo et al. 2017). Além disso, considerando que a quimioterapia é a principal forma terapêutica de escolha para tratamento do câncer, a busca por compostos que sejam mais eficazes, específicos e que apresentem menores efeitos colaterais é fundamental.

Observando o descrito em relação à necessidade de obtenção de novas terapias para o NB, os efeitos antitumorais apresentados pelas chalconas 4HC e ISL em outras linhagens tumorais, e a lacuna na literatura a respeito da ação destes compostos em células de neuroblastoma humano; torna-se relevante o estudo dos mecanismos intracelulares envolvidos na atividade citotóxica desses compostos.

Sendo assim, este estudo teve como objetivo geral, verificar os efeitos citotóxicos das chalconas (4HC e ISL) em células de neuroblastoma humano SH-SY5Y, e avaliar os efeitos intracelulares relacionados a citotoxicidade.

Os objetivos específicos deste estudo foram:

1) Avaliar os efeitos da 4HC em células SH-SY5Y sobre:
    a. Viabilidade celular e sua citotoxicidade, utilizando três metodologias distintas: MTT, confluência celular e níveis de ATP;
    b. Morfologia celular
    c. Proliferação celular, realizando os ensaios de proliferação/migração celular e ciclo celular;
    d. Mecanismos de morte celular utilizando Anexina V/7-AAD;
    e. Função mitocondrial: verificando respiração celular na presença de diferentes substratos da cadeia de transporte de elétrons em células permeabilizadas; potencial de membrana mitocondrial ($\Delta\Psi m$); níveis de espécies reativas de oxigênio;

2) Avaliar os efeitos da ISL em células SH-SY5Y sobre:
    a. Viabilidade celular e sua citotoxicidade, utilizando três metodologias distintas: azul de tripan, confluência celular e níveis de ATP;

b. Proliferação celular, realizando os ensaios de proliferação/migração celular, ciclo celular e níveis das proteínas ERK e p38
c. Mecanismos de morte celular
    i. Necroptose, utilizando o inibidor de necroptose necrostatina-1;
    ii. Autofagia, verificando a expressão da proteína LC3I/II;
    iii. Apoptose, realizando os ensaios de caspases 3/7 e Anexina V/7-AAD;

3 ESTRATÉGIA EXPERIMENTAL

ETAPA I

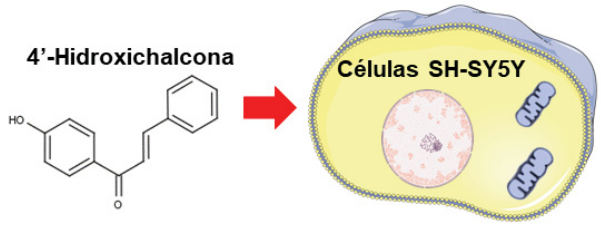

- Viabilidade celular (níveis de ATP, confluência e MTT);
- Morfologia celular (Hematoxilina/Eosina, Microscopia Eletrônica de Transmissão);
- Ciclo celular (Marcação com PI);
- Proliferação/migração celular (Scratch);
- Mecanismo de morte celular (Anexina/7-AAD).
- Respiração celular (Células permeabilizadas – Oxígrafo Oroboros);
- Potencial de membrana mitocondrial (JC-1);
- Níveis de ROS (DCFH-DA);

ETAPA II

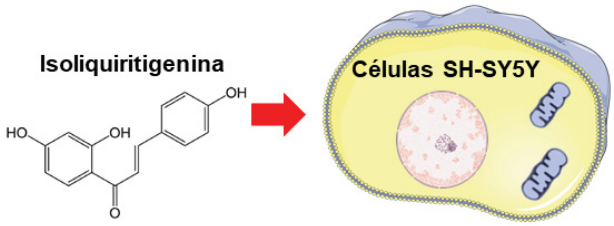

- Viabilidade celular (níveis de ATP, confluência e azul de tripan);
- Ciclo celular (Marcação com PI);
- Proliferação/migração celular (Scratch);
- Proteínas ERK e p38 (Western Blot e Elisa).
- Mecanismo de morte celular
  - ✓ Necroptose (Inibidor - necrostatina);
  - ✓ Autofagia (LC3B I/II);
  - ✓ Apoptose (caspases 3/7 e Anexina/7-AAD);

4 REVISÃO BIBLIOGRÁFICA

4.1 NEUROBLASTOMA

Neuroblastomas (NBs) são tumores sólidos originários do sistema nervoso simpático que ocorrem predominantemente durante a infância. Os NBs são provenientes das simpatogônias – células nervosas indiferenciadas da crista neural, das quais se originam a medula da adrenal e todos os gânglios e plexos simpáticos (Cartum 2012). A etiologia do NB é desconhecida e 75% dos casos apresentam-se em crianças abaixo de 5 anos de idade (Izbicki, Mazur et al. 2003).

Esse tipo de tumor tem incidência de aproximadamente 1 caso a cada 100.000 habitantes nos Estados Unidos (ACS 2018). No Brasil, a incidência anual varia entre 7 e 12 casos por milhão de crianças e jovens até 19 anos e estima-se que ocorram 12.500 novos casos em 2018 (INCA 2018). Além disso, NBs representam cerca de 13% de toda mortalidade relacionada aos casos de câncer infantil no mundo (Louis and Shohet 2015).

A maioria dos estudos de pesquisa sobre NB se concentra em encontrar as melhores combinações de drogas quimioterápicas que promovam maior responsividade (ACS 2018). Vários quimioterápicos, como doxorrubicina, vincristina, ciclofosfamida, cisplatina, topotecano, irinotecano e temozolomida, estão sendo utilizados contra NB (Cheung and Dyer 2013, ACS 2018). No entanto, as abordagens terapêuticas atuais, incluindo cirurgia, radioterapia e quimioterapia, não são completamente eficazes (Louis and Shohet 2015).

4.2 MITOCÔNDRIA COMO POTENCIAL ALVO TERAPÊUTICO NO TRATAMENTO DO CÂNCER

As mitocôndrias são organelas encontradas em células eucarióticas e responsáveis pela produção da maior parte da energia celular (Berry, Trewin et al. 2018). Como principal usina geradora de energia das células, as mitocôndrias podem produzir ATP (adenosina trifosfato) através de uma série de processos bioquímicos conhecidos como fosforilação oxidativa. O transporte de elétrons através da cadeia respiratória mitocondrial é um requisito essencial para a fosforilação oxidativa. Estes processos estão associados à geração de espécies reativas de oxigênio (ERO), que podem ser formadas quando elétrons vazam dos complexos enzimáticos da cadeia (Wen, Zhu et al. 2013).

As características estruturais e funcionais das mitocôndrias fornecem vários alvos primários para a falha bioenergética induzida por xenobióticos (Cui, Wen et al. 2017). As mitocôndrias são altamente vulneráveis à inibição ou desacoplamento do processo de aproveitamento energético.

Compostos químicos podem afetar o funcionamento da mitocôndria interferindo na formação do gradiente eletroquímico de prótons (ΔμH+), através da inibição de um ou mais complexos da cadeia respiratória e do desacoplamento promovido por alterações nas propriedades da membrana mitocondrial (Wallace and Starkov 2000). No desacoplamento ocorre o vazamento de prótons para a matriz mitocondrial independente da produção de ATP (Berry, Trewin et al. 2018). Além disso, a permeabilização da membrana mitocondrial constitui um passo decisivo na execução da morte celular programada (Porporato, Filigheddu et al. 2018).

O mau funcionamento das mitocôndrias leva ao desequilíbrio dos níveis de cálcio, redução dos níveis de ATP, dano oxidativo e morte celular por ativação do processo de morte celular por via intrínseca ou mitocondrial (Dawson and Dawson 2017). Por todos estes motivos a mitocôndria é apontada como um alvo estratégico nas terapias contra o câncer.

Neste contexto, existe um interesse crescente de como a função mitocondrial pode ser alterada por agentes químicos para inibir o crescimento do tumor e induzir a morte celular. Dentre os compostos que podem alterar a função mitocondrial e induzir a morte de células tumorais encontram-se diversos polifenóis, incluindo as chalconas (Stevens, Revel et al. 2017).

4.3 ALGUNS MECANISMOS DE MORTE CELULAR AVALIADOS NESTE TRABALHO

4.3.1 Apoptose

Apoptose é definida como morte celular programada que ocorre de forma ordenada para manter o controle homeostático de um organismo multicelular (Yang, Zhao et al. 2017). Diversos são os fatores que podem desencadear a apoptose, entre eles: permeabilização mitocondrial, danos no DNA e níveis aumentados de espécies reativas do oxigênio (ERO) (Nagata 2018).

Durante a apoptose a célula sofre alterações morfológicas características tais como: retração da célula, perda de aderência com a matriz extracelular e células vizinhas,

condensação da cromatina, fragmentação do DNA e formação dos corpos apoptóticos (Grivicich, Regner et al. 2007, Nagata 2018). Além disso, a apoptose está relacionada com externalização de fosfatidilserina na membrana (Nagata 2018).

A ativação da apoptose pode ser iniciada de duas diferentes maneiras: pela via extrínseca (citoplasmática) ou pela via intrínseca (mitocondrial) (Fig. 1). A via extrínseca é desencadeada por ligantes específicos que quando ligados a um grupo de receptores de morte presentes na membrana celular, esta ligação é capaz de ativar a cascata das caspases, um grupo de cisteína proteases que podem clivar substratos celulares (Mishra, Salehi et al. 2018).

A via intrínseca é ativada por estresse intracelular ou extracelular como a deprivação de fatores de crescimento ou quando ocorre lesão ao DNA por radiação, toxinas ou radicais livres. As mitocôndrias desempenham um papel fundamental na regulação da apoptose (Wang and Youle 2009). Essa organela integra os estímulos de morte celular como a permeabilização mitocondrial que leva a consequente ativação de caspases e/ou liberação de endonuclease G (EndoG) e fator indutor de apoptose (AIF) (Grivicich, Regner et al. 2007).

As caspases podem ser classificadas de acordo com seu papel na apoptose. Caspases iniciadoras estão envolvidas na iniciação da cascata proteolítica, na via extrínseca são as caspases 8/10 e na via intrínseca é a caspase 9. Caspases efetoras são responsáveis pela clivagem de substratos. Independentemente do estímulo, as caspases efetoras que participam do processo são as caspases 3/6/7 (Logue and Martin 2008).

A apoptose também pode ser sinalizada através da liberação da Endo G e do AIF, que normalmente estão confinados à mitocôndria, mas translocam-se para o núcleo em resposta a sinais específicos de morte (Yang, Zhao et al. 2017). A EndoG é um homodímero que está envolvido na replicação do DNA mitocondrial com papel importante na recombinação e reparo do DNA (David, Sasaki et al. 2006). O AIF provoca fragmentação de DNA e condensação da cromatina em células e núcleos isolados de maneira independente de caspases (Susin, Daugas et al. 2000).

Figura 1 – ESQUEMA REPRESENTATIVO DAS VIAS DE ATIVAÇÃO DA APOPTOSE

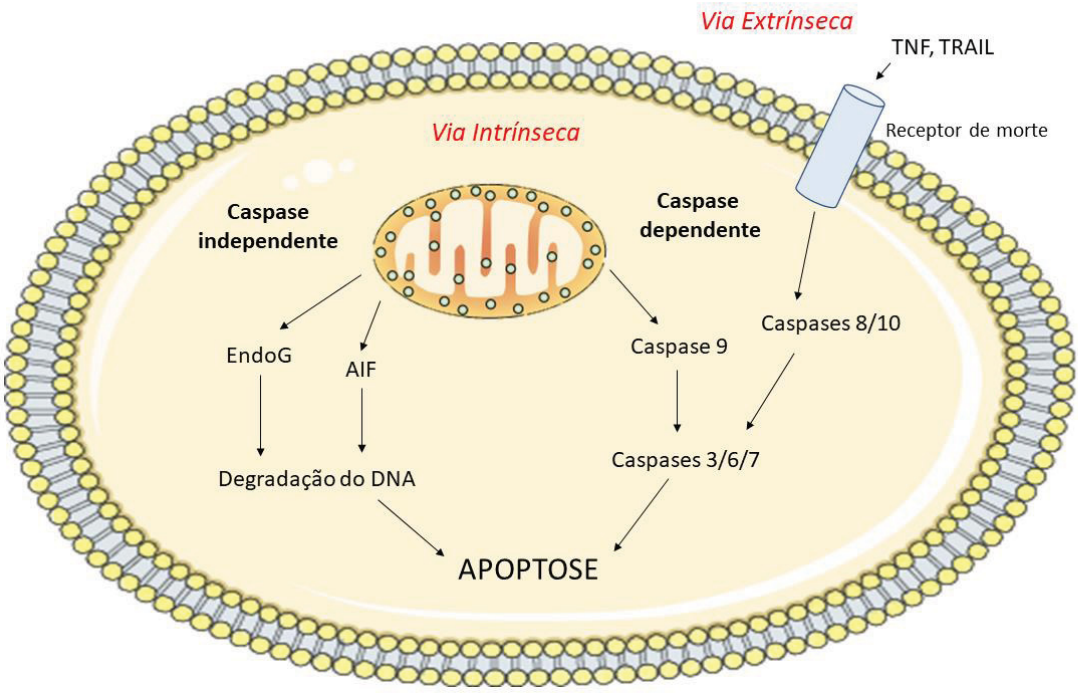

Fonte: O autor (2018)
NOTA: Representação das vias extrínseca e intrínseca da apoptose celular. A via extrínseca, mediada pela ativação de receptores de morte celular localizados na membrana plasmática que desencadeiam ativação de caspases. Já a via intrínseca está relacionada com a permeabilização da mitocôndria, onde pode haver ativação de caspases ou liberação de EndoG ou AIF que levarão à degradação do DNA (Mishra et al., 2018).

Outra organela que também pode estar envolvida com o processo de apoptose é o retículo endoplasmático (RE). O RE é um conjunto de membranas que têm função de síntese e transporte de várias substâncias, entre elas, as proteínas. O RE é altamente sensível a estresses que perturbem os níveis de energia celular, o estado redox ou níveis de Ca^{2+} (Schwarz and Blower 2016). Perturbações na função RE, um processo chamado "estresse do RE", desencadeia a resposta a proteínas mal enoveladas (UPR, do inglês: *Unfolded Protein Response*); um conjunto de reações intracelulares para restaurar a homeostase proteica que levam a redução da tradução protéica e ativação da transcrição de proteínas envolvidas com o enovelamento protéico, como as chaperonas (Sano and Reed 2013). Sob condições em que o estresse do RE é cronicamente prolongado ocorre um acúmulo de proteínas mal enoveladas, o que pode levar ao processo de morte celular por apoptose (Szegezdi, Logue et al. 2006, Tabas and Ron 2011).

Organelas celulares possuem sinalização dinâmica e podem envolver e/ou influenciar o funcionamento e de vários compartimentos e processos celulares. Membranas associadas às mitocôndrias (MAMs, do inglês: *mitochondria-associated membranes*)

colaboram (juntamente com o ER) na resposta a diversos estímulos de estresse, modulação do metabolismo, controle redox e apoptose (Carreras-Sureda, Pihán et al. 2017, van Vliet and Agostinis 2018).

Polifenóis podem regular a apoptose celular através de mecanismos extra ou intracelulares em condições experimentais *in vitro* (Curti, Di Lorenzo et al. 2017). Entre estes polifenóis encontramos alguns flavonoides como xantohumol (Zhang, Chu et al. 2015), buteína (Yang, Hu et al. 2015) e isoliquitigenina (Yang, Zhang et al. 2017).

4.3.2 Autofagia

A autofagia é um processo catabólico de degradação e reciclagem dos componentes celulares. Este processo ocorre principalmente para eliminar macromoléculas desnecessárias, organelas danificadas e patógenos intracelulares (Lee and Lee 2016). Por esse motivo, apresenta um papel crítico na manutenção da homeostase celular em condições de crescimento normal e na preservação da viabilidade celular em condições de estresse (Prieto-Dominguez, Garcia-Mediavilla et al. 2018).

O papel da autofagia na tumorigênese e no tratamento do câncer é complexo. Autofagia está relacionada tanto na supressão quanto na progressão do tumor. Como a autofagia protege as células do estresse metabólico, é razoável que a regulação de autofagia preserve a aptidão celular e a integridade genômica e, assim, previna a tumorigênese. Pelo contrário, as células tumorais estabelecidas podem utilizar a autofagia para sobreviver ao stress, como a limitação de nutrientes e hipóxia. Além disso, o papel citoprotetor da autofagia foi relacionado como um dos mecanismos de sobrevivência das células tumorais (Eskelinen 2011, Singh, Vats et al. 2018).

A via da autofagia prossegue por cinco fases: (1) nucleação, que é a formação de uma estrutura de membrana dupla ou membrana de isolamento, que também é chamada de fagófaro, (2) a expansão da membrana do fagófaro pela associação da proteína LC3-II, (3) a maturação dessa estrutura no autofagossomo e o sequestro do material citoplasmático a ser degradado; (4) a fusão do autofagossomo com o lisossomo, que resulta na formação dos autofagolisossomos e, finalmente, (5) a degradação de materiais biológicos sequestrados pelas enzimas hidrolíticas do lisossomo e a reciclagem de moléculas (principalmente aminoácidos, lipídios, açúcares e nucleotídeos) (Fig. 2) (Maciel-Herrerías and Cabrera-Benítez 2016).

A proteína LC3 (cadeia leve 3 da proteína 1A/1B associada aos microtúbulos) merece uma atenção especial e pode ser utilizada como uma das proteínas marcadoras de autofagia. A proteína LC3 na forma I (LC3-I) sofre clivagem e lipidação quando um sinal pró-autofágico é percebido pela célula, sendo convertida, assim, à forma II (LC3-II). Assim, a avaliação da conversão de LC3-I para LC3-II reflete, pelo menos em parte, a atividade autofágica celular (Yoshii and Mizushima 2017).

A proteína p62 também está relacionada com o processo autofágico. A p62 é seletivamente incorporada pelos autofagossomos através de ligação direta com LC3 e é eficientemente degradada pela autofagia; assim, os níveis totais de expressão celular de p62 correlacionam-se inversamente com a atividade autofágica (Mizushima, Yoshimori et al. 2010).

Beclin 1 tem um papel central na regulação da autofagia. Beclin-1 induz a autofagia por ligação e ativação da fosfatidilinositol 3-quinase tipo 3 (PI3-quinase) também designada Vps34, o que é necessária para a formação dos autofagossomos (Singh, Vats et al. 2018). Beclin 1 também se liga a outras proteínas, como a *Atg*14L, que promovem ou inibem a autofagia por aumentar ou diminuir a atividade Vps34, respectivamente (Eskelinen 2011).

Outros recursos que podem ser utilizados na avaliação do fluxo autofágico são os inibidores da acidificação e função lisossomal, como a bafilomicina A, cloroquina (CQ) e hidroxicloroquina (HCQ) (Ozpolat and Benbrook 2015, Redmann, Benavides et al. 2017) .

O uso de diferentes flavonoides como moduladores da autofagia, isoladamente ou em combinação com outras moléculas, pode ser uma estratégia valiosa no tratamento do câncer (Prieto-Dominguez, Garcia-Mediavilla et al. 2018).

Figura 2 – ESQUEMA REPRESENTATIVO DO PROCESSO AUTOFÁGICO

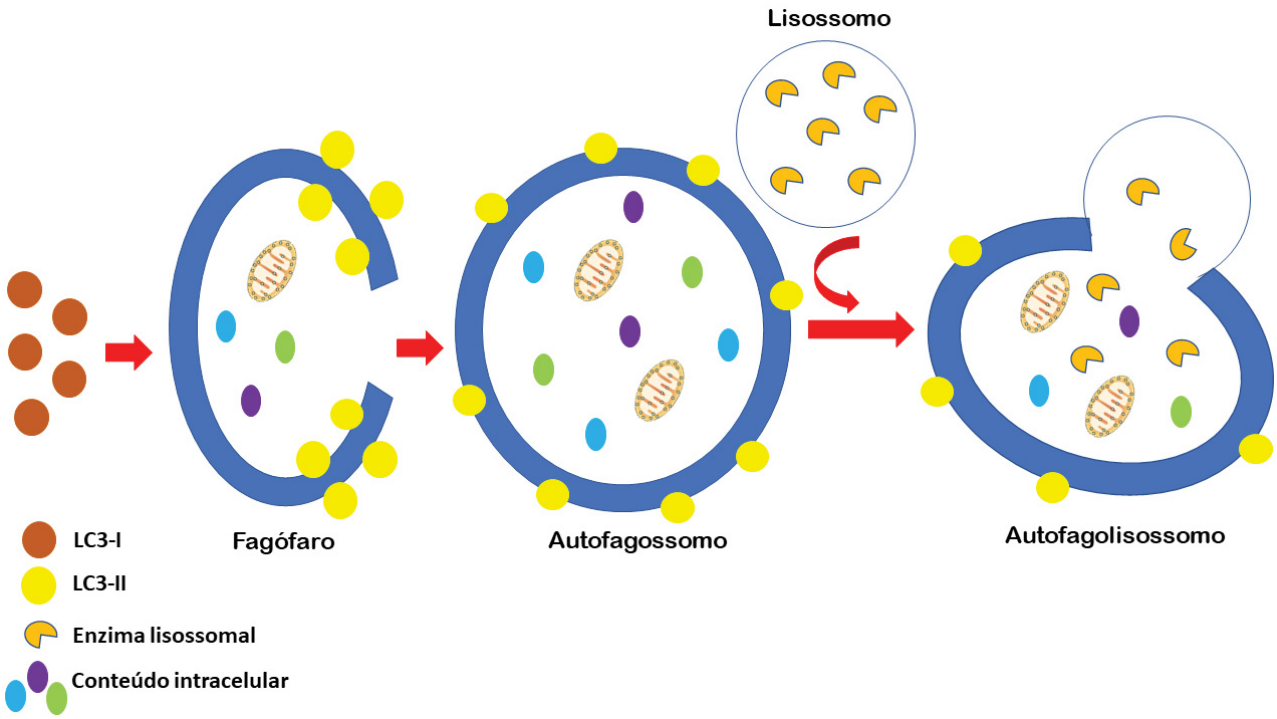

FONTE: O autor (2018).
NOTA: O processo da autofagia inicia-se pela formação de uma membrana dupla dentro da célula (fagófaro). Ocorre o elongamento do fagófaro após a associação da proteína LC3-II à sua membrana. Nessa etapa é formado o autofagossomo que sequestra proteínas e organelas como a mitocôndria. Após a fusão do autofagossomo ao lisossomo, é formado o autofagolisossomo (Maciel-Herrerías and Cabrera-Benítez, 2016).

4.3.3 Necrose e Necroptose

A morte celular por necrose ocorre, geralmente, em resposta à injúria severa às células. Morfologicamente, necrose refere-se a um ganho no volume celular, inchaço das organelas, floculação da cromatina, ruptura de membrana plasmática e subsequente perda de conteúdo celular (Chaabane, User et al. 2013). Em resposta a esse extravasamento celular, ocorre a geração de uma resposta inflamatória, que pode causar morte celular (Lee, Ju et al. 2018). Ainda, durante a necrose ocorrem alterações da função mitocondrial, diminuindo drasticamente a produção de ATP (Anazetti and Melo 2007).

A necroptose é uma forma de necrose programada. Esse tipo de morte celular pode ser iniciada por perturbações do microambiente extracelular ou intracelular detectadas por receptores de morte específicos, incluindo, mas não se limitando, ao receptor do fator de necrose tumoral 1 (TNFR1) (Galluzzi, Vitale et al. 2018). O processo de necroptose

depende de uma via de sinalização mediada por quinases denominadas proteína serina-treonina quinase de interação com receptor (RIPK), mais especificamente RIPK1 e RIPK3. A formação do complexo RIPK1-RIPK3 é capaz de fosforilar a proteína *mixed lineage kinase domain-like* (MLKL). Ocorre a translocação de MLKL fosforilada à membrana celular onde se ligam a espécies específicas de fosfato de fosfatidilinositol e, acionam a permeabilização da membrana plasmática (Silke, Rickard et al. 2015, Galluzzi, Vitale et al. 2018). A necroptose é caracterizada pela rápida permeabilização da membrana plasmática, que está associada à liberação do conteúdo celular e subseqüente exposição de padrões moleculares associados ao dano (DAMPs) (Krysko, Aaes et al. 2017). Embora ocorra sob condições reguladas, a morfologia celular da necroptose é muito semelhante à da necrose (Galluzzi, Vitale et al. 2018).

Figura 3 – ESQUEMA REPRESENTATIVO DA NECROPTOSE

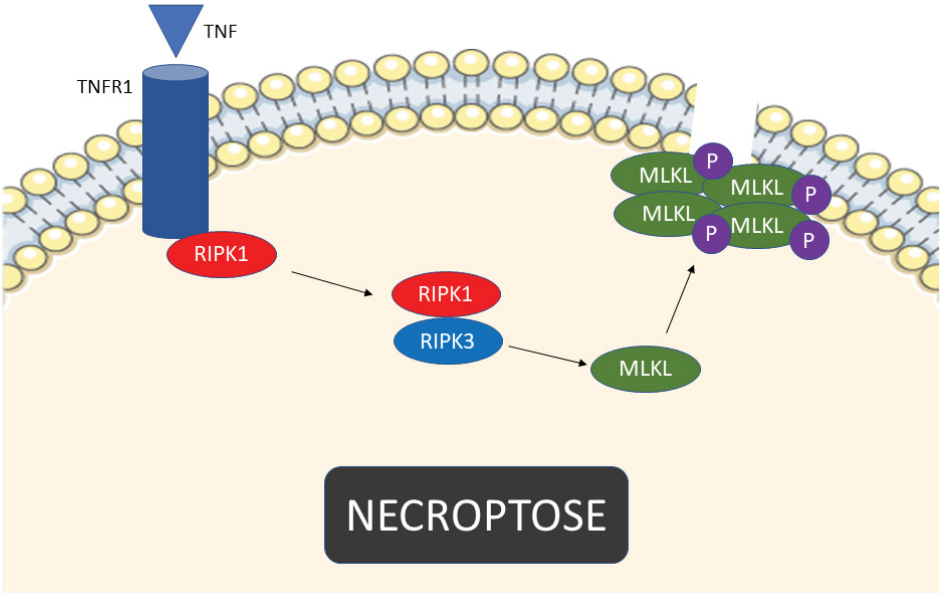

Fonte: O autor (2018)
NOTA: Quando o TNF se liga ao seu receptor (TNFR), ocorre a ubiquitinação de RIPK1. RIPK1 forma um complexo com RIPK3, que oligomeriza e recruta a pseudoquinase, MLKL. O RIPK3 fosforila MLKL, ativando-a e levando a sua translocação para a membrana celular onde forma tetrâmeros para permear a bicamada lipídica (Galluzzi et al., 2018).

Algumas classes de compostos fenólicos são capazes de promover a indução de diferentes tipos de morte celular em células tumorais preferencialmente quando

comparadas com células normais. Entre estes compostos encontramos alguns flavonoides, como a buteína e a isoliquiritigenina (Venu Venkatarame Gowda Saralamma 2017).

4.4 FLAVONOIDES

Os flavonoides são compostos fenólicos encontrados em plantas que possuem várias atividades biológicas estudadas para o tratamento de diversas patologias como alergias, infecções virais, úlceras, câncer e neurodegeneração (Dajas, Andres et al. 2013, Busch, Burkard et al. 2015). Essas atividades biológicas estão relacionadas com a variedade estrutural que os flavonoides possuem (Estrada-Reyes, Ubaldo-Suárez et al. 2012).

Os flavonoides são classificados de acordo com suas estruturas químicas, natureza e distribuição dos substituintes, grau de insaturação e presença ou ausência no anel C em: flavonas, flavonóis, flavanonas, isoflavonas, flavanonóis, flavanas, flavanóis, chalconas, dihidrochalconas e flavan-3,4-dióis (CORRADINI et al., 2011).

Dentre o grupo dos flavonoides, as chalconas têm recebido grande atenção devido a sua estrutura relativamente simples e à diversidade de atividades biológicas que apresentam (Leon-Gonzalez, Acero et al. 2015, Lee, Ju et al. 2018).

Além disso, devido às suas propriedades anti e pró-oxidantes, as chalconas são capazes de afetar funções celulares básicas, entre elas, o crescimento e diferenciação celulares e induzir a morte celular (Sharma, Kumar et al. 2015).

4.4.1 Potencial ação antitumoral das chalconas

Nos últimos anos foram descritas potenciais ações antitumorais de várias chalconas substituídas em diversas linhagens de células tumorais. Entre a chalconas substituídas citadas encontramos algumas hidroxiladas como as descritas a seguir.

Kim e cols. verificaram que a 2-hidroxichalcona e o xanthohumol (2',4,4'-trihidroxi-6'-metoxi-3'-prenilchalcona) foram capazes de induzir apoptose e inibir o crescimento de células tumorais de mama (MDA-MB-231) após 24h de incubação com IC_{50} de 4,6 e 6,7 μM, respectivamente (Kim, Lee et al. 2013).

Shin cols. observaram que a 2-hidroxi-4-metoxi-2',3'-benzochalcona exibiu atividade citotóxica com IC_{50} de 5,2 μM contra células tumorais de pâncreas (Capan1) após 48h de tratamento (Shin, Kim et al. 2013). Esta chalcona induz apoptose através aumento da atividade de caspases 2/9/3/7.

O tratamento de células de hepatocarcinoma (HepG2 e Hep3B) com buteína (3,4,2',4'-tetrahidroxichalcona) na concentração de 30 μM por 24h inibiu o crescimento celular, induzindo o aumento da porcentagem de células na fase G2/M e apoptose (Moon, Kim et al. 2010). Além disso, Yang cols. verificaram que a buteína, na mesma concentração e tempo de tratamento, possui efeitos citotóxicos e induz apoptose em células de câncer de ovário humano (ES-2 e TOV-21G) (Yang, Hu et al. 2015).

Saydam cols. demostraram que a 4,4'-dihidroxichalcona reduz a viabilidade de células de leucemia (HL-60) com IC_{50} = 2 μM após incubação por 72h (Saydam, Aydin et al. 2003).

Além disso, Sabzevari cols. observaram que chalconas hidroxiladas apresentaram efeito citotóxico maior em células de hepatocarcinoma humano (HepG2) quando comparadas a hepatócitos isolados de fígado de rato (Sabzevari, Galati et al. 2004).

Em linhagens de neuroblastoma, algumas chalconas já apresentaram efeito citotóxico. A isobavachalcona (2',4',4-trihidroxi-3'-fenilchalcona) induziu a morte por apoptose de células de neuroblastoma humano (IMR-32 e NB-39) através da via mitocondrial e não apresentou citotoxicidade contra células não tumorais (cultura primária de células granulares cerebelares de ratos) (Nishimura, Tabata et al. 2007).

Ketabforoosh cols. observaram que a 3- bromo- 4,5- dimetoxichalcona apresenta efeito citotóxico em células de neuroblastoma humano (SK-N-MC) com IC_{50} = 1,1 μM após tratamento por 48h (Ketabforoosh, Kheirollahi et al. 2014).

Xanthoangelol (2',4,4'-trihidroxi-3'-geranilchalcona) após tratamento por 48h e IC_{50} de 2,6 μM é capaz de promover estresse oxidativo pelo aumento dos níveis de ERO e induzir a apoptose através da liberação do citocromo *c* e ativação da caspase-9 em células de neuroblastoma (IMR-32) (Motani, Tabata et al. 2008).

As chalconas utilizadas nesse trabalho, 4'-hidroxichalcona (4HC) e isoliquiritigenina (ISL) (Fig. 4), também possuem alguns efeitos biológicos descritos na literatura, incluindo atividade citotóxica em algumas linhagens celulares que serão descritas a seguir.

Figura 4 – FÓRMULAS ESTRUTURAIS DAS CHALCONAS UTILIZADAS NESTE TRABALHO

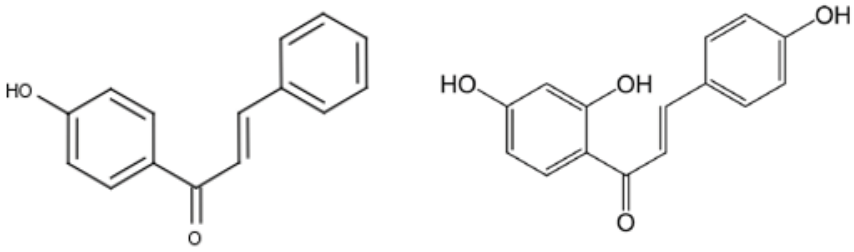

4'-hidroxichalcona Isoliquiritigenina

Fonte: O autor (2018)

4.4.1.1 Potenciais efeitos da 4HC

Sobre a 4HC já foi descrito na literatura efeito citotóxico contra células de leucemia (K562) com IC_{50} de 30 μM após 24h de incubação (Orlikova, Tasdemir et al. 2011). Os autores também observaram que a 4HC foi capaz de inibir a ativação de NF-kβ induzida por TNFα. Além disso, a 4HC apresentou citotoxicidade seletiva para células leucêmicas quando comparadas com células mononucleares saudáveis do sangue periférico.

Gul cols. demostraram que a 4HC e seus derivados apresentam citotoxicidade contra linfócitos T humanos transformados (Jurkat) com $IC_{50} \approx 10$ μM após 48h de incubação e inibem a DNA topoisomerase I em DNA plasmidial (Gul, Cizmecioglu et al. 2009).

Além disso, Martineau descreveu que a 4HC possui efeito desacoplador da fosforilação oxidativa em mitocôndrias isoladas de fígado de rato utilizando a concentração de 100 μM (Martineau 2012).

4.4.1.2 Potencial ação antitumoral da ISL

A ISL é uma chalcona que pode ser encontrada em plantas como alcaçuz (*Glycyrrhiza uralensis)*, cebolas e brotos de feijão (Hsu, Chia et al. 2009).

Estudos farmacocinéticos, metabólicos e de distribuição tecidual em camundongos mostram que a ISL é metabolizada primariamente no fígado, acumula-se em todos os principais órgãos e pode atravessar a barreira hematoencefálica (BHE) (Han, Chin et al. 2013). Esse mesmo estudo demostrou que administração oral (20 mg/kg) de ISL em camundongos resulta em níveis plasmáticos de 19,5 μM na circulação. Além disso, Qiao cols. observaram que a ISL atingiu concentrações máximas dentro de 1h após

administração oral e foi rapidamente eliminada (<5h) nas doses de 10 a 50 mg/kg sem apresentar toxicidade em ratos (Qiao, Zhang et al. 2014).

Yang cols. verificaram que a ISL apresenta efeito citotóxico contra células tumorais da glândula adrenal (PC-12) com IC_{50} = 17,8 μM após 24h de incubação. Os autores descreveram que a ISL induz a apoptose através da ativação da via intrínseca mediada por ERO e causa autofagia nas células PC-12 (Yang, Zhang et al. 2017).

Em células tumorais de endométrio (Ishikawa, HEC-1A e RL95-2), a ISL foi capaz de inibir o crescimento celular e induzir apoptose e autofagia. Os autores observaram que após a incubação com ISL (25 e 50 μM) por 48h houve aumento da porcentagem de células tumorais de endométrio na fase G2/M do ciclo celular, assim como aumento do conteúdo de DNA fragmentado. Além disso, o tratamento com ISL (25 μM) por 12h aumentou a expressão proteica da caspase-7 e LC3BII, vias associadas a apoptose e autofagia (Wu, Chen et al. 2016).

ISL na concentração de 20 μM e no tempo de incubação de 24h foi capaz de promover parada do ciclo celular na fase G2/M em células de câncer de próstata humano (DU145) e de rato (MatLyLu - MLL), promovendo redução da expressão de ciclinas D1 e E, da quinase dependente de ciclina (CDK) 4 e CDC25C, e aumento da expressão de ciclina B1 (Lee, Lim et al. 2009).

Sun cols. observaram que ISL induz estresse oxidativo por perturbar o status redox celular e, assim, aumentar a radiossensibilidade de células de hepatocarcinoma humano (HepG2) (Sun, Zhang et al. 2013).

Além disso, a ISL demonstrou seletividade entre células tumorais e não tumorais. O tratamento com ISL (10-100 μM durante 24 h) inibe a proliferação de células tumorais de próstata (C4-2 e LNCaP) e não tem efeito sobre a viabilidade das células epiteliais não tumorais (IEC-6) (Zhang, Yeung et al. 2010).

Zhou cols. observaram que este composto inibe a proliferação e induz apoptose em células de glioma humano (U87MG) após tratamento por 24h na concentração de 60 μM (Zhou, Song et al. 2013).

Apesar da sua capacidade de passar pela BHE, em células tumorais de sistema nervoso são encontrados poucos estudos sobre os efeitos da ISL, além disso, não são conhecidos seus efeitos sobre células de neuroblastoma humano SH-SY5Y. A sua biodisponibilidade e baixa toxicidade em células normais poderiam colaborar para o uso desta chalcona em tratamento contra neuroblastoma.

5 ARTIGOS CIENTÍFICOS

5.1 4'-HYDROXYCHALCONE INDUCES HUMAN NEUROBLASTOMA CELL DEATH THROUGH MITOCHONDRIAL DYSFUNCTION

Stephane Janaina de Moura Escobar[1,2], Martin Simone[2], Ciro Alberto de Oliveira Ribeiro[3], Glaucia Regina Martinez[1], Sheila Maria Brochado Winnischofer[1], Paul Kenneth Witting[2], Maria Eliane Merlin Rocha[1*]

[1]Department of Biochemistry and Molecular Biology, Federal University of Paraná, Curitiba, PR, Brazil

[2]Redox Biology and Neuropharmacology Groups, Discipline of Pathology, The University of Sydney, Sydney, NSW 2006, Australia

[3] Cellular Toxicology Group, Department of Cellular Biology Federal University of Paraná, Curitiba, PR, Brazil

ABSTRACT

Neuroblastoma is an aggressive form of cancer with high mortality. Hydroxychalcones have received considerable attention because of their cytotoxic activities on cancer cells. However, the effect of the 4'-hydroxychalcone on neuroblastoma cells is unknown. The aim of the present study was to characterize the cytotoxicity of 4HC to neuroblastoma and the importance of mitochondrial effects in its action mechanism using an in vitro model of SH-SY5Y cells. Incubation of cultured SHSY5Y cells with 10-60 μM 4HC (24 h) decreased cell confluency, cellular metabolic activity and depleted intracellular ATP relative to the vehicle-treated control. The mechanism of 4HC-induced cell toxicity likely involves mitochondria dysfunctional as judged by inhibition of mitochondrial respiration, depolarization of mitochondria membrane potential and intracellular and morphological alterations. Furthermore, loss of cell viability was accompanied mainly by increase of phosphatidylserine exposure on the surface of cells, suggesting that the flavonoid may induce apoptosis in SH-SY5Y cells. In addition, treatment inhibited SH-SY5Y cell migration/proliferation in a scratch assay and induced significant changes in the cell cycle progression. Our results showed the effects of 4HC in the human neuroblastoma cell line SH-SY5Y are associated with mitochondrial dysfunctional, depletion of intracellular ATP levels, ROS increase, alteration in cell cycle progression and cellular morphology.

Keywords: hydroxychalcones, mitochondria, respiratory chain, SH-SY5Y

5.1.1. Introduction

Neuroblastoma (NB) is an extracranial solid cancer and the most common cancer in infancy [1]. NB is developed from uncommitted neural crest cells along the sympathetic nervous system and occasionally in central nervous system, including brain [2]. NBs are characterized by poor prognosis and this cancer still accounts for about 15% of all pediatric cancer deaths in North America [3]. The standard treatment for NB is based on the combination of chemotherapeutic drugs such as doxorubicin, vincristine, cyclophosphamide, and cisplatin, however chemoresistance occurs and the tumor become highly aggressive and metastatic [4, 5]. The 5-year survival rate was 95% for children younger than 1 year and 68% for children aged 1 to 14 years who are diagnosed with NB [6]. Hence, novel therapies to address long-term survival rates and with fewer side effects are urgently required.

Flavonoids are polyphenolic compounds which are unique due to their diverse chemical structures and various biological activities like anti-inflammatory [7], anti-oxidative [8] and anti-cancer [9]. Furthermore, flavonoids can act in mitochondria promoting reduction on respiratory rate [10]. Mitochondria are involved with generation of ATP, calcium homeostasis, intracellular sources generation of reactive oxygen species (ROS) and involvement in some types of cell death mechanism, as apoptosis by intrinsic pathway [11]. Because of the essential role to eukaryotic cells, mitochondria are important target organelles in cancer therapeutic strategy and it has attracted much attention over the years [12].

Chalcones, a group of the flavonoids without C ring, are interesting compounds to research due to its simple chemistry, ease of synthesis and a wide variety of promising biological activities [13]. Particularly, cytotoxic activities have been described for hydroxychalcones. Butein (3,4,2,4-tetrahydroxychalcone) [14] and 2-hydroxychalcone [15] induces apoptosis in human hepatoma cancer cells and in breast cancer cells, respectively. Also, isoliquiritigenin (4,2',4'-trihydroxychalcone) showed inhibition of proliferation and alterations in the cell cycle progression in cultured glioma and prostate cancer cells [16, 17].

4'-hydroxychalcone (4HC; Figure 1A) is a synthetic chalcone presenting some biological properties. According to Orlikova and cols. [18] this molecule exhibits significant anti-tumor activities, including inhibition of TNFα-induced NF-kB activation in cultured

leukemic cancer cells (K562 and Jurkat). Some other flavonoids, including chalcones, have been shown to affect enzymatic activities of the mitochondrial respiratory chain in isolated rat liver mitochondria [19-21]. However, no effects of 4HC on mitochondrial respiratory chain and levels of ATP and ROS in neuroblastoma cells SH-SY5Y have been reported.

The aim of the present work is to evaluate the cytotoxic activity of 4HC in human neuroblastoma cells and the contribution of the mitochondrial dysfunction that ultimately leads to cell death. Our data indicate that 4HC significantly decreased SH-SY5Y cell viability, proliferation/migration. This cytotoxic activity of 4HC was associated with inhibition of mitochondrial respiration, depolarization of mitochondria membrane, depletion of intracellular ATP levels, ROS increase, alteration in cell cycle progression and cellular morphological alterations.

5.1.2. Materials and Methods

5.1.2.1 Chemicals

4'-hydroxychalcone (structure shown in Figure 1A), 3-(4,5-dimethylthiazol-2-yl)-2,5-diphenyltetrazolium bromide (MTT) and 2',7'-dichlorofluorescin diacetate (DCFH–DA) were sourced from Sigma-Aldrich (St. Louis, MO, USA). Dimethyl sulfoxide (DMSO) from Merck (São Paulo, SP, Brazil). All buffers were prepared in MilliQ water and adjusted to physiological pH (7.4) prior to use.

5.1.2.2 4'-hydroxychalcone solutions

4'-hydroxychalcone was dissolved in DMSO (final concentration 0.1%), and then further diluted in Dulbecco's Modified Eagle's Medium/Ham's Nutrient Mixture F12 (DMEM/F12) (10–60 μM). The 4'-hydroxychalcone stock solution was stored at -20°C and 8warmed to 25°C just before use.

5.1.2.3 Cell Culture and Treatment

Human neuroblastoma (SH-SY5Y) cells were seeded at 4 x 10^4 cells/cm^2 and grown to confluence at 37°C under 5% CO_2 atmosphere in Dulbecco's Modified Eagle's

Medium/Ham's Nutrient Mixture F12 (DMEM/F12) containing 10% v/v fetal bovine serum, 100 U/mL penicillin, 100 µg/mL streptomycin, 2.5 mM L-glutamine and 1x non-essential amino acid solution. SH-SY5Y cells were treated in the presence or absence of 4HC (final concentration range 10 – 60 µM) for 24 h.

5.1.2.4 Measures of Cell Viability and Cytotoxicity

Intracellular ATP levels. Levels of ATP were determined with a commercial kit as the manufacturer's instructions (Perkin Elmer, Melbourne, Australia). Briefly, SH-SY5Y cells were cultured in 96-well plates and treated with 4HC (0–60 µM) at 37 °C. After 24 h, cells were treated with 50 µL of mammalian cell lysis buffer (100 µL) and the entire plate was shaken (700 r.p.m.) for 5 min. Cell lysates were then mixed with a further 50 µL of substrate solution, the mixture agitated for another 5 min and then incubated in the dark (10 min). Total ATP content was then measured by determining the level of luminescence in each well with an Infinite® 200 PRO TECAN plate reader (Tecan Group Ltd., Männedorf, Switzerland) and finally normalized to corresponding total cell protein determined with the bicinchoninic acid assay.

Confluence. Cells were treated with 4HC (0 – 60 µM) or DMSO (control-vehicle), and the 6-well culture plate was imaged using the IncuCyte™ ZOOM instrument (Essen BioScience, Australia) to assess proliferation by real-time imaging. Data were analyzed using the IncuCyte's built-in Confluence Processing analysis tool (version 1.5), which quantified cell surface area coverage.

MTT assay. The MTT assay is based on the conversion of MTT into formazan crystals by living cells, which determines cellular metabolic activity [22]. Cells were seeded onto 96-well culture plates. After overnight incubation, the cells were treated with various concentrations of 4HC for 24 hours. Cells were incubated for 3 h with 5 mg/ml of MTT, dissolved in phosphate buffered saline (PBS). Followed by the addition of DMSO (200 µl) and then gentle shaking for 2 min so that complete dissolution. Absorbance was recorded at 550 nm using the microplate spectrophotometer system (BioTek Epoch).

5.1.2.5 Hematoxylin and eosin staining

SH-SY5Y cells were seeded onto 24-well cell-culture plates containing glass coverslips. After overnight incubation, the cultures were treated with 4HC (10-40 µM) for 24 h. After

treatment, the coverslips were removed and the cells were immediately fixed in absolute ethanol and then stained with hematoxylin–eosin. The cells were evaluated in Zeiss Axiovert 40 CFL Inverted Microscope.

5.1.2.6 Transmission electron microscopy

For ultrastructure investigations, SY-SY5Y cells were preincubated with 4HC (20-40 μM) for 24 h, preserved in fixative solutions (2.5% glutaraldehyde and 1% paraformaldehyde in 0.1 M cacodylate buffer) for 4h at 4ºC and pH 7.2-7.4. The cell pellets were formed and post-fixed in 1% w/v osmium tetroxide in the same buffer for 1 h at 4ºC, dehydrated in ethanol crescent series, propylene oxide and finally embedded in PoliEmbed 812 DER736 resin (Electron Microscopy Sciences). Ultrathin sections ~70 nm thickness were obtained from Ultramicrotome Leica, contrasted by uranil acetate (0.5% w/v in water) for 20 min and lead citrate [23] for 5 min, and analyzed under the transmission electron microscopy (JEOL TEM 1200 EXII) from Electronic Microscopy Center at Federal University of Parana.

5.1.2.7 Annexin V assay

SH-SY5Y cells were exposed to vehicle (DMSO control) or 4HC (20-40 μM) as described above; the mitochondrial uncoupling agent carbonyl cyanide m-chlorophenyl hydrazone (CCCP; final concentration 100 μM) as positive control. After 12 or 24 h, media was aspirated and collected and each well was treated with 0.25% w/v trypsin for 10 min at 37 °C. Each well was then treated with 1 mL PBS (calcium-free solution) containing 10% v/v FBS and 4 mM EDTA and the isolated cells were combined with the previously collected media, and centrifuged at 200 x g for 5 min followed by resuspension in 2 mL cold PBS (EDTA-free solution) and then another centrifugation step at 200 x g for 5 min. Each resultant cell pellet was immediately dispersed in 100 μL 1x Abcam Flow buffer that contained the following additives: 5 μL Annexin V-CF Blue and 5μL 7-AAD as per the manufacturer's protocol (Abcam Apoptosis Detection Kit; ab214663). This method of cell isolation and labeling was necessary to yield a non-aggregated suspension of single cells suitable for flow cytometric analysis. Finally, the cells were analyzed for the proportion of Annexin V-CF Blue negative, 7-AAD Staining Solution negative; Annexin V-CF Blue positive, 7-AAD Staining Solution negative; Annexin V-CF Blue positive, 7-AAD Staining Solution positive and Annexin V-CF Blue negative, 7-AAD Staining Solution positive with a Gallios Flow

Cytometer (Beckman-Coulter, Lakeview Parkway, IN) and using Kaluza Analysis Software (Beckman Coulter). Finally, numerical data was exported to MSExcel for quantitation.

5.1.2.8 Cell Migration/Proliferation Assay

Migration/Proliferation was determined using a cell scratch assay with real-time monitoring using the IncuCyte™ ZOOM live cell imaging system (Essen BioScience, Sydney, Australia). This system measures scratch closure and calculates the wound width within the area at each time point. A WoundMaker™ (Essen BioScience, Sydney, Australia) tool was used to create uniform, reproducible scratch in a 96-well plate containing SH-SY5Y cells. After application of the scratch-wound, media was aspirated and the wells were washed with PBS to remove any floating cells/cell debris. Next, the cells were treated with vehicle (DMSO) or 4HC (0–60 μM) in the media, and cells sub-cultured at 37°C and imaged at 24, 48 and 72 h-post scratch.

5.1.2.9 Cell Cycle Analysis

Cell cycle analysis was performed with a Muse™ Cell Analyzer (Merck Millipore, Sydney, Australia) following manufacturer's instruction. Briefly, SH-SY5Y cells were treated with vehicle (DMSO) or 4HC (0–60 μM). After a further 24 h incubation, control and 4HC treated-cells were harvested by trypsin digestion and centrifuged; the resultant cell pellet was washed in PBS, permeabilized using Triton X-100 (0.1%) and stained with propidium iodide (PI). Cells were then incubated for 30 min at 20°C in the dark. After staining, the cells were processed for cell cycle analysis and data was reported as a percentage of cells in G0/G1, S and G2/M phases.

5.1.2.10 Cellular respiration

Highly sensitive Oroboros Oxygraphy-2K (Oroboros, Innsbruck, Austria) was used to determine cellular oxygen consumption in cells cultured at 37°C. A reaction medium containing D-mannitol (125 mM), KCl (65 mM), HEPES–KOH buffer (pH 7.4) (10 mM), EGTA (0.1 mM) and BSA (0.1 % w/v) was freshly prepared prior to use in all studies. Initially, preparations of SHSY5Y cells were incubated with digitonin (final concentration 5 μg/mL) for 10 min before monitoring oxygen consumption. Mitochondrial respiration was analyzed in digitonin-permeabilized cells (1 $x10^6$ cells/mL) in the presence of a substrate mix

containing glutamate (10 mM) + malate (1 mM) and succinate (10 mM) as substrates for Complex I and II, respectively, and the reaction was supplemented with ADP (2mM). Where required, rotenone (1 µM) and antimycin A (1 µg/mL) were used as inhibitors for Complex I and III, respectively. Data acquisition and analysis was performed using Oxygraph-2K-DataLab software version 4.3.2.7 (Oroboros instruments, Innsbruk, Austria).

5.1.2.11 Mitochondria membrane potential (MMP)

Fluorochrome dye JC-1 was used to evaluate the changes in MMP. JC-1 monomers aggregate within mitochondria and convert to JC-1 aggregates that emit red light (FL2-H; 595 nm). When MMP collapses and is lower than 120 mV, JC-1 monomers selectively enter mitochondria and emit green light (FL1-H; 539 nm) [24]. The ratio of FL2-H to FL1-H fluorescence of JC-1 depends only on the membrane potential, with a decrease being indicative of membrane depolarization [25]. Briefly, SH-SY5Y cells were incubated with 10, 20 or 40 µM 4HC for 24 h. Following incubation, cells were harvested and cell pellet was gently rinsed with PBS. Cells were then stained with JC-1 (2.5 µM) for 15 min in the dark at 22 °C. Treatment with valinomycin (final concentration 1 µM) for 30 min was used as a positive control. Fluorescent intensity of cells was quantitatively analyzed in FACSCalibur flow cytometer (BD Biosciences Pharmingen, San Diego, CA, USA), and the results were calculated using the proprietary software; BD Accuri C6. Ratios of FL2-H to FL1-H fluorescence were calculated and normalized to control.

5.1.2.12 Intracellular ROS levels

Intracellular ROS levels were determined using DCFH-DA dye [26]. Cells were seeded onto 96-well culture plates. After treatment of SH-SY5Y cells with 4HC for 24 h, excess media was removed and the cells were washed twice with PBS. Cells were then incubated for 30 min with 50 µM of DCFH–DA in PBS. Treatment with H_2O_2 (400 µM) was used as a positive control and immediately after the treatment period, the plates were read using an Infinite 200 TECAN microplate reader. Finally, the level of cellular fluorescence, measured in relative fluorescence units, was then expressed a percentage of control cells (in the presence of 0.1% v/v DMSO), which were arbitrarily assigned a 100% value.

5.1.2.13 Protein determination

Total protein concentration was performed by the Bradford method [27]. For all reported experiments, the system was calibrated using bovine serum albumin.

5.1.2.14 Statistical Analyses

Experimental data was expressed as mean ± SD; n=3 or 4 as specified in figure legends. Comparisons between groups were performed with Prism Software (version 6.07, GraphPad Software Inc, San Diego, CA). Data were analyzed using one-way ANOVA with Tukey's post-hoc analysis for comparisons between treatment and control. Statistical significance was accepted at the $p<0.05$ level.

5.1.3 Results

4HC is cytotoxic to SH-SY5Y cells: The cytotoxic effect of 4HC on cultured neuroblastoma cells was assessed by measuring intracellular ATP levels, cell confluence and cellular metabolic activity (Fig. 1B-D). For this purpose, SH-SY5Y cells were treated with different concentrations of 4HC (10-60 µM) and the parameters listed were monitored at 24 h. Treatment with 4HC significantly decreased ATP levels by ~35-to-90% and SH-SY5Y-cell confluence by ~30-to-70% (Fig. 1B, C). Likewise, MTT assay showed reduction by ~15% in metabolically active cells after treatment with 10 µM 4HC and ranged up to ~70% in cells exposed to 60 µM 4HC (Fig. 1D). To determine the EC_{50} (Effective concentration of 50%) for 4HC were used intracellular ATP levels which indicate the metabolic condition of cells and it is a reproducible and practicable method to assess drug response in cell lines [28]. Thus, the EC_{50} was determined to be 21.5 ± 3.4 µM of 4HC after 24h of treatment (Fig. 1B insert).

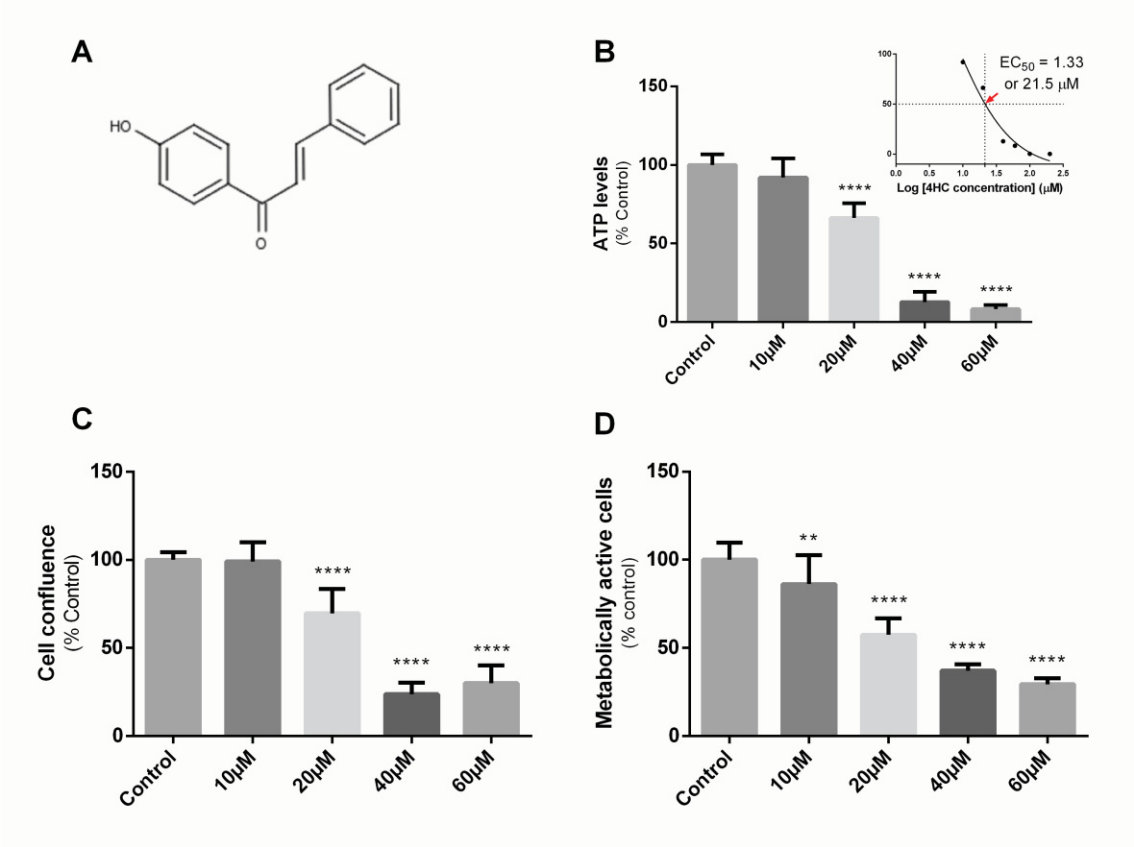

Figure 1. Effects of 4HC on cultured SH-SY5Y cell viability. (A) Chemical structure of 4'-hydroxychalcone. Treatment of cells with increasing concentrations of 4HC impacts cell viability: (B) intracellular ATP levels, (C) cell confluence and (D) MTT assay 24 h after treatment with 4HC at the concentrations indicated. ATP levels obtained to DMSO control (100%) was 2.9 ± 0.2 nmols. Inset (B) shows the assessment of the EC_{50}-concentration for 4HC based on the toxicity data. Data represent mean±SD; n=3 experiments each performed in triplicate. Different to the vehicle-treated (DMSO) control; **p < 0.01; ****p < 0.0001.

Morphological changes promoted by 4HC: Data shown in Figure 2 demonstrates morphological changes promoted by 4HC 24 h after administration of the drug. Concomitant with the changes in cell morphology, a concentration-dependent decrease in SH-SY5Y cell number was determined following treatment with different concentrations of 4HC (10-40 μM) in comparison to control cells (Fig. 2A). In addition, phenotypic changes were observed in 4HC-treated cells including: the occurrence of cell shrinkage, evidence for pyknotic nuclei and condensed cytoplasm (Fig 2B-D), with more pronounced effects on phenotype noted at higher concentrations of 4HC.

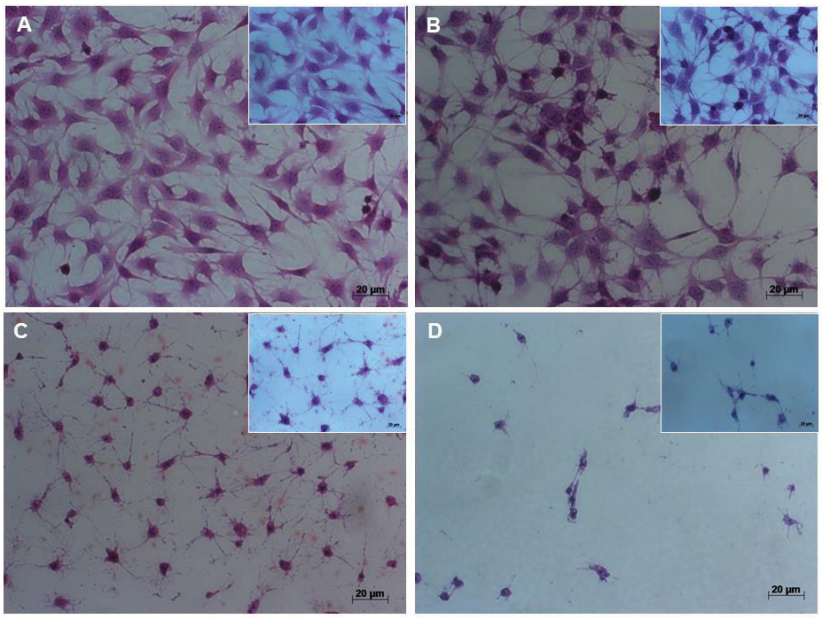

Figure 2. Hematoxylin and eosin staining of SH-SY5Y cell after 4HC treatment. Representative cell images of (A) vehicle treated cells and cells treated with (B) 10 µM 4HC or (C) 20 µM 4HC or (D) 40 µM 4HC. Note cells become less dense and isolated with fewer cellular contact in the presence of higher 4HC dose.

Analysis of ultrastructural changes in SH-SY5Y cells after exposure of 4HC were performed by transmission electron microscopy (TEM). Representative TEM micrographs are indicated in Figure 3. Control SH-SY5Y cells showed morphological characteristics of neuroblastoma cells with nuclei, and prominent clear visible nucleoli with heterochromatin aggregations. Additionally, well-preserved mitochondria, endoplasmic reticule and some vesicular figures were detected (Fig. 3A). After SH-SY5Y cells treatment with 4HC (20-40 µM) ultrastructural change/damage were focused to nuclear, mitochondrial and other organelles. Additionally, the occurrence of vacuolation and an intense formation of external micro vesicles was observed (Figures 3B and C). After exposure to 4HC for 24 h, an aggregation of nuclear chromatin is also evident. Furthermore, close inspection of the micrographs revealed electron-dense mitochondria, dispersed endoplasmic reticule, and the presence of large cytoplasmic vesicles and parallel increases in smaller diameter vesicles (Fig. 3B). Cells treated with higher concentration of 4HC showed the presence of localized to the nuclei but few defined organelles were detected. This group of cells also presented with a large number of secreted micro vesicles and mitochondria showing characteristics of swelling or degeneration (Fig 3C). These changes are more evident in cells exposed to the higher concentration of 4HC when compared to control cells. These ultrastructural features

of 4HC treated cells are indicative of cell apoptosis. These findings were corroborated by the detection of DNA fragmentation, electron dense nuclei and cytoplasm, a lack of identifiable organelles and the increased occurrence of vacuoles and membrane blebbing, all morphological features typical of apoptosis (Figure 3 D).

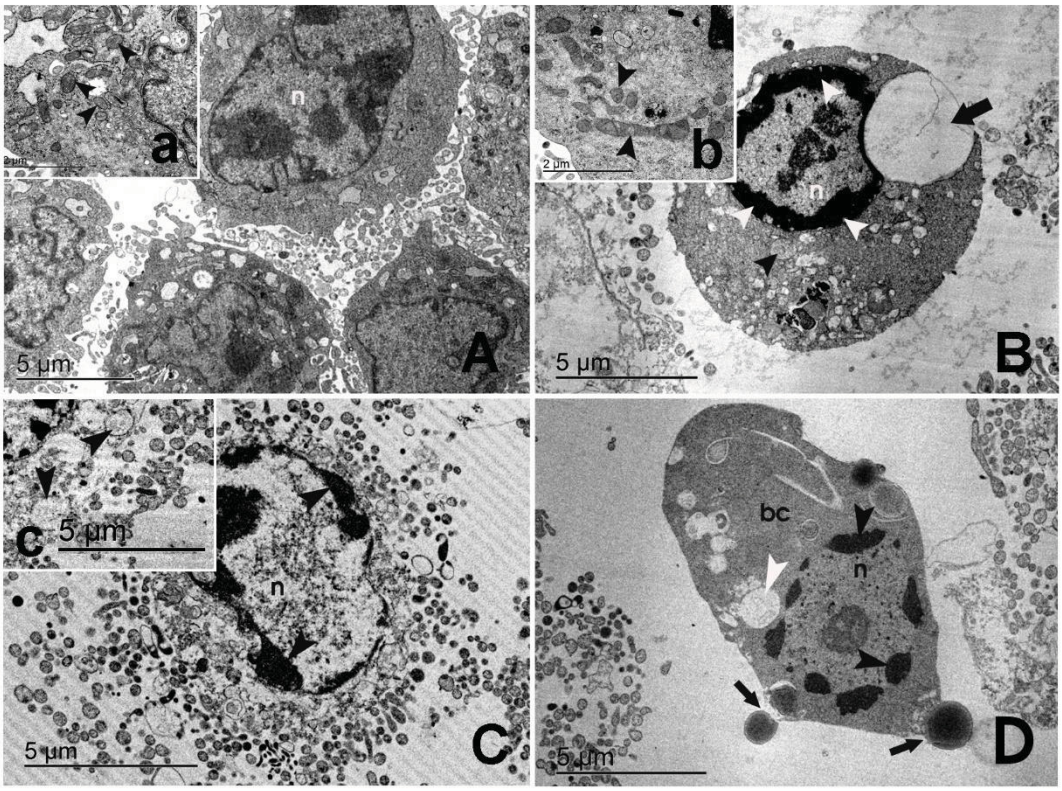

Figure 3. Ultrastructural SH-SY5Y cells changes after 4HC exposure for 24h. A. Control group. Observe the nuclei (n) with normal chromatin distribution and mitochondria (arrows in insert **a**); B. Cells after exposure to 4HC (20µM) observe swelled mitochondria (black arrowhead), the deposition of chromatin around nuclear envelope (white arrowheads) and the presence of large vesicles (arrow). In insert **b** the arrowheads show the mitochondria from control group (arrowheads); C. Cells after exposure to 4HC (40µM). The presence of chromatin accumulation is still present in a more euchromatic nuclei (n) and the number of micro vesicles is very intense in this group of cells. In insert **c** observe the presence of swelled mitochondria (arrowheads) ; D. A typical apoptotic cell death in group exposed to 4HC (20µM). Observe the deposition of chromatin (black arrowheads), the presence of vacuole (white arrowhead), electrondense cytoplasm with not well visible organelles (bc) and blebs (arrows).

The effects of 4HC include phosphatidylserine exposure: To further investigate the mechanism of 4HC-induced SH-SY5Y cell death, Annexin V/7-AAD assays were performed (Fig. 4). This assay provides information on phosphatidylserine exposure on the surface of cells based on Annexin V-positive staining, on membrane permeabilization based on 7-AAD-

positive staining. 4HC treatment increased Annexin V and 7-AAD positives in the lowest concentration (20 µM) by ~6%. Also, when the highest concentration (40 µM) of 4HC was used this effect was more pronounced, reaching 60% of the cell population compared to the vehicle control (*c.f.*, Fig. 4A-C and summary Fig 4D). Furthermore, loss of cell viability was accompanied mainly by increase of Annexin V and 7-AAD positive cells, validating the morphological changes and indicating that the most likely cell death pathway occurs via apoptosis.

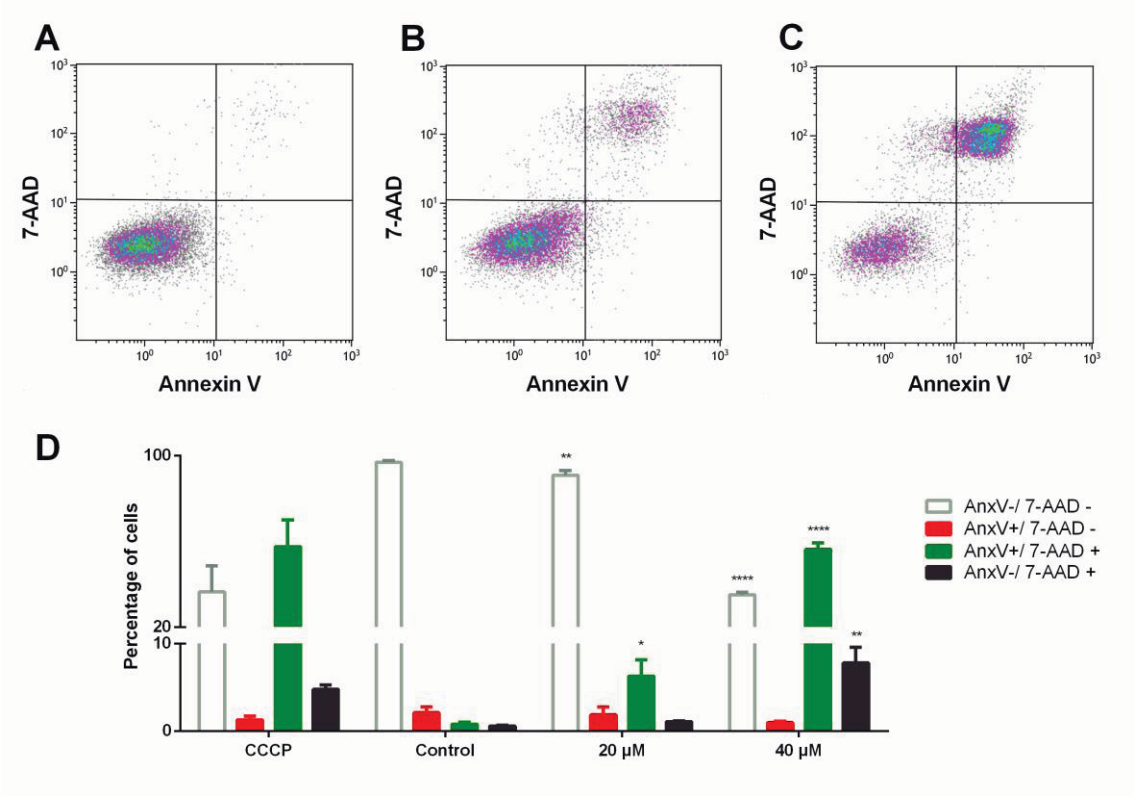

Figure 4. Assessment of 4HC-mediated apoptosis with Annexin-V externalization. Annexin-V positivitiy staining and cell membrane permeabilization were assessed using antibodies against Annexin V and the reporter 7ADD 24 h after insult with 4HC using a Gallio flow cytometer. Representative cell distribution profiles of vehicle (panel A) and cells exposed to 20 µM (panel B) or 40 µM (panel C) 4HC for assessment 24 h after insult. Lower panel D shows the combined data of 24 h post 4HC insult. In these studies the mitochondrial uncoupling agent CCCP (final concentration 100 µM) was included as a positive control. Data represent mean±SD; n=4 independent experiments. Different to the vehicle-treated (DMSO) control; *p < 0.05; **p < 0.01; ****p < 0.0001.

4HC cause disturbs in migration/proliferation and cell cycle profile: In order to determine whether 4HC treatment could influence SH-SY5Y cells migration/proliferation, a

scratch wound healing assay was carried out on a confluent cell monolayer [29]. A notable retardation in scratch healing was observed with 4HC (20-40μM) treatment (Fig. 5A) and it was concentration and time statistically significative, suggesting that 4HC significantly inhibits the migration/proliferation of human neuroblastoma cells.

The effects of 4HC on SH-SY5Y cell cycle progression was analyzed by flow cytometry (Fig. 5B). Significant changes in the cell cycle progression profile of SH-SY5Y occurred after treatment with 20 - 40 μM 4HC for 24 h. The proportion of SH-SY5Y cells in S phase decreased by ~ 7% after treatment with 20 μM 4HC, with concomitant increase of the percentage of cell in G2/M phase (~ 13%). The proportion of cells in S phase remained significantly elevated (~10%) when SH-SY5Y cells were treated with higher concentrations of 4HC (40 μM), in comparison to vehicle-control condition. These findings suggest that 4HC can influence cell proliferation by altering SH-SY5Y cell cycle transition.

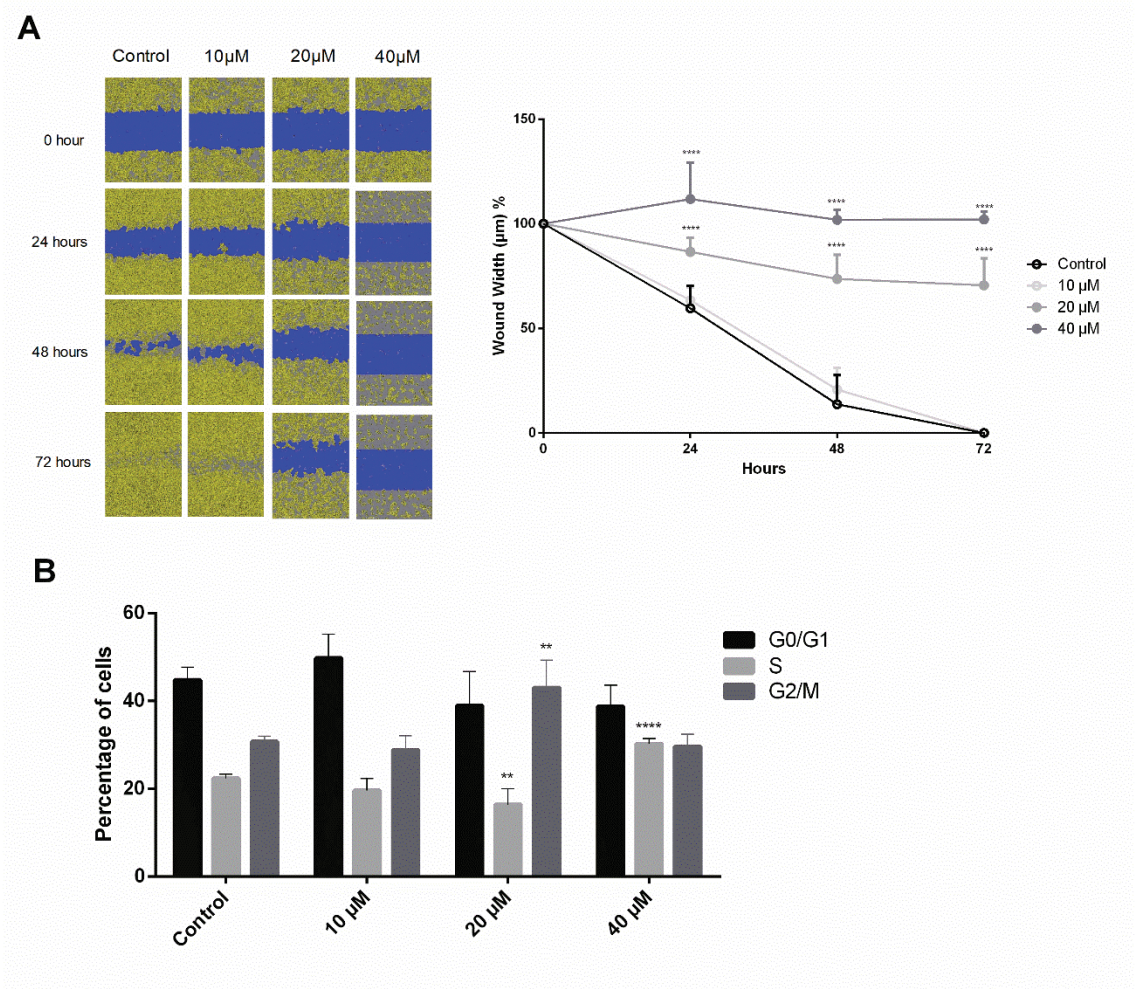

Figure 5. Assessment of cell proliferation/migration and cell cycle progression for SH-SY5Y cells after treatment with increasing concentrations of 4HC. Panel (A) representative images from IncuCyte® ZOOM Live-Cell Analysis System and combined

data showing percentage wound width determined in the scratch assay at 0, 24, 48 and 72 h after treatment of SH-SY5Y cells to increasing concentrations of 4HC. Data represent mean SD; n=2 independent experiments. (B) Cell cycle was analyzed using Muse® Cell Analyzer 24 h after treatment with diferente concentrations of 4HC. Data represent mean±SD; n=3 independent experiments. Different to the vehicle-treated (DMSO) control; **p < 0.01; ****p < 0.0001.

4HC affect mitochondrial respiratory chain: In order to investigate the effect of 4HC on mitochondrial respiratory chain, oxygen consumption was measured (Fig. 6). Basal respiration decreases by ~30% after 4HC treatment with major concentration (40 μM) when compare to control. This reduction in oxygen consumption with 4HC was maintained when glutamate was used as oxidizable substrate (~35%). Where added at 20 μM, 4HC did not significantly affect basal and Complex I respiration rates. However, when succinate was added as an oxidizable substrate to assess Complex II-phase respiration, the respiratory rate decreased by ~50% after treatment with 4HC (final concentrations 20 and 40 μM) compare to controls. These data suggest that 4HC is able to inhibit mitochondrial respiration in permeabilized SH-SY5Y cells. These effects mostly likely result from 4HC impacting on enzymatic complex activities that yield altered electron flow in the respiratory chain or ATP synthase, however, from these data it is not possible to discount potential effects on the mitochondrial membrane.

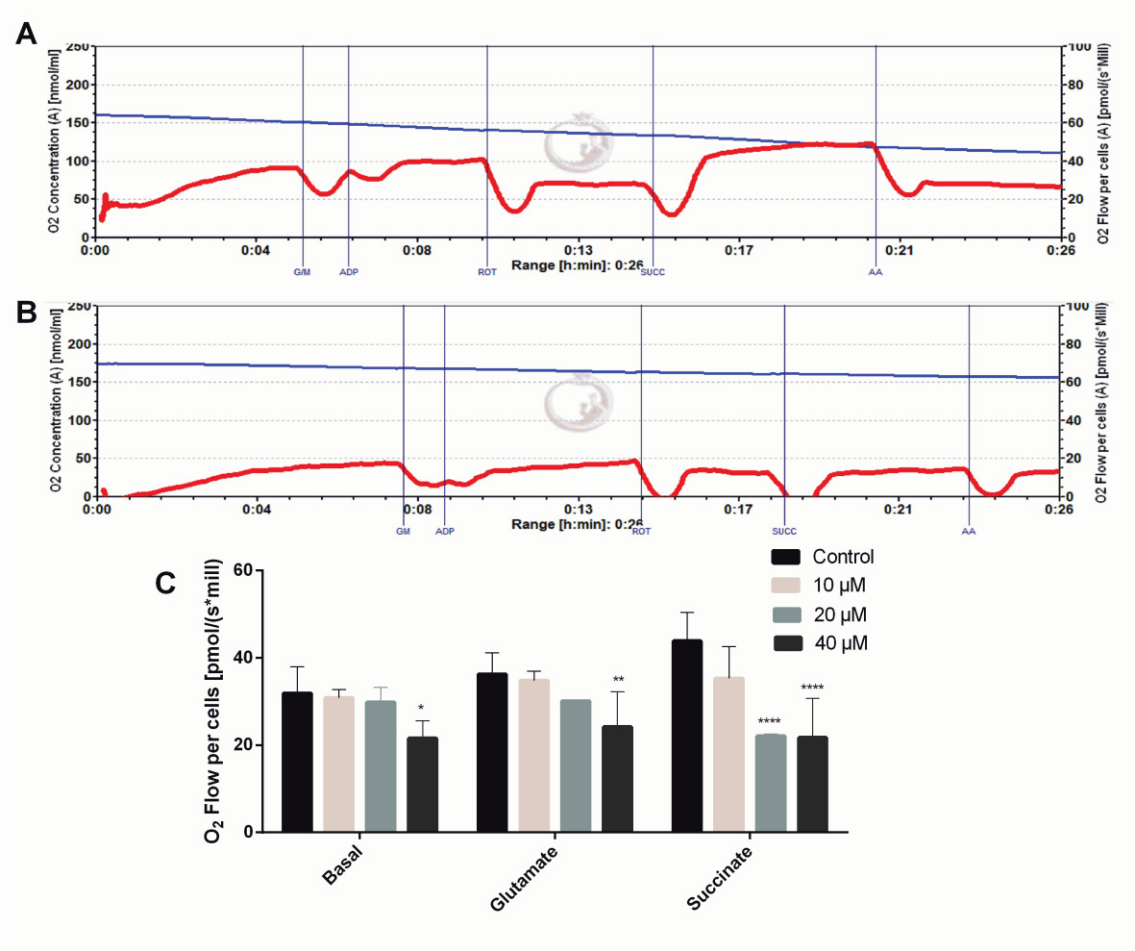

Figure 6. Respiration of SH-SY5Y cell after treatment with 4HC for 24h. Oxygen consumptions at different mitochondrial stages were measured by Oxygraph-2 k high-resolution respirometry. Simultaneous assessment of OCR is depicted in **A** (control) and **B** (40 µM 4HC) with substrates glutamate (G: 10 mM), malate (M: 1 mM), ADP (2 mM), rotenone (Rot: 1 µM), succinate (Succ: 10 mM), and antimycin A (AA: 1 µg/mL). Blue line is the decline of oxygen concentration in chamber of oxygraphy. Red line is the oxygen consumption in response to substrates for Complexes I–II. Panel (C) shows the combined data and assignment of basal, glutamate (Complex I) and succinate (Complex II). Data represent mean±SD; n=3 independent experiments each performed in duplicate. Different to the vehicle-treated (DMSO) control; *p<0.05; **p < 0.01; ****p < 0.0001.

To verify the possible effects of 4HC on mitochondria MMP (mitochondria membrane potential) cultured SH-SY-5Y cells were probed with the fluorescent dye JC-1. Our data demonstrated that neuroblastoma cells did not show significant differences in mitochondrial JC-1 fluorescence in the absence or presence of 4HC added at final concentrations 10-20 µM. However, at higher concentration 4HC (40 µM) caused significant ~50% loss of MMP relative to corresponding control (Fig. 7A), indicating a biphasic effect of the chalcone on MMP.

4HC increases ROS levels: The involvement of ROS in the effects promoted by 4HC on SH-SY5Y cells was verified by monitoring total intracellular ROS levels, using the DCFH-DA probe. Lower concentrations of 4HC (10-20 μM) did not show significant increase of ROS levels in SH-SY5Y cells relative to the control. Only when administered at 40 μM was 4HC able to significantly increase (by ~70%) accumulating ROS, in comparison to the corresponding control (Fig.7B).

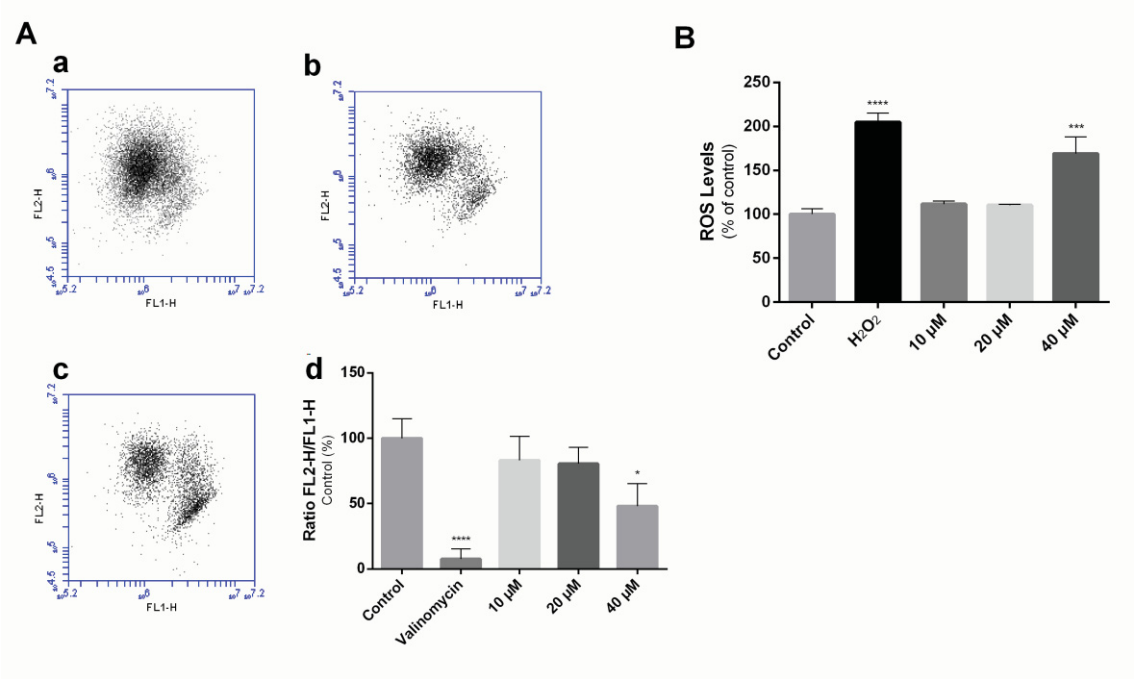

Figure 7. 4HC reduces the mitochondria membrane potential and increases ROS levels in SH-SY5Y cells. (A) Mitochondria membrane potencial was measured using JC-1 staining in SH-SY5Y cells after 4HC treatment. Fluorescence emission of FL2-H at 590 nm (indicating high membrane potential and aggregation of JC-1 dye) and FL1-H at 530 nm (indicating the collapse of membrane potential and the monomer of JC-1 dye) were measured by Flow Cytometry. Representative cell profiles of (a) vehicle treated cells and cells treated with (b) 20 μM or (c) 40 μM 4HC. Panel (d) shows the ratio of FL2-H and FL1-H. Valinomycin (final concentration 1 μM) is included as a positive control that elicits significant mitochondria membrane depolarization. (B) Intracellular ROS levels was measured using the DCFH-DA probe on SH-SY5Y cells after treatment with 4HC for 24 h. H_2O_2 (final concentration 400 μM) is included as a positive control that elicits significant ROS increases. The data were normalized using MTT assay. Data represent mean±SD; n=3 independent. Different to the vehicle-treated (DMSO) control; *p < 0.05; ***p < 0.001, ****p < 0.0001.

5.1.4. Discussion

Over 60% of neuroblastoma tumors are aggressive and become highly metastatic [5] and current therapeutic approaches including surgery, radiotherapy and chemotherapy are

not completely effective [30]. Therefore, novel therapeutic agents that kill tumor cells are highly desirable. Chalcones are potent candidates for antitumor activity due to their seemingly negligible side effects, high therapeutic index, and ease of synthesis [31]. Even though antitumor activities of 4HC have been reported in some types of cancers [18], there is a lack of information about the effects of this chalcone on neuroblastoma tumors. The current study showed that 4HC significantly decreased SH-SY5Y cell viability and proliferation / migration (Figs. 1 and 5) largely in a concentration-dependent manner. This data may be explained by a diversity of physiological disturbs in the cell as mitochondrial changes, misbalance of reducer/oxidative state, morphological damage and cell death.

Mitochondria as a target for anticancer therapies was described in HepG2 cells [32], in human corneal epithelium [33] and in rat brain [34]. Considering this available data, it is relevant that analysis of 4HC toxicology focus initially on mitochondria features. No change was observed in basal respiration nor mitochondrial membrane potential or ROS levels in SH-SY5Y cells exposed to 4HC ≤ 20 μM however, the cells are showing subtle signs of altered metabolism as shown by decreases in intracellular ATP stores and ultra-morphological analysis (Fig 1, 2 and 3). Our data also showed that 4HC added at a final concentration of 40 μM reduces basal respiration. A similar extent of inhibition is observed when succinate and 20 μM or 40 μM 4HC were used suggesting that 4HC may act as an inhibitor of enzymes of the respiratory chain, potentially targeting complexes II and V, which may contribute to the decrease synthesis of ATP detected here in the presence of the added chalcone (Figs. 1 and 7). The changes as observed in mitochondria morphology corroborated with disturbances in mitochondrial respiratory chain, confirming this organelle as a potential target for 4HC.

Our results are in agreement with those observed with other hydroxylated flavonoids (e.g. flavones and flavonols) that have already demonstrated effects on mitochondrial metabolism acting as inhibitors of the enzymes activities in respiratory chain or even on the mitochondrial membrane properties when isolated rat liver mitochondria [21] or HeLa cells [35] were used. The butein (3,4,2,4-tetrahydroxychalcone) increased mitochondrial permeability in human melanoma cells [36] and altered the mitochondrial transmembrane potential in human ovarian cancer cells [37]. Moreover, it was described uncoupling activity of the 4HC in isolated rat liver mitochondria [19]. However, this is the first time that the effects of 4HC on mitochondrial metabolism of SH-SY5Y cells are described.

Data generated in our study demonstrated an increase in ROS levels with concomitant depolarization of mitochondria membrane after treatment with 40 μM 4HC (Fig. 7), suggesting that mitochondria may be a source of ROS generation. Swelled mitochondria (Fig. 3) as described in the current study are found in cell death confirming the changes in respiratory findings. In support of this conclusion, it was reported that alterations in mitochondrial morphology has an important role in regulating ROS [38] and ATP levels [39]. Furthermore, ROS production is known to promote further mitochondrial and cellular damage in an injurious cycle [40]. Sabzevari and colleagues [41] have suggested that chalcone cytotoxicity on tumor cells likely stems from an ability to promote mitochondrial dysfunction, which can be linked, at least in part, to the promotion of cell death via intrinsic pathways.

It was also identified that cell cycle and migration/ proliferation (Fig. 5) were changed, indicating that the alteration of SH-SY5Y cell cycle promoted by 4HC can influence cell proliferation. Also, it was previously reported that another chalcone, butein, increases G2/M phase and induces apoptosis in human hepatoma cancer cells (HepG2 and Hep3B) through ROS generation [42]. The current data suggest also a similar mechanism as ROS generation was stimulated by 4HC exposure.

In general, morphological effects, as described, are the reflex that all cellular mechanisms failure to cell survives. The alterations in chromatin showed behind cells death important cytotoxic effect that can induce other disturbs, like alteration of proteins and enzymes expression, leading for example to the decrease in cellular viability. Additionally, the cytoplasmic vacuolization as observed may represent a failure in the mechanism of cytoskeleton organization leading to both accumulation of cellular production or uncompleted lysosomal digestion.

Of specific interest is the increased number of exosomal vesicles detected upon exposure of cultures SH-SY5Y cells with the higher concentrations of 4HC. According to Isola and colleagues [43], exosomes are naturally occurring as small membranes enclosed microvesicles with a characteristic size 30 – 120 nm diameter, which are released by various cells types. These cellular structures may also be related with treatment resistance in cancer cells [44]. In this regard, the gradual 4HC-dose dependent increase in exosome production by cells could be explained by the cell attempting to eliminate 4HC. While this assumed effort to eliminate the xenobiotic resulted in a delayed cell death (in the presence of ≤ 20

μM), this mechanism was eventually overwhelmed and unable to eliminate sufficient drug to avoid the toxic effects at higher 4HC concentrations.

These results and the ultrastructure changes observed in SH-SY5Y cells as nuclear alterations, cytoskeleton impairment and other morphological findings as cytoplasmic vacuolation are described as strong evidences of cell death through a pro-apoptotic mechanism (Figure 3 D). Furthermore, loss of cell viability was accompanied primarily by increase of phosphatidylserine exposure on the surface of cells (Fig. 4), indicating that the flavonoid likely induces the intrinsic mitochondrial apoptotic pathway in SH-SY5Y cells.

Chalcones are effective inducers of apoptosis by different pathways [31] and mitochondrial dysfunction could result in the activation of this type of death. Moreover, it should also be noted that hydroxy groups play a crucial role in the cytotoxic [41] and apoptotic effects [45] of chalcones. It has been described that xanthoangelol (3'-C-geranyl-2',4,4'-trihydroxychalcone) induces the mitochondrial apoptotic pathway in human chronic myelogenous leukemia (K562 cells) [46]. In neuroblastoma model, isobavachalcone (2',4',4-trihydroxy-3'-prenylchalcone) induced apoptosis on IMR-32 and NB-39 cells. In addition, isobavachalcone also demonstrated selective effect against non-tumoral cells (cerebellar granule cells) [47].

The present study demonstrated in first time that 4HC inhibited the growth of neuroblastoma cells and probably mitochondrial dysfunctional is involved in the action mechanism. Furthermore, the results suggest that the effects of this chalcone on cell proliferation, ROS levels and oxygen consumption contributed to the observed cytotoxic effects of 4HC on SH-SY5Y cells. Finally, the current findings suggest that 4HC is a promising molecule to studies as potential anticancer agent for treatment of neuroblastoma tumor.

5.1.5. Acknowledgement

We acknowledge funding from the Australian Research Council (Discovery grants DP130103711 and DP160102063 to PKW); funding from the Sydney Medical School, The University of Sydney and the award of a Brazilian Science Exchange Scholarship (CNPq) to SJME as part of the Science without Borders initiative. We also acknowledge the assistance of Mrs Shirley Nakhla and the Bosch Institute Live Cell Analysis Facility, The University of Sydney.

5.1.6. References

[1] J.R. Park, A. Eggert, H. Caron, Neuroblastoma: Biology, Prognosis, and Treatment, Hematology/Oncology Clinics of North America, 24 (2010) 65-86.
[2] H. Sidhar, R.K. Giri, Induction of Bex genes by curcumin is associated with apoptosis and activation of p53 in N2a neuroblastoma cells, Scientific Reports, 7 (2017).
[3] I. Penna, A. Gigoni, D. Costa, S. Vella, D. Russo, A. Poggi, F. Villa, A. Brizzolara, C. Canale, A. Mescola, A. Daga, C. Russo, M. Nizzari, T. Florio, P. Menichini, A. Pagano, The inhibition of 45A ncRNA expression reduces tumor formation, affecting tumor nodules compactness and metastatic potential in neuroblastoma cells, Oncotarget, 8 (2017) 8189-8205.
[4] D. Tibullo, C. Giallongo, F. Puglisi, D. Tomassoni, G. Camiolo, M. Cristaldi, M.V. Brundo, C.D. Anfuso, G. Lupo, T. Stampone, G. Li Volti, F. Amenta, R. Avola, V. Bramanti, Effect of Lipoic Acid on the Biochemical Mechanisms of Resistance to Bortezomib in SH-SY5Y Neuroblastoma Cells, Molecular Neurobiology, (2017) 1-7.
[5] N.K.V. Cheung, M.A. Dyer, Neuroblastoma: Developmental Biology, Cancer Genomics, and Immunotherapy, Nat Rev Cancer, 13 (2013) 397-411.
[6] M.A. Smith, S.F. Altekruse, P.C. Adamson, G.H. Reaman, N.L. Seibel, Declining childhood and adolescent cancer mortality, Cancer, 120 (2014) 2497-2506.
[7] X.-M. Chen, A.R. Tait, D.D. Kitts, Flavonoid composition of orange peel and its association with antioxidant and anti-inflammatory activities, Food Chemistry, 218 (2017) 15-21.
[8] H. Zhang, R. Tsao, Dietary polyphenols, oxidative stress and antioxidant and anti-inflammatory effects, Current Opinion in Food Science, 8 (2016) 33-42.
[9] V.C. George, G. Dellaire, H.P.V. Rupasinghe, Plant flavonoids in cancer chemoprevention: role in genome stability, The Journal of nutritional biochemistry, 45 (2017) 1-14.
[10] D.J. Dorta, A.A. Pigoso, F.E. Mingatto, T. Rodrigues, C.R. Pestana, S.A. Uyemura, A.C. Santos, C. Curti, Antioxidant activity of flavonoids in isolated mitochondria, Phytotherapy research : PTR, 22 (2008) 1213-1218.
[11] S. Wen, D. Zhu, P. Huang, Targeting cancer cell mitochondria as a therapeutic approach, Future Medicinal Chemistry, 5 (2012) 53-67.
[12] X. Gao, B. Schottker, Reduction-oxidation pathways involved in cancer development: a systematic review of literature reviews, Oncotarget, (2017).
[13] D.K. Mahapatra, S.K. Bharti, V. Asati, Anti-cancer chalcones: Structural and molecular target perspectives, European journal of medicinal chemistry, 98 (2015) 69-114.
[14] M.K. Pandey, S.K. Sandur, B. Sung, G. Sethi, A.B. Kunnumakkara, B.B. Aggarwal, Butein, a tetrahydroxychalcone, inhibits nuclear factor (NF)-kappaB and NF-kappaB-regulated gene expression through direct inhibition of IkappaBalpha kinase beta on cysteine 179 residue, The Journal of biological chemistry, 282 (2007) 17340-17350.
[15] S.Y. Kim, I.-S. Lee, A. Moon, 2-Hydroxychalcone and xanthohumol inhibit invasion of triple negative breast cancer cells, Chemico-Biological Interactions, 203 (2013) 565-572.
[16] G.S. Zhou, L.J. Song, B. Yang, Isoliquiritigenin inhibits proliferation and induces apoptosis of U87 human glioma cells in vitro, Molecular medicine reports, 7 (2013) 531-536.
[17] Y.M. Lee, D.Y. Lim, H.J. Choi, J.I. Jung, W.Y. Chung, J.H. Park, Induction of cell cycle arrest in prostate cancer cells by the dietary compound isoliquiritigenin, Journal of medicinal food, 12 (2009) 8-14.

[18] B. Orlikova, D. Tasdemir, F. Golais, M. Dicato, M. Diederich, The aromatic ketone 4′-hydroxychalcone inhibits TNFα-induced NF-κB activation via proteasome inhibition, Biochemical pharmacology, 82 (2011) 620-631.
[19] L.C. Martineau, Large enhancement of skeletal muscle cell glucose uptake and suppression of hepatocyte glucose-6-phosphatase activity by weak uncouplers of oxidative phosphorylation, Biochim Biophys Acta, 1820 (2012) 133-150.
[20] D.J. Dorta, A.A. Pigoso, F.E. Mingatto, T. Rodrigues, I.M. Prado, A.F. Helena, S.A. Uyemura, A.C. Santos, C. Curti, The interaction of flavonoids with mitochondria: effects on energetic processes, Chem Biol Interact, 152 (2005) 67-78.
[21] P. Dabaghi-Barbosa, A. Mariante Rocha, A. Franco da Cruz Lima, B. Heleno de Oliveira, M. Benigna Martinelli de Oliveira, E. Gunilla Skare Carnieri, S.M.S.C. Cadena, M. Eliane Merlin Rocha, Hispidulin: Antioxidant properties and effect on mitochondrial energy metabolism†, Free Radical Research, 39 (2005) 1305-1315.
[22] T. Mosmann, Rapid colorimetric assay for cellular growth and survival: application to proliferation and cytotoxicity assays, Journal of immunological methods, 65 (1983) 55-63.
[23] E.S. Reynolds, The use of lead citrate at high pH as an electron-opaque stain in electron microscopy, The Journal of cell biology, 17 (1963) 208-212.
[24] Y. Cui, P. Lu, G. Song, Q. Liu, D. Zhu, X. Liu, Involvement of PI3K/Akt, ERK and p38 signaling pathways in emodin-mediated extrinsic and intrinsic human hepatoblastoma cell apoptosis, Food Chem. Toxicol., 92 (2016) 26-37.
[25] X. Yuan, B. Zhang, L. Gan, Z.H. Wang, B.C. Yu, L.L. Liu, Q.S. Zheng, Z.P. Wang, Involvement of the mitochondrion-dependent and the endoplasmic reticulum stress-signaling pathways in isoliquiritigenin-induced apoptosis of HeLa cell, Biomedical and environmental sciences : BES, 26 (2013) 268-276.
[26] X.S. Wan, Z. Zhou, A.R. Kennedy, Adaptation of the dichlorofluorescein assay for detection of radiation-induced oxidative stress in cultured cells, Radiation research, 160 (2003) 622-630.
[27] M.M. Bradford, A rapid and sensitive method for the quantitation of microgram quantities of protein utilizing the principle of protein-dye binding, Analytical biochemistry, 72 (1976) 248-254.
[28] O.R. Koechli, B.U. Sevin, J.P. Perras, R. Angioli, M. Untch, A. Steren, C. Ramachandran, H.E. Averette, Comparative chemosensitivity profiles in three human breast cancer cell lines with the ATP-cell viability assay, Oncology, 51 (1994) 552-558.
[29] S.T. Johnston, E.T. Shah, L.K. Chopin, D.L. Sean McElwain, M.J. Simpson, Estimating cell diffusivity and cell proliferation rate by interpreting IncuCyte ZOOM™ assay data using the Fisher-Kolmogorov model, BMC Systems Biology, 9 (2015) 1-13.
[30] C.U. Louis, J.M. Shohet, Neuroblastoma: molecular pathogenesis and therapy, Annual review of medicine, 66 (2015) 49-63.
[31] R. Sharma, R. Kumar, R. Kodwani, S. Kapoor, A. Khare, R. Bansal, S. Khurana, S. Singh, J. Thomas, B. Roy, R. Phartyal, S. Saluja, S. Kumar, A Review on Mechanisms of Anti Tumor Activity of Chalcones, Anti-cancer agents in medicinal chemistry, 16 (2015) 200-211.
[32] K.G. Lima, G.C. Krause, E.F.G. da Silva, L.L. Xavier, L.A.M. Martins, L.M. Alice, L.B. da Luz, R.B. Gassen, E.C. Filippi-Chiela, G.V. Haute, M.C.R. Garcia, G.A. Funchal, L. Pedrazza, C.K. Reghelin, J.R. de Oliveira, Octyl gallate reduces ATP levels and Ki67 expression leading HepG2 cells to cell cycle arrest and mitochondria-mediated apoptosis, Toxicol In Vitro, 48 (2018) 11-25.
[33] M. Shan, T.J. Fan, Cytotoxicity of carteolol to human corneal epithelial cells by inducing apoptosis via triggering the Bcl-2 family protein-mediated mitochondrial pro-apoptotic pathway, Toxicol In Vitro, 35 (2016) 36-42.

[34] G. Jevtic, T. Nikolic, A. Mircic, T. Stojkovic, M. Velimirovic, V. Trajkovic, I. Markovic, A.M. Trbovich, N.V. Radonjic, N.D. Petronijevic, Mitochondrial impairment, apoptosis and autophagy in a rat brain as immediate and long-term effects of perinatal phencyclidine treatment - influence of restraint stress, Progress in neuro-psychopharmacology & biological psychiatry, 66 (2016) 87-96.
[35] T. Herrerias, A.A. Oliveira, M.L. Belem, B.H. Oliveira, E.G.S. Carnieri, S.M.S.C. Cadena, G.R. Noleto, G.R. Martinez, M.B.M. Oliveira, M.E.M. Rocha, Effects of natural flavones on membrane properties and citotoxicity of HeLa cells, Revista Brasileira Farmacognologia, 20 (2010) 403-408.
[36] Z. Cui, E. Song, D.N. Hu, M. Chen, R. Rosen, S.A. McCormick, Butein induces apoptosis in human uveal melanoma cells through mitochondrial apoptosis pathway, Current eye research, 37 (2012) 730-739.
[37] P.Y. Yang, D.N. Hu, I.C. Lin, F.S. Liu, Butein Shows Cytotoxic Effects and Induces Apoptosis in Human Ovarian Cancer Cells, The American journal of Chinese medicine, 43 (2015) 769-782.
[38] Y. Wang, Y. Nartiss, B. Steipe, G.A. McQuibban, P.K. Kim, ROS-induced mitochondrial depolarization initiates PARK2/PARKIN-dependent mitochondrial degradation by autophagy, Autophagy, 8 (2012) 1462-1476.
[39] P. Paumard, J. Vaillier, B. Coulary, J. Schaeffer, V. Soubannier, D.M. Mueller, D. Brèthes, J.P. di Rago, J. Velours, The ATP synthase is involved in generating mitochondrial cristae morphology, The EMBO Journal, 21 (2002) 221-230.
[40] D.B. Zorov, M. Juhaszova, S.J. Sollott, Mitochondrial ROS-induced ROS release: an update and review, Biochim Biophys Acta, 1757 (2006) 509-517.
[41] O. Sabzevari, G. Galati, M.Y. Moridani, A. Siraki, P.J. O'Brien, Molecular cytotoxic mechanisms of anticancer hydroxychalcones, Chemico-Biological Interactions, 148 (2004) 57-67.
[42] D.O. Moon, M.O. Kim, Y.H. Choi, J.W. Hyun, W.Y. Chang, G.Y. Kim, Butein induces G(2)/M phase arrest and apoptosis in human hepatoma cancer cells through ROS generation, Cancer Lett, 288 (2010) 204-213.
[43] A.L. Isola, K. Eddy, S. Chen, Biology, Therapy and Implications of Tumor Exosomes in the Progression of Melanoma, Cancers, 8 (2016).
[44] K.G. Chen, J.C. Valencia, B. Lai, G. Zhang, J.K. Paterson, F. Rouzaud, W. Berens, S.M. Wincovitch, S.H. Garfield, R.D. Leapman, V.J. Hearing, M.M. Gottesman, Melanosomal sequestration of cytotoxic drugs contributes to the intractability of malignant melanomas, Proceedings of the National Academy of Sciences, 103 (2006) 9903-9907.
[45] A.N. Pande, S. Biswas, N.D. Reddy, B. Jayashree, N. Kumar, C.M. Rao, In vitro and in vivo anticancer studies of 2'-hydroxy chalcone derivatives exhibit apoptosis in colon cancer cells by HDAC inhibition and cell cycle arrest, EXCLI Journal, 16 (2017) 448-463.
[46] Y. Teng, L. Wang, H. Liu, Y. Yuan, Q. Zhang, M. Wu, L. Wang, H. Wang, Z. Liu, P. Yu, 3'-Geranyl-mono-substituted chalcone Xanthoangelovl induces apoptosis in human leukemia K562 cells via activation of mitochondrial pathway, Chem Biol Interact, 261 (2017) 103-107.
[47] R. Nishimura, K. Tabata, M. Arakawa, Y. Ito, Y. Kimura, T. Akihisa, H. Nagai, A. Sakuma, H. Kohno, T. Suzuki, Isobavachalcone, a chalcone constituent of Angelica keiskei, induces apoptosis in neuroblastoma, Biological & pharmaceutical bulletin, 30 (2007) 1878-1883.

5.2 ANTI-PROLIFERATIVE AND CYTOTOXIC ACTIVITIES OF THE FLAVONOID ISOLIQUIRITIGENIN IN THE HUMAN NEUROBLASTOMA CELL LINE SH-SY5Y

Stephane J. de M. Escobar,[1,2] Genevieve M. Fong,[2] Sheila M. B. Winnischofer,[1] Martin Simone,[2] Lenka Munoz,[3] Joanne M. Dennis,[2] Maria Eliane M. Rocha,[1] Paul K. Witting[2,*]

[1]Department of Biochemistry and Molecular Biology, Federal University of Paraná, Curitiba, PR, Brazil

[2]Redox Biology and [3]Neuropharmacology Groups, Discipline of Pathology, The University of Sydney, Sydney, NSW 2006, Australia

ABSTRACT

Neuroblastoma is a common childhood cancer with high mortality. We evaluated the capacity of the flavonoid, isoliquiritigenin (4,2',4'-trihydroxychalcone; ISL) to inhibit cellular proliferation and migration in the human neuroblastoma cell line SH-SY5Y. Incubation of cultured SH-SY5Y cells with 10-100 μM ISL (24 h) decreased cell confluency and depleted intracellular ATP relative to the vehicle-treated control. ISL-mediated cell toxicity did not involve intracellular caspase 3/7 activation or externalization of phosphatidylserine on the cell membrane, all indicating that the flavonoid did not induce apoptosis. By contrast, an inhibitor of necroptosis, necrostatin-1, significantly restored ATP levels in ISL-treated neuroblastoma cells indicative of enhanced viability. In addition, ISL treatment inhibited SH-SY5Y cell migration/proliferation in a scratch assay and arrested cell cycle transition by significantly decreasing the number of cells in G0/G1 phase and increasing populations in S (primarily) and G2/M (lesser extent) phases. The intracellular ratio of phosphorylated/total ERK 1/2 and p38 remained unchanged after ISL treatment (up to 40 μM); ERK activation was only determined at ISL dose well above the experimental EC_{50} value as judged by ELISA analyses and this did not correlate with ISL cytotoxicity at lower dose <40 μM; Western blot assay confirmed the detection of phosphorylated (p-)ERK1/2 and (p-)p38 in ISL treated cells. Together the results suggest that ISL exerts anti-proliferative and cytotoxic activity on SHSY5Y cells through the loss of ATP, induction of cell cycle arrest, and cell death largely via a necroptotic mechanism in the absence of apoptosis.

5.2.1. Introduction

Neuroblastoma is a childhood cancer of the sympathetic nervous system originating in the adrenal medulla or paraspinal tissue. It is the most common childhood extracranial solid tumor and also the most common childhood cancer to be diagnosed in the first year of life. Neuroblastoma affects up to 700 children per year in the United States and accounts for 10-20% of all malignant cancers in children < 5 years [1]. Neuroblastoma disease is diverse in clinical presentation, largely sporadic and markedly heterogeneous, ranging from spontaneous regression to recalcitrant tumor progression making prognosis difficult. Over 60% of neuroblastoma tumors are aggressive and become highly metastatic [2] and current therapeutic approaches including surgery, radiotherapy and chemotherapy are not completely effective [3]. Hence, mortality amongst children with high-risk relapse neuroblastoma remains unacceptably high and novel therapies to address long-term survival rates are urgently required [4].

Screening natural source compounds for anti-proliferative and anti-tumor activities may identify novel therapeutics for neuroblastoma and other cancers [5]. Of particular interest is the targeted use of natural compounds to activate programmed cell death pathways that control cell survival and proliferation. Programmed cell death is important in many physiological processes but alterations thereof are implicated in cancer [6]. For example, it is widely accepted that defective apoptosis pathways promote malignancy by allowing transformed cells to evade death. The potential to exploit cell death pathways for therapeutic advantage has stimulated screening and development of natural compounds that decrease cancer cell viability through pro-apoptotic activities [7, 8] or other pathways. More recently, necroptosis has been described as a programmed cell necrosis pathway without active caspase involvement [9]. Several natural compounds induce necroptosis in malignant cells including green tea polyphenols [10] and shikonin [11].

Flavonoids are endogenous plant polyphenols that exhibit several biological activities including anti-cancer activity [5]. The chalcone subclass of flavonoids are pharmacologically active and show anti-inflammatory [12], anti-oxidative [13] and anti-cancer [14, 15] properties *in vitro* and *in vivo*. Several chalcones exert anti-cancer activity by promoting apoptotic cell death [16, 17], modifying cell signal transduction [18, 19] and inducing cell cycle arrest [8, 20, 21].

Isoliquiritigenin (*trans*-4,2',4'-trihydroxychalcone; ISL, Figure 1A is a chalcone analogue found abundantly in the licorice plant (*Glycyrrhiza uralensis)*, shallot and bean sprouts [22]. ISL is reported to have several useful pharmacological properties including anti-inflammatory, anti-oxidative, anti-diabetic and cardio-protective effects [23-25]. ISL also exhibits significant anti-tumor activities through the inhibition of proliferation and blockage of cell cycle progression at the S and G2/M phases in cultured glioma and prostate cancer cells [26, 27]. Interestingly, ISL selectively inhibits the proliferation of prostate cancer cells compared with normal epithelial cells [28] suggesting that it may be cytotoxic to a variety of cancer cells but relatively benign to normal cell types; a desirable characteristic in chemotherapeutics. Other studies also demonstrate the selective toxicity with ISL inhibiting

murine breast cancer growth and neo-angiogenesis in xenograft models with relatively little toxicity toward vascular endothelial cells [8, 29].

The aim of the present work is to evaluate the cytotoxic activity of ISL in the human neuroblastoma cell line SH-SY5Y. Our data indicate that ISL effectively depleted intracellular ATP concentrations and significantly decreased SH-SY5Y cell viability, proliferation and migration. This cytotoxic activity of ISL was associated with cell cycle arrest and induction of the programmed cell death pathway, necroptosis that was independent of markers of apoptosis including caspase 3/7 activity and externalization of phosphatidylserine at the cell membrane.

5.2.2. Materials and Methods

5.2.2.1 Chemicals

Unless specified, all general biochemicals were of the highest quality available and sourced commercially from Sigma (Sydney, Australia). Isoliquiritigenin (*trans*-4,2',4'-trihydroxychalcone), dimethyl sulfoxide (DMSO), necrostatin-1 and materials for cell culture were sourced from Sigma (Sydney, Australia). All buffers were prepared in MilliQ water and adjusted to physiological pH (7.4) prior to use.

5.2.2.2 Cell Culture and Treatment

Human neuroblastoma (SH-SY5Y) cells were obtained from CellBank Australia (Sydney, Australia) seeded at 2 x 10^5 cells/mL in a 6-well plate and grown to confluence at 37°C under 5% $CO_{2\,(g)}$ atmosphere in Dulbecco's Modified Eagle's Medium/Ham's Nutrient Mixture F12 (DMEM/F12) containing 10% v/v fetal bovine serum, 100 U/mL penicillin, 100 µg/mL streptomycin, 2.5 mM L-glutamine and 1x non-essential amino acid solution. Cultured cells were routinely assessed for mycoplasma using the MycoAlert™ PLUS Mycoplasma Detection Kit (Lonza, Sydney, Australia); all cells employed in this study were free of mycoplasma contamination. Confluent SH-SY5Y cells were treated in the presence or absence of ISL (final concentration 10 – 100 µM) for 24 h. In some studies, SH-SY5Y cells were pre-incubated for 2 h with necrostatin-1 (final concentration 50 µM; this concentration selectively inhibits necroptosis [30]) before supplementation with ISL to assess the effects of the flavonoid on cell death pathways.

5.2.2.3 Measurement of Cell Viability

Cell counting. After treatment, cells were treated with 1 x trypsin-EDTA (5 min, 37 °C) and the cell pellet collected by centrifugation (365 x *g*, 5 min), suspended in PBS and mixed 1:1 v/v with trypan blue. Viable cells were routinely quantified using the trypan blue exclusion

assay as determined with a BioRad TC10 automated cell counter (Bio-Rad, Sydney, Australia).

Confluence. Cells were treated with ISL (0 – 100 µM) or DMSO 0.1% (as control), and the 6-well culture plate was imaged using the IncuCyte™ ZOOM instrument (Essen BioScience, Australia) to assess proliferation by real-time imaging. Data were analyzed using the IncuCyte's built-in Confluence Processing analysis tool (*v*1.5), which quantified areal cell coverage and the level of confluence as independent measures of viability.

Intracellular ATP concentration. After treatment with vehicle or ISL (at the indicated dose), cells were isolated and the levels of ATP were determined with a commercial kit as per the manufacturer's instructions (Perkin Elmer, Melbourne, Australia). Briefly, SH-SY5Y cells were cultured in 96-well plates and treated with ISL (0–100 µM) at 37 °C. After 24 h, cells were treated with 50 µL of mammalian cell lysis buffer (100 µL) and the entire plate was shaken (700 r.p.m.) for 5 min. Cell lysates were mixed with 50 µL of substrate solution, the mixture agitated for 5 min and then incubated in the dark (10 min). Total ATP content was then measured by assessing levels of luminescence with an Infinite® 200 PRO TECAN plate reader (Tecan Group Ltd., Männedorf, Switzerland). Finally, all data was normalized to corresponding total cell protein determined in cell lysates with the Bicinchoninic Acid assay®.

5.2.2.4 Measurement of Caspase 3/7 activity

Cultured SH-SY5Y cells were exposed to vehicle (DMSO control) or 0-100 µM of ISL as described above. After 24 h, the cells were analyzed for early and late-stage apoptosis and cell death using a Muse Caspase-3/7 kit and Muse Cell Analyzer (Merck Millipore, Sydney, Australia) according to the manufacturer's instructions. This assay permits simultaneous evaluation of apoptotic status based on caspase-3/7 activation and membrane permeabilization (surrogate for total cell death). The assay provides plots of the relative percentage of cells that are live (7-AAD negative, apoptosis negative), caspase-3/7 (7-AAD negative, caspase-3/7 positive), apoptotic/dead (7-AAD positive, caspase-3/7 positive) or dead (7-AAD positive, caspase-3/7 negative).

5.2.2.5 Measurement of apoptosis with Annexin V binding to phosphatidylserine

Externalization of phosphatidylserine was used to complement assessments of apoptosis by monitoring of caspase activation in cultured cells. Thus, SH-SY5Y cells were exposed to vehicle (DMSO control) or 60 µM of ISL as described above; the mitochondrial uncoupling agent carbonyl cyanide m-chlorophenyl hydrazone (CCCP) as positive control. After 12 or 24 h, media was aspirated and collected and each well was treated with 0.25% w/v trypsin for 10 min at 37 °C. Each well was then treated with 1 mL PBS (calcium-free solution) containing 10% v/v FBS and 4 mM EDTA and the isolated cells were combined with the previously collected media, and centrifuged at 200 x g for 5 min followed by resuspension in 2 mL cold PBS (EDTA-free solution) and then another centrifugation step at 200 x g for 5 min. Each resultant cell pellet was immediately dispersed in 100 µL 1x Abcam Flow buffer

that contained the following additives: 5 µL Annexin V-CF Blue and 5µL 7-AAD as per the manufacturer's protocol (Abcam Apoptosis Detection Kit; ab214663). This method of cell isolation and labeling was necessary to yield a non-aggregated suspension of single cells suitable for flow cytometric analysis. Finally, the cells were analyzed for the proportion of intact live cells (Annexin V-CF Blue negative, 7-AAD Staining Solution negative), early apoptotic (Annexin V-CF Blue positive, 7-AAD Staining Solution negative) and late apoptotic or necrotic cells (Annexin V-CF Blue positive, 7-AAD Staining Solution positive) with a Gallios Flow Cytometer (Beckman-Coulter, Lakeview Parkway, IN) and using Kaluza Analysis Software (Beckman Coulter). Finally, numerical data was exported to MSExcel for quantitation.

5.2.2.6 Cell Migration/Proliferation Assay

Migration/Proliferation was determined using a cell scratch assay with real-time monitoring using the IncuCyte™ ZOOM live cell imaging system (Essen BioScience, Sydney, Australia). This system measures scratch closure and calculates the wound width within the area at each time point. A WoundMaker™ (Essen BioScience, Sydney, Australia) tool was used to create uniform, reproducible injury in a 96-well plate containing SH-SY5Y cells. After injury, the medium was aspirated and the wells were washed with PBS to remove any floating cells/cell debris. Next, the cells were treated with vehicle (DMSO) or ISL (0–60 µM) in the media, and cells sub-cultured at 37°C and imaged 24, 48 and 72 h-post injury.

5.2.2.7 Cell Cycle Analysis

Cell cycle analysis was performed with a Muse™ Cell Analyzer (Merck Millipore, Sydney, Australia) following manufacturer's instruction. Briefly, SH-SY5Y cells were treated with vehicle (DMSO) or ISL (at the final dose indicated). After a further 24 h incubation, control and ISL treated-cells were harvested by trypsin digestion and centrifuged; the resultant cell pellet was washed in PBS, permeabilized using Triton X-100 (0.1%) and stained with propidium iodide (PI). Cells were then incubated for 30 min at 20°C in the dark. After staining, the cells were processed for cell cycle analysis and data was reported as a percentage of cells in G0/G1, S and G2/M phases.

5.2.2.8 Assessing intracellular protein concentration with ELISA

Cultured SH-SY5Y cells were treated with vehicle (DMSO) or with ISL (0-60 µM) and the levels of phosphorylated proteins *p*-p38 (relative to total p38) and ERK 1/2 (relative to total ERK) were determined in cell pellets using respective commercial ELISA kits (Abcam, Sydney, Australia) following manufacturer's instructions.

5.2.2.9 Western Blotting

Western blot analyses were performed as described in detail elsewhere [31]. Briefly, cell lysates were added 30µg/µL of protein and then loaded onto commercial IN-GEL (BioRad, Sydney Auistralia) SDS-PAGE, separated, transferred to polyvinylidene difluoride (PVDF) membranes, and assessed for the following phosphorylated proteins LC3B I/II (Genesearch, Sydney Australia; primary antibody final dilution 1:2000 v/v), ERK 1/2 (Genesearch, Sydney Australia; *p*-44/42 MAPK; primary antibody final dilution 1:1000 v/v) and p38 (Genesearch, Sydney Australia; *p*-180/182 MAPK; primary antibody final dilution 1:2000 v/v) and probed using appropriate secondary antibodies (Cell Signaling Technology, Sapphire Biosciences, Sydney, Australia). Images were captured and analyzed using the ChemiDoc MP imaging system (Bio-Rad, Sydney, Australia) and ImageLab software (version 4.1, Bio-Rad, Sydney, Australia). In all cases, stain-free images of all protein bands were obtained prior to protein transfer. Corresponding images were used to verify equal loading of total protein onto the various lanes after SDS-PAGE separation as assayed with Image J (v1.5i; freeware available at *https://imagej.nih.gov/ij*). Total protein assessed in each lane was then employed for the normalization of the corresponding specific proteins detected by Western blotting in the same lane.

5.2.2.10 Statistical Analyses

Experimental data was expressed as mean ± SD; n=3 or 4 independent cell experiments as specified in figure legends. Comparisons between groups were performed with Prism Software (version 6.07, GraphPad Software Inc, San Diego, CA). All quantitative data were analyzed using one-way ANOVA with Tukey's post-hoc analysis for comparisons between treatments and control. Statistical significance was accepted at the $p<0.05$ level.

5.2.3. Results

The effect of ISL on neuroblastoma cell viability was assessed in SH-SY5Y cells using several parameters to distinguish cell death pathways such as apoptosis, autophagy and necrosis; for reference the chemical structure for ISL is shown in Fig. 1A. Initial viability measurements included determination of trypan blue exclusion, cell confluence and intracellular ATP concentration (Fig. 1B-D). Incubation of SH-SY5Y cells with ISL (20-100 µM) for 24 h significantly decreased cell viability by ~15-45% and cell confluence by ~15-70%, respectively (Fig. 1B, C). Consistent with this demonstrable loss in viability, ATP concentration was depleted significantly by ~15% in cells incubated with 10 µM ISL and ranged up to ~90% ATP depletion in cells exposed to 100 µM ISL (Fig. 1D). Intracellular ATP levels indicate the metabolic condition of viable cells, moreover, it is a reproducible and practicable method to assess drug response in cell lines [32]. So, ATP levels were used to determine an EC_{50} for the treatment with ISL. Thus, 24 h after incubation of SH-SY5Y cells with ISL the EC_{50} (Effective concentration of 50%) was determined to be 25.4 µM (Fig. 1D inset; note the log scale used for ISL concentration).

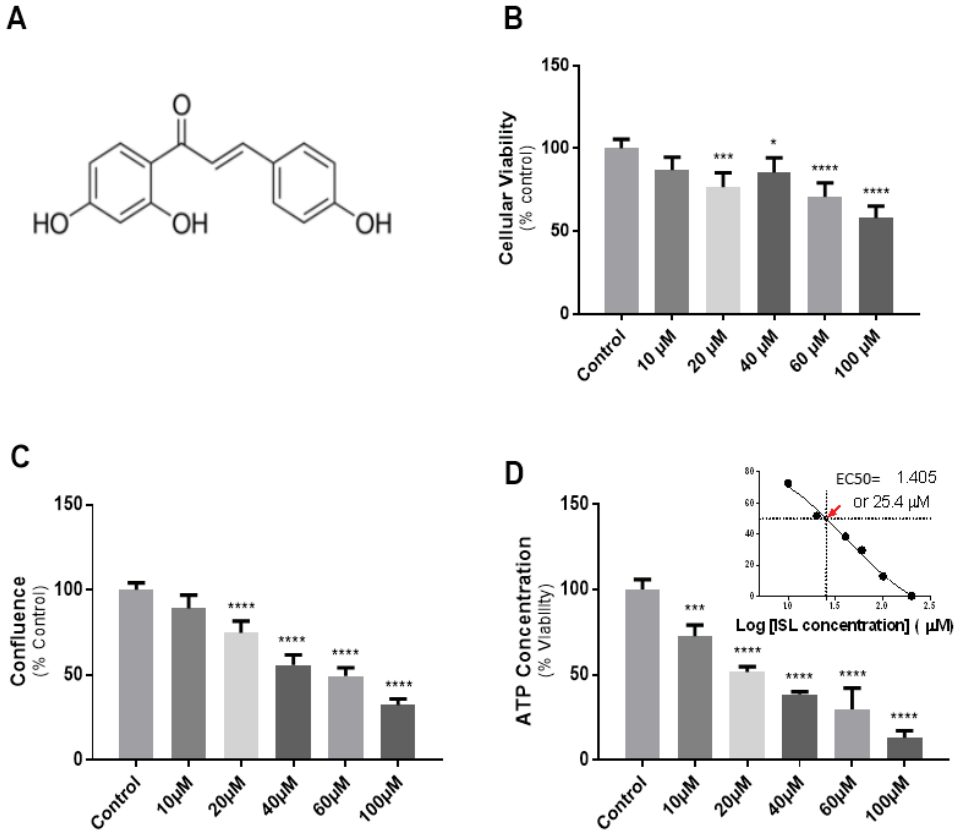

Figure 1. Effects of ISL on cultured SH-SY5Y cell viability. (A) Chemical structure of trans-isoliquiritigenin. Treatment of cells with increasing dose of ISL impacts cell viability: (B) Cell counts using trypan blue, (C) cell confluence and (D) intracellular ATP concentrations 24 h after insult with ISL at the doses indicated. Inset (D) shows the assessment of the EC_{50}-concentration for ISL based on the toxicity data. Data represent mean±SD; n=3 experiments each performed in triplicate. Different to the vehicle-treated (DMSO) control; *p < 0.05; ***p < 0.001; ****p < 0.0001.

To further investigate the mechanism of ISL-induced SH-SY5Y cell death, simultaneous evaluation of live, early-to-late-stage apoptotic or dead cells was determined by assessing total caspase 3/7 activity. This assay provides information on apoptosis status based on effector caspases 3/7 and also cell death via membrane permeabilization as a gross marker of necrosis. Consistent with viability data shown in Fig. 1, supplementing cells with ISL induced neuroblastoma cell death ranging from ~ 20% to 45% at flavonoid concentrations 20 – 100 μM compared to the vehicle control (*c.f.*, Fig. 2A-C and summary Fig 2D). However, loss of cell viability attributed to apoptosis did not reach statistical significance and indeed little apoptosis was detected in cells exposed to ISL (<2%) under all conditions tested, indicating cell death was most likely independent of this pathway (Fig. 2A-D). In these studies hydrogen peroxide (H_2O_2; final concentration 200 μM) was employed as a positive control that stimulated near complete cell death after 24 h (Fig. 2D).

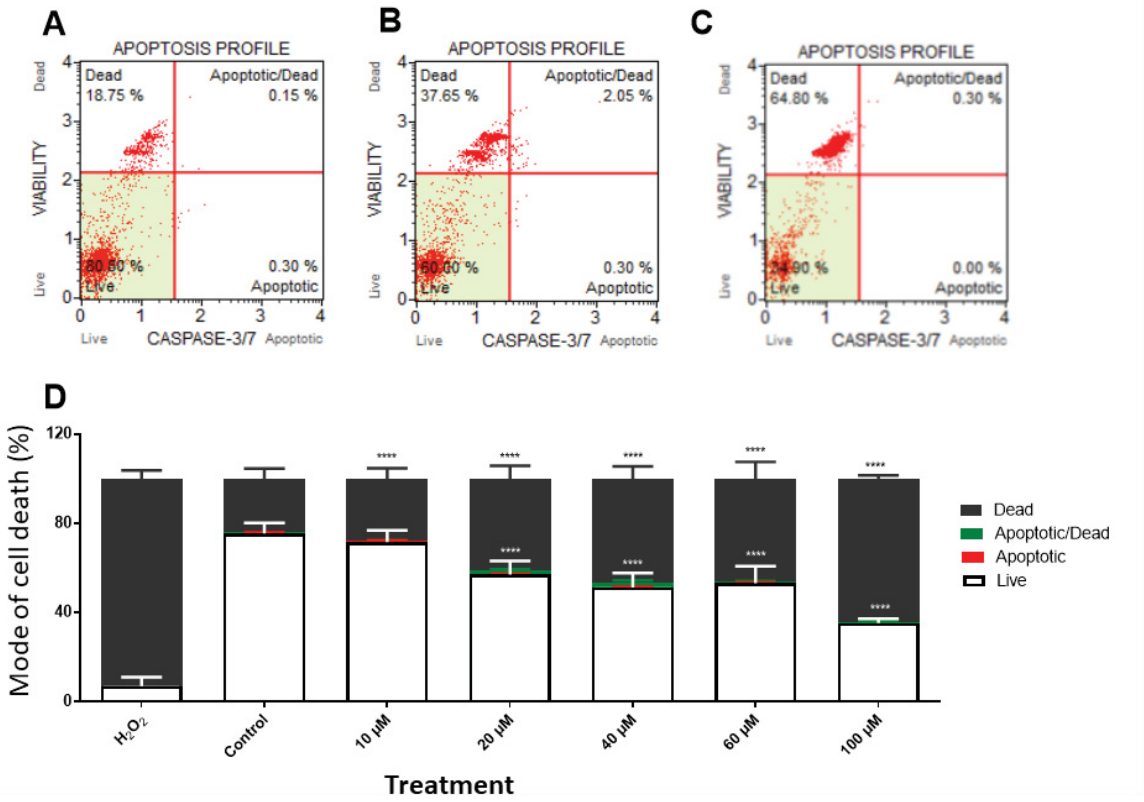

Figure 2. Effect of ISL on caspase 3/7 activity in SH-SY5Y cells. Caspases 3/7 activation and cell membrane permeabilization were analyzed using a Muse® Cell Analyser 24 h after insult with ISL at the doses indicated. Representative cell profiles of (A) vehicle treated cells and cells treated with (B) 20 µM ISL or (C) 100 µM ISL. Panel (D) shows the combined data and assignment of live, apoptotic and dead cells. H_2O_2 (final concentration 200 µM) is included as a positive control that elicits significant cell death primarily through necrosis. Data represent mean±SD; n=3 independent experiments each performed in triplicate. Different to the vehicle-treated (DMSO) control; ****p < 0.0001.

Complimentary assessment of apoptosis using the binding of Annexin V under identical treatment conditions (Fig. 3A-D) showed cell death occurred largely independent of Annexin V-positive apoptosis, which was a minor contributor to overall cell death irrespective of whether the cells were isolated 12 or 24 h (*c.f.*, Fig. 3A-C and summary Fig. 3D) post treatment with ISL. Thus, 12 h post insult (mean ± SD, n=4); 0.3 ± 0.3% cells were positive for Annexin V; 4.1 ± 2.0 % cells were positive for 7ADD, while 3.3 ± 1.2 % cells were positive for overall cell death. Similarly, when assessed for cell death markers 24 h post insult (mean±SD, n=4); 0.7 ± 0.3% cells were positive for Annexin V; 3.7 ± 1.2 % cells were positive for 7ADD, while overall 28.4 ± 10.5% cells were positive for cell death. Together these data indicated that ISL stimulated a loss in cell viability, which was primarily associated activation of necrotic pathways. As expected the mitochondrial uncoupling agent CCCP (positive control) promoted significant cell death with loss in cell viability primarily through necrosis > apoptosis (Fig. 3D). Together these findings indicate that ISL did not induce SH-SY5Y cell death via a classical (caspase-dependent) apoptosis pathway.

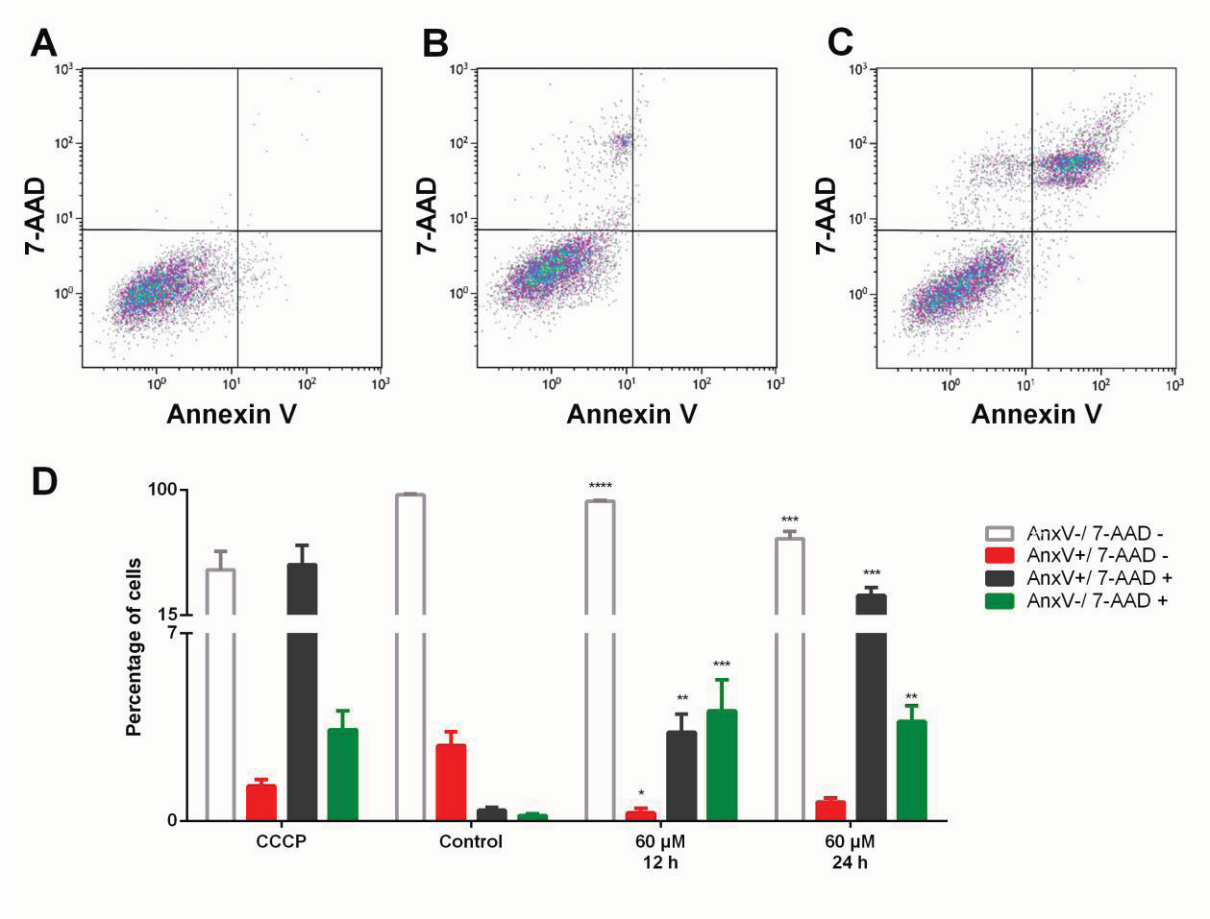

Figure 3. Assessment of ISL-mediated apoptosis with Annexin-V externalization. Annexin-V positivity and cell membrane permeabilization were assessed using antibodies against Annexin V and the reporter 7ADD 12 and 24 h after insult with ISL (doses as indicated) using a Gallio flow cytometer. Representative cell distribution profiles of vehicle (panel A) and cells exposed to 60 µM ISL and isolated for assessment 12 (panel B) or 24 h (panels C) after insult. Lower panel D shows the combined data and assignment of live, apoptotic and dead cells 12 or 24 h post ISL insult (note the break in the Y-axis scale). In these studies the mitochondrial uncoupling agent CCCP (final concentration 100 µM) was included as a positive control. Data represent mean±SD; n=4 independent experiments. Different to the vehicle-treated (DMSO) control; *p < 0.05; **p < 0.01; ***p < 0.001; ****p < 0.0001.

In order to demonstrate that a necroptotic pathway was central to neuroblastoma cell death stimulated by ISL, the effect of a necroptosis inhibitor, necrostatin-1, on the intracellular concentration of ATP was examined (Fig. 4). SH-SY5Y neuroblastoma cells pre-incubated with necrostatin-1 and then subjected to ISL treatment showed significant increases in ATP concentration when compared to corresponding ISL-treated cells in the absence of necrostatin-1 (Fig. 4). Notably, necrostatin-1 pretreatment effectively prevented the loss of ATP induced by ISL concentrations up to 20 µM and also significantly reduced ATP loss at higher ISL concentrations. These data suggest that a significant proportion of SH-SY5Y cell death can be attributed to necroptosis, especially at lower ISL concentrations corresponding to doses up to its experimentally determined EC_{50} value.

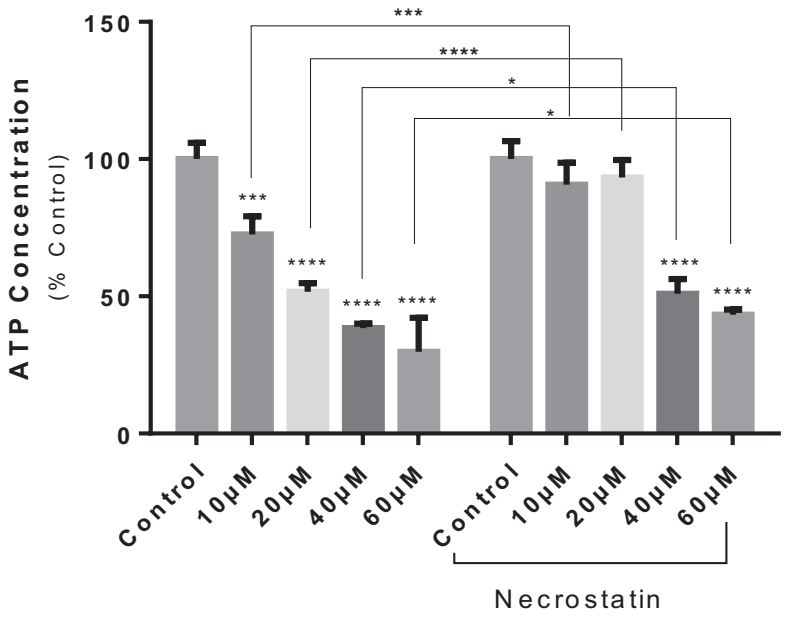

Figure 4. Assessment of intracellular ATP after administering ISL and necrostatin-1 to SH-SY5Y cells. Cells were either pre-incubated with necrostatin-1 (50 μM) or buffer alone as a control for 2 h and then exposed to ISL at the doses indicated. After 24 h further incubation, intracellular ATP concentration was determined using a commercial kit. Data represent mean±SD; n=3 independent experiments each performed in duplicate. Different to the corresponding vehicle treated (DMSO) control or different to the corresponding condition in the absence of necrostatin-1; *$p < 0.05$; ***$p < 0.001$; ****$p < 0.0001$.

Polyphenols can enhance autophagy [33], a controlled physiological cellular response dependent on signaling proteins such as the ubiquitin-like protein, LC3. The conversion of LC3 from cytosolic LC3-I, to the active, membrane bound form LC3-II, during autophagosome formation can be used as markers for monitoring autophagy [34]. LC3-I and LC3-II proteins were analyzed in SH-SY5Y neuroblastoma cells after incubation with 10-60 μM ISL (Fig. 5). Levels of LC3B-I were detected under all conditions tested, whereas LC3B-II was weakly detected and trended to increase with increasing ISL concentrations up to 40 μM (Fig. 5 A-C). Both LC3-I (~4 fold) and LC3-II (~5 fold) increased significantly in cells treated with 60 μM ISL (Fig. 5B and C). However, the LC3-II/I ratio remained largely unchanged and similar to the ratio determined for control (non-treated) cells, with the exception of a significant 1.5-fold increase in cells treated with 60 μM ISL (Fig. 5D).

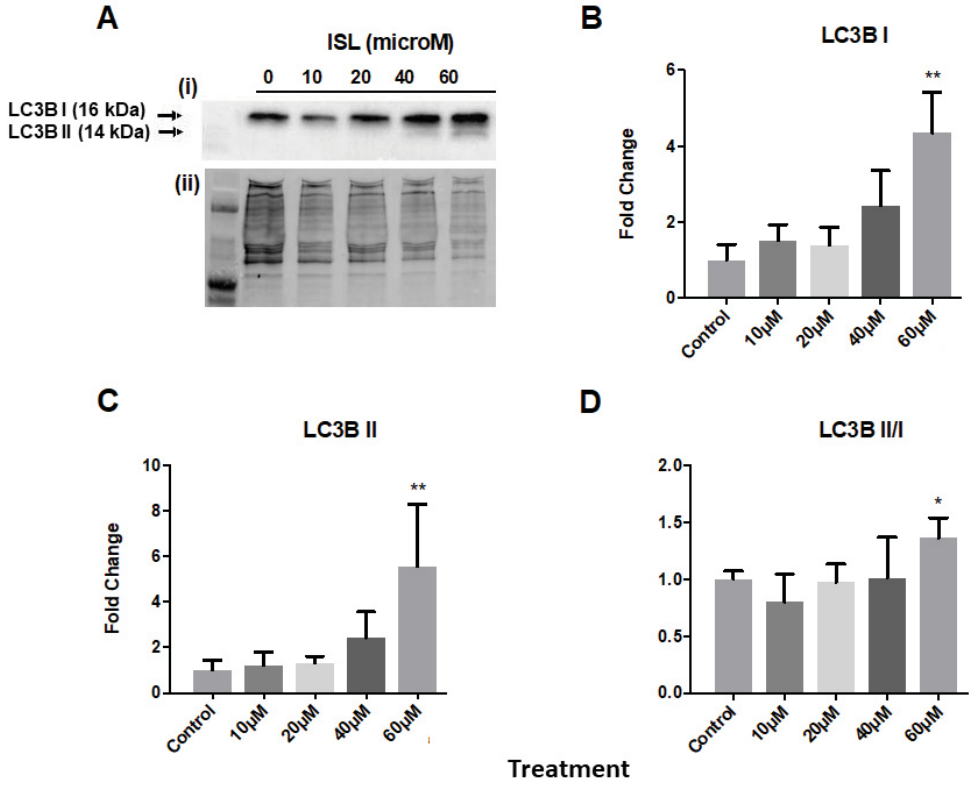

Figure 5. Assessment of autophagy in SH-SY5Y cells after insult with ISL. Panel (A(i)) representative accumulation of LC3B I and II proteins determined with western blot 24 h after treatment of SH-SY-5Y cells with increasing doses of ISL; (A(ii)) shows the corresponding in gel assessment of protein loading. Estimates of protein levels for (B) LC3BI and (C) LC3BII normalized to total protein determined in gel as described in the methods section. Semi-quantitative data are expressed as mean±SD; n=3 independent experiments. Different to corresponding data in presence of DMSO (vehicle control) alone: **p < 0.01.

Next, a scratch test was used to determine whether ISL treatment could influence SH-SY5Y migration/proliferation [35]. A notable retardation in scratch healing was observed with ISL treatment (Fig. 6) that reached significance for concentrations of ISL $\geq$ 20 μM and at time points between 24 – 72 h (Fig. 6B). Treatment of SH-SY5Y cells with 10 μM ISL significantly affected wound healing 48 h post drug administration (Fig 6B). Overall, the results suggest that ISL significantly inhibits the migration/proliferation of human neuroblastoma cells at effective doses ranging 20-60 μM.

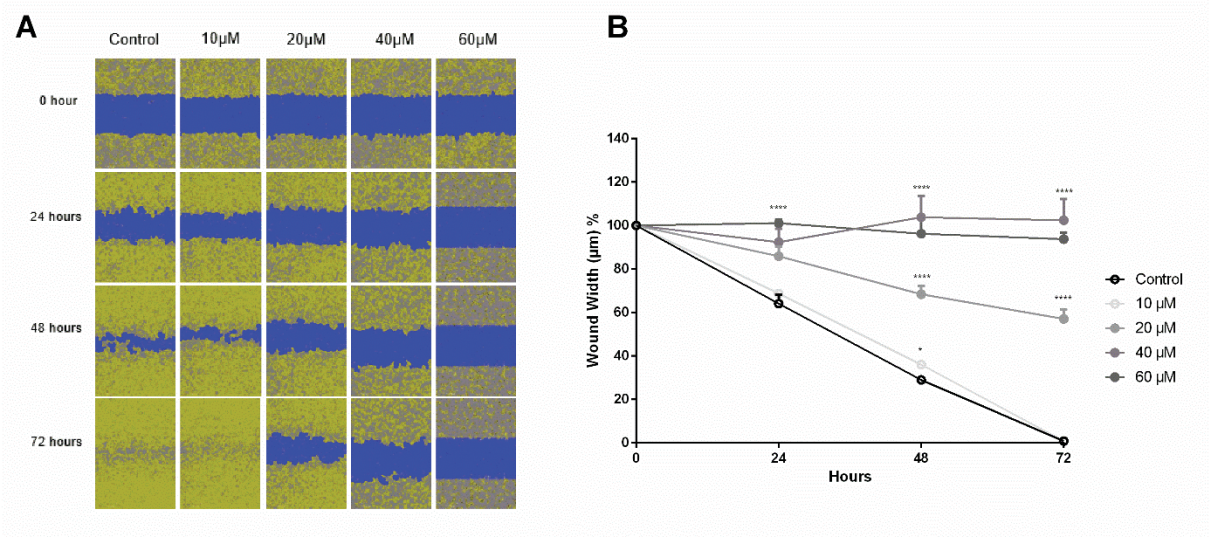

Figure 6. Assessment of SH-SY5Y cell migration/proliferation after treatment with increasing dose of ISL. Panel (A) representative images from IncuCyte® ZOOM Live-Cell Analysis System 0, 24, 48 and 72 h after exposure of SH-SY5Y cells to increasing dose of ISL. (B) Combined data showing percentage wound width determined in the scratch assays at 24 h post ISL treatment. Data represent mean SD; n=4 independent experiments. Different to the vehicle-treated (DMSO) control; *p < 0.05; ****p < 0.0001.

The impact of ISL on SH-SY5Y cell cycle was analyzed by flow cytometry (Fig. 7). Significant changes in the cell cycle profile of SH-SY5Y were induced 24 h after incubation with 40 - 60 μM ISL. For example, the proportion of cells in G0/G1 phase decreased by ~17% and cell populations in S and G2/M phases correspondingly increased by ~10% each after exposure to 40 μM ISL. The proportion of cells in S phase remained significantly elevated at ISL concentration 60 μM compared to control (untreated) cells, whereas the proportion of cells in the G2/M phase decreased to near control levels under these conditions. These findings suggest that ISL can influence cell proliferation primarily by arresting SH-SY5Y cell cycle transition particularly in the S (synthesizing) phase of the cell cycle with a consistently impact also evident at the G2/M phase although to a lesser extent.

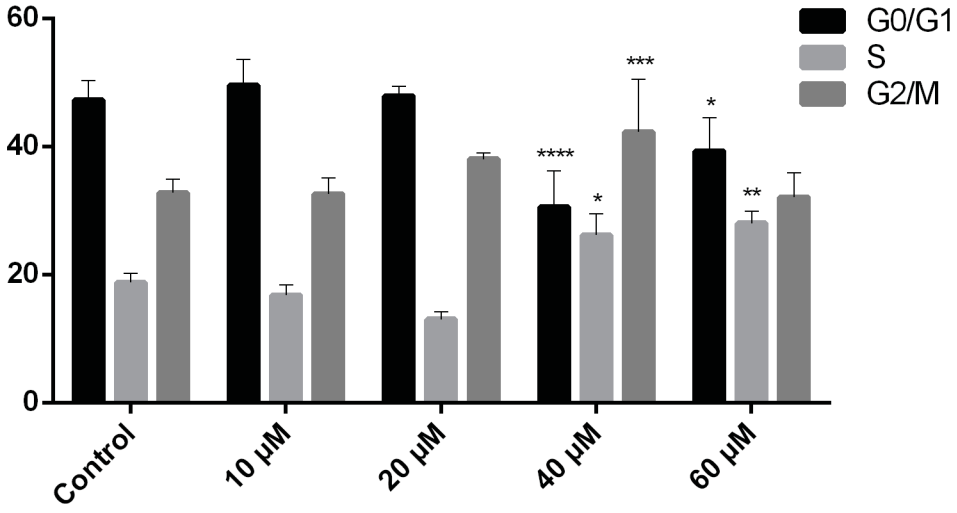

Figure 7. Assessment of cell cycle progression for SH-SY5Y cells treated with ISL. Neuroblastoma cell populations was analyzed using Muse® Cell Analyzer 24 h after treatment with various ISL doses. Data represent mean±SD; n=3 independent experiments each performed in duplicate. Different to the vehicle-treated (DMSO) control; *p < 0.05; **p < 0.01; ***p < 0.001; ****p < 0.0001.

Mitogen-activated protein kinases (MAPK) regulate proliferation, differentiation cell cycle functions and may be up-regulated in response to external stress. Therefore, the effects of ISL treatment on SH-SY5Y neuroblastoma cell MAPK proteins ERK1/2 (Fig. 8A-C) and p38 (Fig 8D-F) were evaluated. The levels of phosphorylated ERK1/2 and p38 were unchanged in SH-SY5Y cells treated with ISL at concentrations up to 40 µM final concentration. By contrast, ISL added well above the EC_{50}-value (that is, 60 µM) promoted significant increases in phosphorylated (*p*-)ERK 1/2 (~2.5 fold, Fig. 8B). In comparison, total p38 tended to decrease with low ISL concentrations (20–40 µM) whereas levels of phosphorylated (*p*-)p38 remained relatively stable at all ISL doses tested (Fig. 8E-G). This resulted in a ~ 3-fold increase in the ratio *p*-p38 /total p38 compared to control cells following treatment with 20 µM ISL, however, no other ISL dose elicited an alteration in *p*-p38 over the same dose range that promoted a corresponding loss in cell viability (*c.f.*, Fig. 1C and D with Fig. 8E).

To confirm the quantitative outcomes determined for *p*-ERK 1/2 and *p*-p38 as determined by ELISA, the phosphorylated proteins were also detected qualitatively by western blot (Fig. 8D and G, respectively). This assay confirmed the increased expression of *p*-ERK1/2 after treatment with ISL (Fig. 8D) only at dose well above the calculated EC_{50} (final concentrations 60 µM). While relatively little change was observed in *p*-p38 after ISL treatment when assessed by ELISA (Fig. 8E-G) corresponding western blot analysis showed a trend to decreased *p*-p38 levels (Fig. 8H). Taken together these determinations of ERK and p38 MAPK phophorylation suggest that little activation occurs in the dose range

close to the EC_{50} value for ISL and in general only doses 3 times the EC_{50}-value determined here for ISL lead to altered MAPK activation.

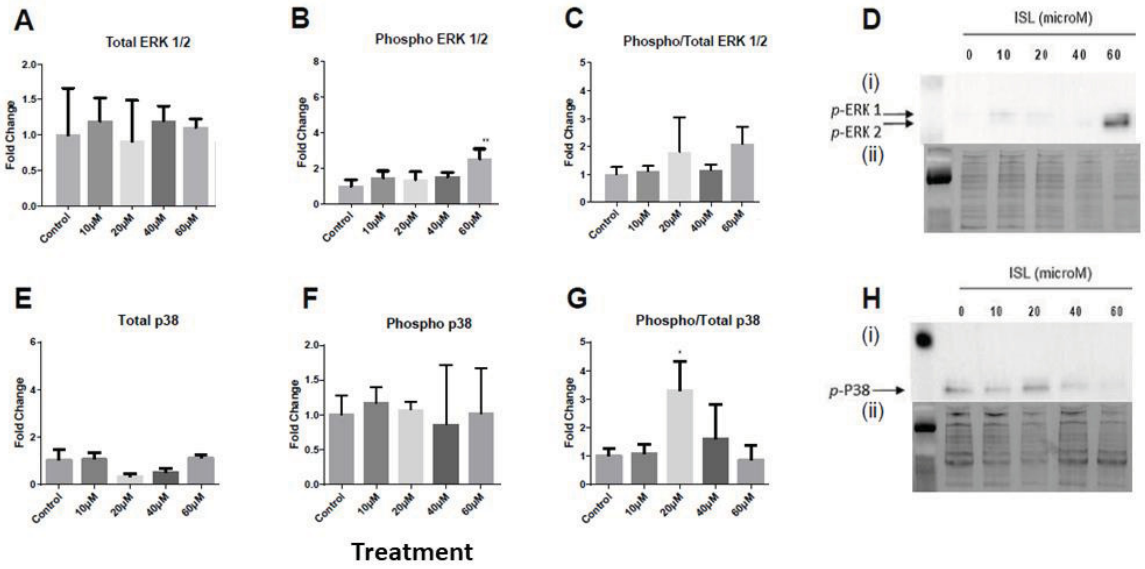

Figure 8. Testing intracellular activation of ERK 1/2 and p38 after treatment of SH-SY5Y cells with ISL. Cells were incubated with various doses of ISL and after 24h the levels of (A) total ERK 1/2, (B) phosphorylated ERK 1/2, (C) ratio of phosphorylated/total ERK 1/2 protein, (D(i)) representative images from phosphorylated ERK 1/2 protein western blot 24 h after insult with ISL at various doses and (D(ii)) shows the corresponding in gel assessment of protein loading. (E), total p38, (F) phosphorylated p38, (G) ratio of phosphorylated/total p38 protein determined by ELISA, (H(i)) Representative images from phosphorylated p38 protein western blot 24 h after exposure to ISL at the indicated doses and (H(ii)) shows the corresponding in gel assessment of protein loading. Data represent mean±SD; n=3 independent experiments. Different to the vehicle-treated (DMSO) control; *p < 0.05; **p < 0.01; ****p < 0.0001.

5.2.4. Discussion

Neuroblastoma has a high mortality rate representing 15% of all cancer deaths during childhood [36]. Current therapies are not effective and only 50% of patients survive beyond a 5-year period after diagnosis [37]. It is important to develop novel therapies to increase survival rates. The natural flavonoid ISL, has been considered as a potential therapeutic agent for cancer, demonstrating anti-tumor efficacy in various malignant cell types, including glioma [26], prostate [28], liver [38] and uterine cervical cancer [22]. Herein, we demonstrated that ISL induces neuroblastoma cell death likely through a mechanism of necroptosis with little evidence supporting a pro-apoptotic activity for this natural product

(see Figs. 1 & 2). The evidence supporting flavonoid cytotoxicity toward neuroblastoma cells includes (i) ISL dose-dependent decrease in cell viability with (ii) a concomitant decrease in intracellular ATP that is (iii) reversed by pre-incubation with the necroptosis inhibitor necrostatin-1 and (iv) ISL stimulated a marked decrease in cell migration, as well as cell cycle arrest. To the best of our knowledge this is the first report of isoliquiritigenin inducing neuroblastoma cell death. Our data also indicate that MAPKs ERK and p38 remained in the inactive state and phosphorylation/activation of these MAPK was only noted at doses 3 times the EC_{50}-value determined here for ISL cytotoxicity. The observed decreases in neuroblastoma cell viability and altered cell cycle transition may be linked to ISL-induced loss of intracellular ATP. This disturbance in cellular energetics primarily enhanced necrotic cell death in the absence any marked cell death through apoptosis. These combined activities indicate that ISL may offer some therapeutic potential and impact positively on the pathogenesis of this childhood cancer.

Several diverse classes of natural compounds show promise as potential therapeutics to combat neuroblastoma [39]. Flavonoids such as apigenin, (-)-epigallocatechin, (-)-epigallocatechin-3-gallate and genistein all decrease SH-SY5Y cell viability by a mechanism involving the induction of apoptosis through caspase activation [40]. Similarly, the chalcones xanthoangelol [16] and isobavachalcone [41], also mitigate neuroblastoma primarily by apoptosis induction. Whether these and other flavonoids also induce cell death via necroptosis in neuroblastoma is not clear, however, flavonoid-induced necroptosis by green tea polyphenols [10] and shikonin [11] is reported for other malignant cells. Notably, ISL induces both apoptotic and necrotic cell death in human glioma cells [26]. This data further indicates that ISL can induce cell death pathways independent of apoptosis in cancer cells.

Necroptosis is a form of programmed necrosis and represents an emerging mechanism of non-apoptotic cell death that is caspase-independent and regulated by receptor-interacting serine/threonine protein kinases (RIPK). Necrostatin-1 is a small molecule inhibitor of RIPK1 and suppresses necroptosis in several settings [42]. Pre-treatment of SH-SY5Y cells with necrostatin-1 prior to addition of ISL resulted in significant recovery of intracellular ATP levels suggesting that necroptosis may be responsible for ISL-induced loss of viability in neuroblastoma cells. However, necrostatin-1 is not specific to RIPK1; it is also known to inhibit indolamine-2,3-dioxygenase (IDO), which means that it can exert effects on the immune system and this pathway is also implicated in neuroprotection [43]. Also, herein we employed necrostatin-1 to analyze ATP levels and we did not look at concomitant recovery of cell viability. Therefore, further experiments using this inhibitor of RIPK and IDO and other inhibitors of necroptosis are warranted in order to confirm this cell death pathway. Irrespective of these prospective studies, our data do confirm that ISL does not enhance cell death via a caspase-dependent, pro-apoptotic mechanism.

Intracellular ATP determines cell death pathways with depletion of ATP favoring necrosis/necroptosis in cancer cells [44-46]. Mitochondria, as energy organelles controlling ATP formation, may be pivotal in determining modes of cell death and disturbances in key mitochondrial processes such as transmembrane potential, adenine nucleotide translocase

and the mitochondrial permeability transition pore complex may be involved in necroptotic induction [47]. Interestingly, flavonoids show differential structure-function effects on mitochondrial respiration, uncoupling and mitochondrial permeability transition that aligns with a variable ability to decrease mitochondrial ATP levels. Thus, flavonoids such as quercetin and galangin that substantially inhibit mitochondrial respiration or uncoupling and cause depletion of ATP may be conducive to necrosis induction [48]. Similarly, ISL can trigger dissipation of mitochondrial membrane potential and release of cytochrome C in studies where the flavonoid inhibits cancer cell growth [25]. Herein ISL dose-dependently depleted intracellular ATP and induced necroptosis thereby implicating ISL-mediated alteration to cellular bioenergetics in SH-SY5Y cells. Whether direct interaction of ISL with mitochondrial processes contributes to the flavonoid's cytotoxic mechanism in neuroblastoma cells warrants further investigation.

Autophagy and necroptosis may be interlinked cellular processes. For example, autophagy can suppress necrotic cell death in various cell lines and inhibition of autophagy can enhance necroptosis [49]. The autophagosome markers LC3BI and II tended to increase with ISL concentrations $\geq$40 μM in SH-SY5Y cells with a significant increase in LC3BI at 60 μM (Fig. 5) suggestive of induction of autophagy at the higher doses of ISL tested. However, doses of ISL $\leq$ 40 μM, that were associated with a loss in SH-SY5Y cell viability, did not significantly increase autophagy suggesting that its induction may be limited to doses of ISL significantly higher than the EC_{50}-value and/or that autophagy proceeds that of necroptosis under the experimental conditions used herein. Autophagy is stress-responsive and enables tumor cell survival under adverse conditions via restoration of cellular nutrient and ATP [50]. It may be envisaged that ATP depletion induced by ISL in neuroblastoma cells activates an autophagic response. However, this was not the case at least under the conditions employed here. Pharmacological induction of autophagy by flavonoids can be chemotherapeutic via promoting non-apoptotic cell death and overcoming chemotherapy resistance in some cancers [33, 50]. In this regard, ISL has been demonstrated to aggravate autophagy, induce G2/M cell cycle arrest and overcome drug resistance in breast cancer cells [51]. Thus, necroptosis and autophagy may combine to stimulate ISL-induced cell death in some cancer cell types.

Flavonoids are known to promiscuously activate numerous intracellular signaling pathways [52]. At least in the case for ERK, activation is known to play an important role in necroptotic cell death [53]. In addition, activation of ERK1/2 is associated with autophagy [54] and ISL is reported to activate ERK1/2 and promote apoptosis/autophagy in human endometrial cancer cells [55]. Moreover, the flavonoid curcumin, induces G2/M arrest and autophagy in malignant glioma via inhibition of Akt/mTOR/p70S6K and activation of ERK1/2 pathways [33]. By contrast, the study herein identified that MAPKs ERK and p38 remained inactivated during ISL-mediated toxicity and that the MAPKs only became activated through phosphorylation at ISL dose ($\geq$60 μM). Two other kinases, RIPK1 and RIPK3, are suggested to act upstream of ATP depletion during necroptosis in human HT29 colon and HepG2 liver cancer cells [56]. It is unclear whether ISL is capable of modulating RIPK activation directly or indirectly by stimulating TNF production [57]. Further investigation of the precise effects

of ISL on the convergent kinase pathways in neuroblastoma and other cancer cells will be important in defining a robust chemotherapeutic potential for this flavonoid.

In contrast to ERK, total and phosphorylated p38 protein tended to decrease with ISL treatment in neuroblastoma cells. The singular significant increase in p-p38/total p38 at [ISL] = 20 μM (Fig 8F) may be explained by loss of total p38 rather than phosphorylative activation. The biological consequences of p38 activation are complex and probably cell type specific as in some instances p38 can promote cell death and apoptosis while in other cell types p38 activation enhances cell survival, growth and proliferation by participating in G1 and G2/M phases of the cell cycle [58]. Increased cell proliferation is a common characteristic in numerous cancers and cell-cycle regulatory systems are important in preventing malignancy [59]. Treatment of SH-SY5Y cells with ISL resulted in apparent S-phase cell cycle arrest suggesting that ISL may affect checkpoint cyclin proteins and/or DNA synthesis that occur at this stage. Further, ISL reduced migration, suggesting that it possibly inhibits the ability of cells to spread thus impacting on neuroblastoma malignancy (Figure 6). These observations are consistent with outcomes from studies demonstrating ISL-induced cell cycle arrest in other cancer cell types [26, 27]. Further, panduratin A [20], butein [60], chalcone (1,3-diphenyl-2-propenone) [61] and 2'-hydroxy-2,3,4',6'-tetramethoxychalcone [62], compounds with similar chemical structure to ISL, all induce cell cycle arrest and decrease prostate, liver, bladder and lung cancer cell viability, respectively.

The efficacy of ISL as a chemotherapeutic in neuroblastoma and other cancers is reliant on efficient delivery to the target tissue potentially without clearance via metabolism (although metabolites may be therapeutic). Pharmacokinetic, metabolic and tissue distribution studies in mice show that ISL is metabolized primarily in the liver, accumulates in all major organs and can cross the blood brain barrier (BBB) [63]. Also, intravenous (10 mg/kg) and oral (20 mg/kg) administration of ISL to mice results in plasma levels in the micromolar range, for example, Han et al. [68], demonstrated that infusion of ISL (20 mg/kg), dissolved in a mixture of polyethyleneglycol and water (1:1, v/v), directly into the jugular vein yielded a maximal concentration of 19.5 μM ISL in the circulation; a value close to the EC_{50} value calculated in this study. In addition, there are methods that allow drugs to be delivered to neuroblastoma cancers using nano-carriers that are also known to enhance the active concentration for drugs [64, 65]; this mode of delivery may enhance the ability of ISL to accumulate in target cancerous tissues. Recently, chemists have developed phosphate and ammonium salt pro-drug forms of ISL that exhibit improved water solubility and solution stability [66]. Future studies using these ISL pro-drugs or nano-carrier delivered ISL in cell and animal model of neuroblastoma will address the efficacy of these modes of ISL drug delivery.

In conclusion, the evidence provided herein demonstrates that ISL treatment induces anti-proliferative and cytotoxic effects on neuroblastoma cells involving a combined loss of ATP, induction of cell cycle arrest, and cell death largely via a necroptotic mechanism in the absence of substantial activation of apoptosis. These findings suggest that ISL may be a promising chemopreventive agent for neuroblastoma provided therapeutic doses can be achieved in affected tissues.

5.2.5. Acknowledgement

All work was conducted in the Charles Perkins Centre and specifically the Redox Biology lab. The named researchers were responsible for the design and implementation of the experimental studies described herein. We acknowledge funding from the Australian Research Council (Discovery grants DP130103711 and DP160102063 to PKW); funding from the Sydney Medical School, The University of Sydney and the award of a Brazilian Science Exchange Scholarship (CNPq) to SJME as part of the Science without Borders initiative. We also acknowledge the assistance of Mrs Shirley Nakhla and the Bosch Institute Live Cell Analysis Facility, The University of Sydney.

5.2.6. References

[1] U.S.C.S.W.G. CDC, United States Cancer Statistics: 1999–2012 Incidence and Mortality Web-based Report. Incidence and Mortality Web-based Report. Atlanta: U.S. Department of Health and Human Services, Centers for Disease Control and Prevention and National Cancer Institute, (2015).
[2] N.K.V. Cheung, M.A. Dyer, Neuroblastoma: Developmental Biology, Cancer Genomics, and Immunotherapy, Nat Rev Cancer, 13 (2013) 397-411.
[3] C.U. Louis, J.M. Shohet, Neuroblastoma: molecular pathogenesis and therapy, Annual review of medicine, 66 (2015) 49-63.
[4] T.R. Mielcke, A. Mascarello, E. Filippi-Chiela, R.F. Zanin, G. Lenz, P.C. Leal, L.D. Chiaradia, R.A. Yunes, R.J. Nunes, A.M. Battastini, F.B. Morrone, M.M. Campos, Activity of novel quinoxaline-derived chalcones on in vitro glioma cell proliferation, European journal of medicinal chemistry, 48 (2012) 255-264.
[5] C. Busch, M. Burkard, C. Leischner, U.M. Lauer, J. Frank, S. Venturelli, Epigenetic activities of flavonoids in the prevention and treatment of cancer, Clinical Epigenetics, 7 (2015) 1-18.
[6] V. Nikoletopoulou, M. Markaki, K. Palikaras, N. Tavernarakis, Crosstalk between apoptosis, necrosis and autophagy, Biochim Biophys Acta, 1833 (2013) 3448-3459.
[7] M. Hassan, H. Watari, A. AbuAlmaaty, Y. Ohba, N. Sakuragi, Apoptosis and molecular targeting therapy in cancer, BioMed research international, 2014 (2014) 150845.
[8] A.J. Leon-Gonzalez, N. Acero, D. Munoz-Mingarro, I. Navarro, C. Martin-Cordero, Chalcones as Promising Lead Compounds on Cancer Therapy, Current medicinal chemistry, 22 (2015) 3407-3425.
[9] D.E. Christofferson, J. Yuan, Necroptosis as an alternative form of programmed cell death, Current opinion in cell biology, 22 (2010) 263-268.
[10] W. Lin, S. Tongyi, Role of Bax/Bcl-2 family members in green tea polyphenol induced necroptosis of p53-deficient Hep3B cells, Tumour biology : the journal of the International Society for Oncodevelopmental Biology and Medicine, 35 (2014) 8065-8075.
[11] Z. Fu, B. Deng, Y. Liao, L. Shan, F. Yin, Z. Wang, H. Zeng, D. Zuo, Y. Hua, Z. Cai, The anti-tumor effect of shikonin on osteosarcoma by inducing RIP1 and RIP3 dependent necroptosis, BMC Cancer, 13 (2013) 1-10.
[12] L.D. Chiaradia, R. dos Santos, C.E. Vitor, A.A. Vieira, P.C. Leal, R.J. Nunes, J.B. Calixto, R.A. Yunes, Synthesis and pharmacological activity of chalcones derived from 2,4,6-trimethoxyacetophenone in RAW 264.7 cells stimulated by LPS: Quantitative structure–activity relationships, Bioorganic & Medicinal Chemistry, 16 (2008) 658-667.
[13] M. Sikander, S. Malik, D. Yadav, S. Biswas, D.P. Katare, S.K. Jain, Cytoprotective activity of a trans-chalcone against hydrogen peroxide induced toxicity in hepatocellular

carcinoma (HepG2) cells, Asian Pacific journal of cancer prevention : APJCP, 12 (2011) 2513-2516.
[14] Y.L. Hsu, P.L. Kuo, W.S. Tzeng, C.C. Lin, Chalcone inhibits the proliferation of human breast cancer cell by blocking cell cycle progression and inducing apoptosis, Food and chemical toxicology : an international journal published for the British Industrial Biological Research Association, 44 (2006) 704-713.
[15] E. Szliszka, Z.P. Czuba, B. Mazur, A. Paradysz, W. Krol, Chalcones and dihydrochalcones augment TRAIL-mediated apoptosis in prostate cancer cells, Molecules (Basel, Switzerland), 15 (2010) 5336-5353.
[16] K. Tabata, K. Motani, N. Takayanagi, R. Nishimura, S. Asami, Y. Kimura, M. Ukiya, D. Hasegawa, T. Akihisa, T. Suzuki, Xanthoangelol, a major chalcone constituent of Angelica keiskei, induces apoptosis in neuroblastoma and leukemia cells, Biological & pharmaceutical bulletin, 28 (2005) 1404-1407.
[17] Y.F. Kuo, Y.Z. Su, Y.H. Tseng, S.Y. Wang, H.M. Wang, P.J. Chueh, Flavokawain B, a novel chalcone from Alpinia pricei Hayata with potent apoptotic activity: Involvement of ROS and GADD153 upstream of mitochondria-dependent apoptosis in HCT116 cells, Free radical biology & medicine, 49 (2010) 214-226.
[18] H. Jing, X. Zhou, X. Dong, J. Cao, H. Zhu, J. Lou, Y. Hu, Q. He, B. Yang, Abrogation of Akt signaling by Isobavachalcone contributes to its anti-proliferative effects towards human cancer cells, Cancer Lett, 294 (2010) 167-177.
[19] M.K. Pandey, B. Sung, K.S. Ahn, B.B. Aggarwal, Butein suppresses constitutive and inducible signal transducer and activator of transcription (STAT) 3 activation and STAT3-regulated gene products through the induction of a protein tyrosine phosphatase SHP-1, Molecular pharmacology, 75 (2009) 525-533.
[20] J.M. Yun, M.H. Kweon, H. Kwon, J.K. Hwang, H. Mukhtar, Induction of apoptosis and cell cycle arrest by a chalcone panduratin A isolated from Kaempferia pandurata in androgen-independent human prostate cancer cells PC3 and DU145, Carcinogenesis, 27 (2006) 1454-1464.
[21] A. Boumendjel, X. Ronot, J. Boutonnat, Chalcones derivatives acting as cell cycle blockers: potential anti cancer drugs?, Current drug targets, 10 (2009) 363-371.
[22] Y.L. Hsu, C.C. Chia, P.J. Chen, S.E. Huang, S.C. Huang, P.L. Kuo, Shallot and licorice constituent isoliquiritigenin arrests cell cycle progression and induces apoptosis through the induction of ATM/p53 and initiation of the mitochondrial system in human cervical carcinoma HeLa cells, Molecular nutrition & food research, 53 (2009) 826-835.
[23] R. Gaur, K.S. Yadav, R.K. Verma, N.P. Yadav, R.S. Bhakuni, In vivo anti-diabetic activity of derivatives of isoliquiritigenin and liquiritigenin, Phytomedicine, 21 (2014) 415-422.
[24] X. Zhang, P. Zhu, X. Zhang, Y. Ma, W. Li, J.M. Chen, H.M. Guo, R. Bucala, J. Zhuang, J. Li, Natural antioxidant-isoliquiritigenin ameliorates contractile dysfunction of hypoxic cardiomyocytes via AMPK signaling pathway, Mediators of inflammation, 2013 (2013) 390890.
[25] F. Peng, Q.H. Du, C. Peng, N. Wang, H.L. Tang, X.M. Xie, J.G. Shen, J.P. Chen, A Review: The Pharmacology of Isoliquiritigenin, Phytotherapy Research, 29 (2015) 969-977.
[26] G.S. Zhou, L.J. Song, B. Yang, Isoliquiritigenin inhibits proliferation and induces apoptosis of U87 human glioma cells in vitro, Molecular medicine reports, 7 (2013) 531-536.
[27] Y.M. Lee, D.Y. Lim, H.J. Choi, J.I. Jung, W.Y. Chung, J.H. Park, Induction of cell cycle arrest in prostate cancer cells by the dietary compound isoliquiritigenin, Journal of medicinal food, 12 (2009) 8-14.

[28] X. Zhang, E.D. Yeung, J. Wang, E.E. Panzhinskiy, C. Tong, W. Li, J. Li, Isoliquiritigenin, a natural anti-oxidant, selectively inhibits the proliferation of prostate cancer cells, Clinical and experimental pharmacology & physiology, 37 (2010) 841-847.
[29] Z. Wang, N. Wang, S. Han, D. Wang, S. Mo, L. Yu, H. Huang, K. Tsui, J. Shen, J. Chen, Dietary compound isoliquiritigenin inhibits breast cancer neoangiogenesis via VEGF/VEGFR-2 signaling pathway, PLoS One, 8 (2013) e68566.
[30] K. Yamanaka, Y. Saito, T. Yamamori, Y. Urano, N. Noguchi, 24(S)-hydroxycholesterol induces neuronal cell death through necroptosis, a form of programmed necrosis, The Journal of biological chemistry, 286 (2011) 24666-24673.
[31] T. Mahmood, P.C. Yang, Western Blot: Technique, Theory, and Trouble Shooting, North American Journal of Medical Sciences, 4 (2012) 429-434.
[32] O.R. Koechli, B.U. Sevin, J.P. Perras, R. Angioli, M. Untch, A. Steren, C. Ramachandran, H.E. Averette, Comparative chemosensitivity profiles in three human breast cancer cell lines with the ATP-cell viability assay, Oncology, 51 (1994) 552-558.
[33] N. Hasima, B. Ozpolat, Regulation of autophagy by polyphenolic compounds as a potential therapeutic strategy for cancer, Cell Death Dis, 5 (2014) e1509-.
[34] R.A. Gottlieb, A.M. Andres, J. Sin, D.P.J. Taylor, Untangling Autophagy Measurements: All Fluxed Up, Circulation Research, 116 (2015) 504-514.
[35] S.T. Johnston, E.T. Shah, L.K. Chopin, D.L. Sean McElwain, M.J. Simpson, Estimating cell diffusivity and cell proliferation rate by interpreting IncuCyte ZOOM™ assay data using the Fisher-Kolmogorov model, BMC Systems Biology, 9 (2015) 1-13.
[36] T. Sanda, K. Akahanse, B.J. Abraham, N. Weichert, A. Durbin, L. Anders, S.H. Tan, A.W.Y. Yam, L.N. Lawton, R.A. Young, J.M. Maris, A.T. Look, Transcriptional regulatory program controlled by the oncogenic transcription factor LMO1 in neuroblastoma, Cancer Research, 76 (2016) 2007-2007.
[37] A.L. Gaviglio, G.C. Blobe, Heparin-binding epidermal growth factor-like growth factor is a pro-differentiating factor in neuroblastoma, Cancer Research, 76 (2016) 1182-1182.
[38] C. Sun, H. Zhang, X.F. Ma, X. Zhou, L. Gan, Y.Y. Liu, Z.H. Wang, Isoliquiritigenin Enhances Radiosensitivity of HepG2 Cells via Disturbance of Redox Status, Cell Biochemistry and Biophysics, 65 (2013) 433-444.
[39] K.T. Yasukawa, Keiichi, Promising Natural Products As Anti-Cancer Agents against Neuroblastoma, Horizons in Cancer Research, 59 (2015) 91-113.
[40] A. Das, N.L. Banik, S.K. Ray, Mechanism of apoptosis with the involvement of calpain and caspase cascades in human malignant neuroblastoma SH-SY5Y cells exposed to flavonoids, International journal of cancer, 119 (2006) 2575-2585.
[41] R. Nishimura, K. Tabata, M. Arakawa, Y. Ito, Y. Kimura, T. Akihisa, H. Nagai, A. Sakuma, H. Kohno, T. Suzuki, Isobavachalcone, a chalcone constituent of Angelica keiskei, induces apoptosis in neuroblastoma, Biological & pharmaceutical bulletin, 30 (2007) 1878-1883.
[42] A. Degterev, Z. Huang, M. Boyce, Y. Li, P. Jagtap, N. Mizushima, G.D. Cuny, T.J. Mitchison, M.A. Moskowitz, J. Yuan, Chemical inhibitor of nonapoptotic cell death with therapeutic potential for ischemic brain injury, Nat Chem Biol, 1 (2005) 112-119.
[43] P. Vandenabeele, S. Grootjans, N. Callewaert, N. Takahashi, Necrostatin-1 blocks both RIPK1 and IDO: consequences for the study of cell death in experimental disease models, Cell Death and Differentiation, 20 (2013) 185-187.
[44] A. Kaczmarek, P. Vandenabeele, Dmitri V. Krysko, Necroptosis: The Release of Damage-Associated Molecular Patterns and Its Physiological Relevance, Immunity, 38 (2013) 209-223.

[45] M. Leist, B. Single, A.F. Castoldi, S. Kuhnle, P. Nicotera, Intracellular adenosine triphosphate (ATP) concentration: a switch in the decision between apoptosis and necrosis, The Journal of experimental medicine, 185 (1997) 1481-1486.
[46] Y. Eguchi, S. Shimizu, Y. Tsujimoto, Intracellular ATP levels determine cell death fate by apoptosis or necrosis, Cancer Res, 57 (1997) 1835-1840.
[47] P. Vandenabeele, L. Galluzzi, T. Vanden Berghe, G. Kroemer, Molecular mechanisms of necroptosis: an ordered cellular explosion, Nat Rev Mol Cell Biol, 11 (2010) 700-714.
[48] D.J. Dorta, A.A. Pigoso, F.E. Mingatto, T. Rodrigues, I.M. Prado, A.F. Helena, S.A. Uyemura, A.C. Santos, C. Curti, The interaction of flavonoids with mitochondria: effects on energetic processes, Chem Biol Interact, 152 (2005) 67-78.
[49] Y.T. Wu, H.L. Tan, Q. Huang, C.N. Ong, H.M. Shen, Activation of the PI3K-Akt-mTOR signaling pathway promotes necrotic cell death via suppression of autophagy, Autophagy, 5 (2009) 824-834.
[50] R. Mathew, V. Karantza-Wadsworth, E. White, Role of autophagy in cancer, Nat Rev Cancer, 7 (2007) 961-967.
[51] Z. Wang, N. Wang, P. Liu, Q. Chen, H. Situ, T. Xie, J. Zhang, C. Peng, Y. Lin, J. Chen, MicroRNA-25 regulates chemoresistance-associated autophagy in breast cancer cells, a process modulated by the natural autophagy inducer isoliquiritigenin, Oncotarget, 5 (2014) 7013-7026.
[52] H. Zhang, R. Tsao, Dietary polyphenols, oxidative stress and antioxidant and anti-inflammatory effects, Current Opinion in Food Science, 8 (2016) 33-42.
[53] M. Zhang, J. Li, R. Geng, W. Ge, Y. Zhou, C. Zhang, Y. Cheng, D. Geng, The inhibition of ERK activation mediates the protection of necrostatin-1 on glutamate toxicity in HT-22 cells, Neurotoxicity research, 24 (2013) 64-70.
[54] U. Sivaprasad, A. Basu, Inhibition of ERK attenuates autophagy and potentiates tumour necrosis factor-α-induced cell death in MCF-7 cells, Journal of Cellular and Molecular Medicine, 12 (2008) 1265-1271.
[55] C.H. Wu, H.Y. Chen, C.W. Wang, T.M. Shieh, T.C. Huang, L.C. Lin, K.L. Wang, S.M. Hsia, Isoliquiritigenin induces apoptosis and autophagy and inhibits endometrial cancer growth in mice, Oncotarget, 7 (2016) 73432-73447.
[56] S. Jouan-Lanhouet, M.I. Arshad, C. Piquet-Pellorce, C. Martin-Chouly, G. Le Moigne-Muller, F. Van Herreweghe, N. Takahashi, O. Sergent, D. Lagadic-Gossmann, P. Vandenabeele, M. Samson, M. Dimanche-Boitrel, TRAIL induces necroptosis involving RIPK1/RIPK3-dependent PARP-1 activation, Cell Death and Differentiation, 19 (2012) 2003-2014.
[57] L. Munoz, Non-kinase targets of protein kinase inhibitors, Nat Rev Drug Discov, advance online publication (2017).
[58] T. Zarubin, J. Han, Activation and signaling of the p38 MAP kinase pathway, Cell research, 15 (2005) 11-18.
[59] M.-D. Shi, C.-K. Shiao, Y.-C. Lee, Y.-W. Shih, Apigenin, a dietary flavonoid, inhibits proliferation of human bladder cancer T-24 cells via blocking cell cycle progression and inducing apoptosis, Cancer Cell International, 15 (2015) 33.
[60] D.O. Moon, M.O. Kim, Y.H. Choi, J.W. Hyun, W.Y. Chang, G.Y. Kim, Butein induces G(2)/M phase arrest and apoptosis in human hepatoma cancer cells through ROS generation, Cancer Lett, 288 (2010) 204-213.
[61] K.H. Shen, J.K. Chang, Y.L. Hsu, P.L. Kuo, Chalcone arrests cell cycle progression and induces apoptosis through induction of mitochondrial pathway and inhibition of nuclear factor kappa B signalling in human bladder cancer cells, Basic & clinical pharmacology & toxicology, 101 (2007) 254-261.

[62] Y.K. Rao, T.Y. Kao, J.L. Ko, Y.M. Tzeng, Chalcone HTMC causes in vitro selective cytotoxicity, cell-cycle G1 phase arrest through p53-dependent pathway in human lung adenocarcinoma A549 cells, and in vivo tumor growth suppression, Bioorganic & medicinal chemistry letters, 20 (2010) 6508-6512.
[63] S.Y. Han, Y.W. Chin, Y.H. Choi, A new approach for pharmacokinetic studies of natural products: measurement of isoliquiritigenin levels in mice plasma, urine and feces using modified automated dosing/blood sampling system, Biomedical chromatography : BMC, 27 (2013) 741-749.
[64] I. Cossu, G. Bottoni, M. Loi, L. Emionite, A. Bartolini, D. Di Paolo, C. Brignole, F. Piaggio, P. Perri, A. Sacchi, F. Curnis, M.C. Gagliani, S. Bruno, C. Marini, A. Gori, R. Longhi, D. Murgia, A.R. Sementa, M. Cilli, C. Tacchetti, A. Corti, G. Sambuceti, S. Marchio, M. Ponzoni, F. Pastorino, Neuroblastoma-targeted nanocarriers improve drug delivery and penetration, delay tumor growth and abrogate metastatic diffusion, Biomaterials, 68 (2015) 89-99.
[65] B. Delalat, V.C. Sheppard, S. Rasi Ghaemi, S. Rao, C.A. Prestidge, G. McPhee, M.L. Rogers, J.F. Donoghue, V. Pillay, T.G. Johns, N. Kroger, N.H. Voelcker, Targeted drug delivery using genetically engineered diatom biosilica, 6 (2015) 8791.
[66] K. Boyapelly, M.A. Bonin, H. Traboulsi, A. Cloutier, S.C. Phaneuf, D. Fortin, A.M. Cantin, M.V. Richter, E. Marsault, Synthesis and Characterization of a Phosphate Prodrug of Isoliquiritigenin, Journal of natural products, (2017).

6 DISCUSSÃO FINAL

O neuroblastoma tem uma alta taxa de mortalidade e as terapias disponíveis não são completamente eficazes (ACS 2018). Portanto, é importante desenvolver novas terapias para aumentar as taxas de sobrevivência. Dentre os grupos de possíveis compostos com ação antitumoral destacam-se as chalconas (Leon-Gonzalez, Acero et al. 2015). As hidroxichalconas 4HC e ISL, utilizadas neste trabalho, têm sido consideradas como potenciais agentes terapêuticos para o câncer (Orlikova, Tasdemir et al. 2011, Peng, Du et al. 2015). Observou-se que ambos os compostos possuem atividade citotóxica contra células SH-SY5Y, porém o mecanismo de morte induzido por eles não foi o mesmo.

Sobre a 4HC, nossos dados sugerem que essa chalcona pode induzir a morte de células de neuroblastoma por apoptose via intrínseca (mitocondrial). Essa hipótese é suportada pela (i) diminuição significativa da viabilidade celular, (ii) depleção dos níveis intracelulares de ATP, (iii) redução da proliferação/migração, (iv) aumento da exposição de fosfatidilserina na superfície das células, (v) alterações morfológicas e (vi) disfunção mitocondrial após tratamento com 4HC em células de neuroblastoma (SH-SY5Y). Os resultados observados relacionados com a disfunção mitocondrial observada nas células SH-SY5Y tratadas com 4HC foram: a inibição da respiração mitocondrial, despolarização da membrana mitocondrial, aumento de ERO e alterações morfológicas da organela.

A ISL induz a morte de células de neuroblastoma provavelmente através do mecanismo de necroptose. As evidências que suportam esta hipótese envolvidas com a citotoxicidade dessa chalcona em relação às células de neuroblastoma (SH-SY5Y) incluem (i) diminuição da viabilidade celular dependente da concentração de ISL com (ii) uma concomitante diminuição dos níveis de ATP intracelular que foi (iii) revertida por pré-tratamento com o inibidor da necroptose (necrostatina-1). No entanto, para confirmar a hipótese de morte por necroptose promovida pela ISL seriam necessários mais experimentos, como a expressão das principais proteínas envolvidas nesse processo RIPK1/3 e MLKL. He e cols. descreveram que em células tumorais de pulmão (A549) e de bexiga (UM-UC-3) a chalcona-24 (2-hidroxi-3,3’,4’,5’-tetrametoxi chalcona) foi capaz de induzir a morte celular via necroptose através da modulação das proteínas RIP1 e RIP3 (He, Wang et al. 2014).

ERK1/2 e p38 são proteínas que poderiam estar relacionadas com a redução da proliferação e alteração do ciclo celular promovidas pela ISL. ERK1/2 são proteínas que participam na regulação de uma grande variedade de processos, incluindo adesão celular,

progressão do ciclo celular, migração celular, sobrevivência celular, diferenciação e proliferação (Roskoski 2012). Além disso, sabe-se a proteína p38 regula tanto o ponto de verificação do ciclo celular G2/M quanto G1/S em resposta ao estresse celular, como danos no DNA (Thornton and Rincon 2009). No entanto, nossos dados indicam que as proteínas ERK e p38 permaneceram no estado inativo e a fosforilação/ativação dessas proteínas foi observada apenas em concentrações 3-4 vezes o valor de EC_{50} determinado para ISL, o que sugere que essas proteínas não estão relacionadas com os efeitos promovidos pelo composto.

O efeito do tratamento nas células SH-SY5Y com as diferentes concentrações de ISL sobre alguns parâmetros de apoptose e autofagia foram avaliados. Não houve aumento da atividade de caspases 3/7 ou da exposição de fosfatidilserina na superfície celular, sugerindo que não está ocorrendo morte por apoptose pela via clássica de ativação de caspases. No entanto, outras vias de ativação de apoptose como a liberação de EndoG e AIF poderiam ser avaliadas para confirmar a participação desse processo na morte celular induzida por ISL. Sobre a autofagia, a razão das proteínas LC3II/I demonstrou-se aumentada apenas na concentração de 60 µM de ISL, o que pode sugerir que o processo autofágico pode estar relacionado com a tentativa de sobrevivência da célula, porém mais análises seriam necessárias para confirmar essa hipótese.

Ambos os compostos utilizados nesse estudo, 4HC e ISL, promoveram redução na migração/proliferação celular, bem como alteração do ciclo celular. Entre as alterações observadas no ciclo celular destaca-se principalmente o aumento do percentual de células na fase S a partir da concentração de 40 µM para ambos os compostos. Nossos resultados estão de acordo com os observados por outros autores que verificaram que em células de cultura primária de glioblastoma humano, a 3'-metoxi-4'-hidroxi-2-naftil chalcona, um derivado de chalcona com hidroxila na posição 4', também foi capaz de aumentar o percentual de células na fase S (Bittencourt, Oliveira et al. 2016). A alteração da progressão do ciclo celular promovida pelos compostos utilizados nesse trabalho poderia ser explicada, pelo menos em parte, por um possível efeito da 4HC e da ISL sobre a topoisomerase I. As topoisomerases são responsáveis pelo controle da topologia do DNA e sua atividade é um elemento essencial da replicação do DNA. A topoisomerase I induz quebras de fita simples na molécula de DNA levando ao relaxamento do DNA superenovelado produzido durante a replicação e posterior transcrição do DNA (Janočková, Plšíková et al. 2015).

Na literatura outros autores já verificaram em ensaios *in vitro,* utilizando DNA plasmidial, que a 4HC e a ISL são capazes de inibir a enzima topoisomerase I (Gul,

Cizmecioglu et al. 2009, Zhao, Chang et al. 2015). Zhao e cols. compararam os efeitos inibitórios sobre a topoisomerase I da camptotecina (CPT), um alcalóide utilizado como controle positivo, com os da ISL em células de glioma (U87) e verificaram (utilizando pBR322DNA e análise por eletroforese) que a partir da concentração de 2,5 μM de ISL já foi observado um efeito inibitório da topoisomerase I próximo ao da camptotecina (2μM). Além disso, estes autores verificaram que o efeito inibitório da ISL sobre o crescimento de células de glioma (U87) foi inferior ao da CPT (IC_{50} para a CPT e ISL foram 0,509 ± 0.36 μM e 6,265 ± 0.89 μM, respectivamente), contudo a toxicidade da ISL em relação às células normais de cérebro (compradas da JRDUN Biotechnogy -Shanghai) era muito menor (menos da metade) que a da CPT quando utilizadas as concentrações entre 10 e 50 μM. Morris e cols. demostraram que a CPT inibe a topoisomerase I impedindo a religação de quebras de DNA de fita única mediadas por esta enzima, produzindo assim, alterações no DNA potencialmente letais durante a sua replicação (Morris and Geller 1996). A CPT já foi usada clinicamente, porém possui alta toxicidade e instabilidade *in vivo* (Basili and Moro 2009). O uso de inibidores eficazes da topoisomerase I com baixa toxicidade é importante por promoverem inibição do crescimento e da metástase de células tumorais (Zhao, Chang et al. 2015). Desta forma, a ISL e a 4HC tornam-se compostos promissores para estudo de sua potencial capacidade antitumoral.

Os valores de EC_{50} em células de neuroblastoma para ambas as chalconas foram próximos, sendo: 25,4 ± 3,4 μM para ISL e 21,5 ± 1,4 μM para 4HC. Sugerindo que a presença dos dois grupos hidroxilas que a ISL possui a mais que a 4HC poderiam não alterar significativamente a ação citotóxica do composto. Além disso, Sabzevari cols. analisaram a citotoxicidade de hidroxichalconas em cultura primária de hepatócitos e verificaram que a ISL e a 4HC, entre as chalconas testadas, foram as que tiveram menor efeito citotóxico com LD_{50} (2h) de 215 ± 27 μM e 200 ± 22 μM, respectivamente (Sabzevari, Galati et al. 2004).

Com base nos resultados obtidos nesse trabalho e os dados já descritos na literatura, podemos concluir que ambas as chalconas, ISL e 4HC, possuem características favoráveis para serem estudadas como potenciais compostos para o tratamento de neuroblastoma.

7 CONCLUSÕES

Em relação aos efeitos da 4HC sobre as células de neuroblastoma humano (SH-SY5Y), pode-se concluir que:

- Sua citotoxicidade sobre células SH-SY5Y é dependente da concentração e pode estar relacionada com a disfunção mitocondrial;
- Promove modificação da progressão do ciclo celular e redução da proliferação/migração celular;
- Promove disfunção mitocondrial, evidenciada por alterações morfológicas, inibição da respiração celular e redução do potencial de membrana mitocondrial, possivelmente associados à redução dos níveis de ATP intracelular e ao aumento dos níveis de ERO. Estes efeitos estariam colaborando para a indução da morte celular por apoptose via intrínseca (mitocondrial) em células de neuroblastoma humano (SH-SY5Y.

Em relação aos efeitos da ISL sobre as células de neuroblastoma humano (SH-SY5Y), pode-se concluir que:

- Reduz significativamente a viabilidade de células SH-SY5Y de maneira dependente da concentração e induz a morte celular associada com a redução dos níveis de ATP intracelular;
- Promove a redução da proliferação/migração celular e altera a progressão do ciclo celular;
- Possivelmente induz a morte celular por necroptose, uma vez que o pré-tratamento com o inibidor desta via de morte (necrostatina-1) promoveu a recuperação parcial dos níveis de ATP.

REFERÊNCIAS

ACS, A. C. S. (2018). "Cancer Statistics Center." American Cancer Society.

ACS, A. C. S. (2018). "Key Statistics About Neuroblastoma." American Cancer Society.

ACS, A. C. S. (2018). "What's New in Neuroblastoma Research?" American Cancer Society.

Anazetti, M. C. and P. S. Melo (2007). "Morte Celular por Apoptose: uma visão bioquímica e molecular." Metrocamp Pesquisa **1**(1): 37-58.

Basili, S. and S. Moro (2009). "Novel camptothecin derivatives as topoisomerase I inhibitors." Expert Opin Ther Pat **19**(5): 555-574.

Berry, B. J., A. J. Trewin, A. M. Amitrano, M. Kim and A. P. Wojtovich (2018). "Use the Protonmotive Force: Mitochondrial Uncoupling and Reactive Oxygen Species." J Mol Biol.

Bittencourt, L. F., K. A. Oliveira, C. B. Cardoso, F. G. Lopes, T. Dal-Cim, L. D. Chiaradia-Delatorre, A. Mascarello, S. W. Maluf, R. A. Yunes, R. C. Garcez, C. I. Tasca and C. B. Nedel (2016). "Novel synthetic chalcones induces apoptosis in human glioblastoma cells." Chem Biol Interact **252**: 74-81.

Busch, C., M. Burkard, C. Leischner, U. M. Lauer, J. Frank and S. Venturelli (2015). "Epigenetic activities of flavonoids in the prevention and treatment of cancer." Clinical Epigenetics **7**(1): 1-18.

Carreras-Sureda, A., P. Pihán and C. Hetz (2017). "The Unfolded Protein Response: At the Intersection between Endoplasmic Reticulum Function and Mitochondrial Bioenergetics." Frontiers in Oncology **7**(55).

Cartum, J. (2012). "Neuroblastoma: o enigmático tumor da infância." Pediatria Moderna **48**: 296-301.

Chaabane, W., S. D. User, M. El-Gazzah, R. Jaksik, E. Sajjadi, J. Rzeszowska-Wolny and M. J. Łos (2013). "Autophagy, Apoptosis, Mitoptosis and Necrosis: Interdependence Between Those Pathways and Effects on Cancer." Archivum Immunologiae et Therapiae Experimentalis **61**(1): 43-58.

Cheung, N. K. V. and M. A. Dyer (2013). "Neuroblastoma: Developmental Biology, Cancer Genomics, and Immunotherapy." Nat Rev Cancer **13**(6): 397-411.

Chiaradia, L. D., R. dos Santos, C. E. Vitor, A. A. Vieira, P. C. Leal, R. J. Nunes, J. B. Calixto and R. A. Yunes (2008). "Synthesis and pharmacological activity of chalcones derived from 2,4,6-trimethoxyacetophenone in RAW 264.7 cells stimulated by LPS: Quantitative structure–activity relationships." Bioorganic & Medicinal Chemistry **16**(2): 658-667.

Cui, Q., S. Wen and P. Huang (2017). "Targeting cancer cell mitochondria as a therapeutic approach: recent updates." Future Med Chem **9**(9): 929-949.

Curti, V., A. Di Lorenzo, M. Dacrema, J. Xiao, S. M. Nabavi and M. Daglia (2017). "In vitro polyphenol effects on apoptosis: An update of literature data." Semin Cancer Biol **46**: 119-131.

Dajas, F., A. C. Andres, A. Florencia, E. Carolina and R. M. Felicia (2013). "Neuroprotective actions of flavones and flavonols: mechanisms and relationship to flavonoid structural features." Cent Nerv Syst Agents Med Chem **13**(1): 30-35.

David, K. K., M. Sasaki, S. W. Yu, T. M. Dawson and V. L. Dawson (2006). "EndoG is dispensable in embryogenesis and apoptosis." Cell Death Differ **13**(7): 1147-1155.
Dawson, T. M. and V. L. Dawson (2017). "Mitochondrial Mechanisms of Neuronal Cell Death: Potential Therapeutics." Annual Review of Pharmacology and Toxicology **57**(1): 437-454.

Echeverria, C., J. F. Santibañez, O. Donoso-Tauda, C. A. Escobar and R. Ramirez-Tagle (2009). "Structural Antitumoral Activity Relationships of Synthetic Chalcones." International Journal of Molecular Sciences **10**(1): 221-231.

Eskelinen, E. L. (2011). "The dual role of autophagy in cancer." Curr Opin Pharmacol **11**(4): 294-300.

Estrada-Reyes, R., D. Ubaldo-Suárez and A. G. Araujo-Escalona (2012). "Los flavonoides y el Sistema Nervioso Central." Salud mental **35**: 375-384.

Gali-Muhtasib, H., R. Hmadi, M. Kareh, R. Tohme and N. Darwiche (2015). "Cell death mechanisms of plant-derived anticancer drugs: beyond apoptosis." Apoptosis **20**(12): 1531-1562.

Galluzzi, L., I. Vitale, S. A. Aaronson, J. M. Abrams, D. Adam, P. Agostinis, E. S. Alnemri, L. Altucci, I. Amelio, D. W. Andrews, M. Annicchiarico-Petruzzelli, A. V. Antonov, E. Arama, E. H. Baehrecke, N. A. Barlev, N. G. Bazan, F. Bernassola, M. J. M. Bertrand, K. Bianchi, M. V. Blagosklonny, K. Blomgren, C. Borner, P. Boya, C. Brenner, M. Campanella, E. Candi, D. Carmona-Gutierrez, F. Cecconi, F. K. Chan, N. S. Chandel, E. H. Cheng, J. E. Chipuk, J. A. Cidlowski, A. Ciechanover, G. M. Cohen, M. Conrad, J. R. Cubillos-Ruiz, P. E. Czabotar, V. D'Angiolella, T. M. Dawson, V. L. Dawson, V. De Laurenzi, R. De Maria, K. M. Debatin, R. J. DeBerardinis, M. Deshmukh, N. Di Daniele, F. Di Virgilio, V. M. Dixit, S. J. Dixon, C. S. Duckett, B. D. Dynlacht, W. S. El-Deiry, J. W. Elrod, G. M. Fimia, S. Fulda, A. J. Garcia-Saez, A. D. Garg, C. Garrido, E. Gavathiotis, P. Golstein, E. Gottlieb, D. R. Green, L. A. Greene, H. Gronemeyer, A. Gross, G. Hajnoczky, J. M. Hardwick, I. S. Harris, M. O. Hengartner, C. Hetz, H. Ichijo, M. Jaattela, B. Joseph, P. J. Jost, P. P. Juin, W. J. Kaiser, M. Karin, T. Kaufmann, O. Kepp, A. Kimchi, R. N. Kitsis, D. J. Klionsky, R. A. Knight, S. Kumar, S. W. Lee, J. J. Lemasters, B. Levine, A. Linkermann, S. A. Lipton, R. A. Lockshin, C. Lopez-Otin, S. W. Lowe, T. Luedde, E. Lugli, M. MacFarlane, F. Madeo, M. Malewicz, W. Malorni, G. Manic, J. C. Marine, S. J. Martin, J. C. Martinou, J. P. Medema, P. Mehlen, P. Meier, S. Melino, E. A. Miao, J. D. Molkentin, U. M. Moll, C. Munoz-Pinedo, S. Nagata, G. Nunez, A. Oberst, M. Oren, M. Overholtzer, M. Pagano, T. Panaretakis, M. Pasparakis, J. M. Penninger, D. M. Pereira, S. Pervaiz, M.

E. Peter, M. Piacentini, P. Pinton, J. H. M. Prehn, H. Puthalakath, G. A. Rabinovich, M. Rehm, R. Rizzuto, C. M. P. Rodrigues, D. C. Rubinsztein, T. Rudel, K. M. Ryan, E. Sayan, L. Scorrano, F. Shao, Y. Shi, J. Silke, H. U. Simon, A. Sistigu, B. R. Stockwell, A. Strasser, G. Szabadkai, S. W. G. Tait, D. Tang, N. Tavernarakis, A. Thorburn, Y. Tsujimoto, B. Turk, T. Vanden Berghe, P. Vandenabeele, M. G. Vander Heiden, A. Villunger, H. W. Virgin, K. H. Vousden, D. Vucic, E. F. Wagner, H. Walczak, D. Wallach, Y. Wang, J. A. Wells, W. Wood, J. Yuan, Z. Zakeri, B. Zhivotovsky, L. Zitvogel, G. Melino and G. Kroemer (2018). "Molecular mechanisms of cell death: recommendations of the Nomenclature Committee on Cell Death 2018." Cell Death Differ **25**(3): 486-541.

Gaur, R., K. S. Yadav, R. K. Verma, N. P. Yadav and R. S. Bhakuni (2014). "In vivo anti-diabetic activity of derivatives of isoliquiritigenin and liquiritigenin." Phytomedicine **21**(4): 415-422.

George, V. C., G. Dellaire and H. P. V. Rupasinghe (2017). "Plant flavonoids in cancer chemoprevention: role in genome stability." The Journal of Nutritional Biochemistry **45**: 1-14.

Grivicich, I., A. Regner and A. B. d. Rocha (2007). "Morte Celular por Apoptose." Revista Brasileira de Cancerologia **53**(3): 335-343.

Gul, H. I., M. Cizmecioglu, S. Zencir, M. Gul, P. Canturk, M. Atalay and Z. Topcu (2009). "Cytotoxic activity of 4'-hydroxychalcone derivatives against Jurkat cells and their effects on mammalian DNA topoisomerase I." J Enzyme Inhib Med Chem **24**(3): 804-807.

Gupta, D. and D. K. Jain (2015). "Chalcone derivatives as potential antifungal agents: Synthesis, and antifungal activity." J Adv Pharm Technol Res **6**(3): 114-117.

Han, S. Y., Y. W. Chin and Y. H. Choi (2013). "A new approach for pharmacokinetic studies of natural products: measurement of isoliquiritigenin levels in mice plasma, urine and feces using modified automated dosing/blood sampling system." Biomed Chromatogr **27**(6): 741-749.

He, W., Q. Wang, B. Srinivasan, J. Xu, M. T. Padilla, Z. Li, X. Wang, Y. Liu, X. Gou, H. M. Shen, C. Xing and Y. Lin (2014). "A JNK-mediated autophagy pathway that triggers c-IAP degradation and necroptosis for anticancer chemotherapy." Oncogene **33**(23): 3004-3013.

Hsu, Y. L., C. C. Chia, P. J. Chen, S. E. Huang, S. C. Huang and P. L. Kuo (2009). "Shallot and licorice constituent isoliquiritigenin arrests cell cycle progression and induces apoptosis through the induction of ATM/p53 and initiation of the mitochondrial system in human cervical carcinoma HeLa cells." Mol Nutr Food Res **53**(7): 826-835.

INCA (2018). "Câncer Infantil." Instituto Nacional de Câncer.

Izbicki, T., J. Mazur and E. Izbicka (2003). "Epidemiology and etiology of neuroblastoma: an overview." Anticancer Res **23**(1b): 755-760.

Janočková, J., J. Plšíková, J. Kašpárková, V. Brabec, R. Jendželovský, J. Mikeš, J. Kovaľ, S. Hamuľaková, P. Fedoročko, K. Kuča and M. Kožurková (2015). "Inhibition of DNA

topoisomerases I and II and growth inhibition of HL-60 cells by novel acridine-based compounds." European Journal of Pharmaceutical Sciences **76**: 192-202.

Ketabforoosh, S. H., A. Kheirollahi, M. Safavi, N. Esmati, S. K. Ardestani, S. Emami, L. Firoozpour, A. Shafiee and A. Foroumadi (2014). "Synthesis and anti-cancer activity evaluation of new dimethoxylated chalcone and flavanone analogs." Arch Pharm (Weinheim) **347**(11): 853-860.

Kim, S. Y., I.-S. Lee and A. Moon (2013). "2-Hydroxychalcone and xanthohumol inhibit invasion of triple negative breast cancer cells." Chemico-Biological Interactions **203**(3): 565-572.

Krysko, O., T. L. Aaes, V. E. Kagan, K. D'Herde, C. Bachert, L. Leybaert, P. Vandenabeele and D. V. Krysko (2017). "Necroptotic cell death in anti-cancer therapy." Immunological Reviews **280**(1): 207-219.

Lee, S. Y., M. K. Ju, H. M. Jeon, E. K. Jeong, Y. J. Lee, C. H. Kim, H. G. Park, S. I. Han and H. S. Kang (2018). "Regulation of Tumor Progression by Programmed Necrosis." Oxid Med Cell Longev **2018**: 3537471.

Lee, Y. K. and J. A. Lee (2016). "Role of the mammalian ATG8/LC3 family in autophagy: differential and compensatory roles in the spatiotemporal regulation of autophagy." BMB Rep **49**(8): 424-430.

Lee, Y. M., D. Y. Lim, H. J. Choi, J. I. Jung, W. Y. Chung and J. H. Park (2009). "Induction of cell cycle arrest in prostate cancer cells by the dietary compound isoliquiritigenin." J Med Food **12**(1): 8-14.

Leon-Gonzalez, A. J., N. Acero, D. Munoz-Mingarro, I. Navarro and C. Martin-Cordero (2015). "Chalcones as Promising Lead Compounds on Cancer Therapy." Curr Med Chem **22**(30): 3407-3425.

Logue, S. E. and S. J. Martin (2008). "Caspase activation cascades in apoptosis." Biochem Soc Trans **36**(Pt 1): 1-9.

Lopez, J. and S. W. Tait (2015). "Mitochondrial apoptosis: killing cancer using the enemy within." Br J Cancer **112**(6): 957-962.

Louis, C. U. and J. M. Shohet (2015). "Neuroblastoma: molecular pathogenesis and therapy." Annu Rev Med **66**: 49-63.

Maciel-Herrerías, M. and S. Cabrera-Benítez (2016). "El papel de la autofagia en enfermedades pulmonares." Neumología y cirugía de tórax **75**: 227-236.

Martineau, L. C. (2012). "Large enhancement of skeletal muscle cell glucose uptake and suppression of hepatocyte glucose-6-phosphatase activity by weak uncouplers of oxidative phosphorylation." Biochim Biophys Acta **1820**(2): 133-150.

Mishra, A. P., B. Salehi, M. Sharifi-Rad, R. Pezzani, F. Kobarfard, J. Sharifi-Rad and M. Nigam (2018). "Programmed Cell Death, from a Cancer Perspective: An Overview." Mol Diagn Ther.

Mizushima, N., T. Yoshimori and B. Levine (2010). "Methods in Mammalian Autophagy Research." Cell **140**(3): 313-326.

Moon, D. O., M. O. Kim, Y. H. Choi, J. W. Hyun, W. Y. Chang and G. Y. Kim (2010). "Butein induces G(2)/M phase arrest and apoptosis in human hepatoma cancer cells through ROS generation." Cancer Lett **288**(2): 204-213.

Morris, E. J. and H. M. Geller (1996). "Induction of neuronal apoptosis by camptothecin, an inhibitor of DNA topoisomerase-I: evidence for cell cycle-independent toxicity." J Cell Biol **134**(3): 757-770.

Motani, K., K. Tabata, Y. Kimura, S. Okano, Y. Shibata, Y. Abiko, H. Nagai, T. Akihisa and T. Suzuki (2008). "Proteomic analysis of apoptosis induced by xanthoangelol, a major constituent of Angelica keiskei, in neuroblastoma." Biol Pharm Bull **31**(4): 618-626.
Nagata, S. (2018). "Apoptosis and Clearance of Apoptotic Cells." Annual Review of Immunology **36**(1): 489-517.

Nikoletopoulou, V., M. Markaki, K. Palikaras and N. Tavernarakis (2013). "Crosstalk between apoptosis, necrosis and autophagy." Biochim Biophys Acta **1833**(12): 3448-3459.

Nishimura, R., K. Tabata, M. Arakawa, Y. Ito, Y. Kimura, T. Akihisa, H. Nagai, A. Sakuma, H. Kohno and T. Suzuki (2007). "Isobavachalcone, a chalcone constituent of Angelica keiskei, induces apoptosis in neuroblastoma." Biol Pharm Bull **30**(10): 1878-1883.

Orlikova, B., D. Tasdemir, F. Golais, M. Dicato and M. Diederich (2011). "The aromatic ketone 4′-hydroxychalcone inhibits TNFα-induced NF-κB activation via proteasome inhibition." Biochemical Pharmacology **82**(6): 620-631.

Ozpolat, B. and D. M. Benbrook (2015). "Targeting autophagy in cancer management – strategies and developments." Cancer Manag Res **7**: 291-299.

Park, J. R., A. Eggert and H. Caron (2010). "Neuroblastoma: Biology, Prognosis, and Treatment." Hematology/Oncology Clinics of North America **24**(1): 65-86.

Peng, F., Q. H. Du, C. Peng, N. Wang, H. L. Tang, X. M. Xie, J. G. Shen and J. P. Chen (2015). "A Review: The Pharmacology of Isoliquiritigenin." Phytotherapy Research **29**(7): 969-977.

Porporato, P. E., N. Filigheddu, J. M. B. Pedro, G. Kroemer and L. Galluzzi (2018). "Mitochondrial metabolism and cancer." Cell Res **28**(3): 265-280.

Prieto-Dominguez, N., M. V. Garcia-Mediavilla, S. Sanchez-Campos, J. L. Mauriz and J. Gonzalez-Gallego (2018). "Autophagy as a Molecular Target of Flavonoids Underlying their Protective Effects in Human Disease." Curr Med Chem **25**(7): 814-838.

Qiao, H., X. Zhang, T. Wang, L. Liang, W. Chang and H. Xia (2014). "Pharmacokinetics, biodistribution and bioavailability of isoliquiritigenin after intravenous and oral administration." Pharm Biol **52**(2): 228-236.

Ramirez-Tagle, R., C. A. Escobar, V. Romero, I. Montorfano, R. Armisén, V. Borgna, E. Jeldes, L. Pizarro, F. Simon and C. Echeverria (2016). "Chalcone-Induced Apoptosis through Caspase-Dependent Intrinsic Pathways in Human Hepatocellular Carcinoma Cells." Int J Mol Sci **17**(2).

Redmann, M., G. A. Benavides, T. F. Berryhill, W. Y. Wani, X. Ouyang, M. S. Johnson, S. Ravi, S. Barnes, V. M. Darley-Usmar and J. Zhang (2017). "Inhibition of autophagy with bafilomycin and chloroquine decreases mitochondrial quality and bioenergetic function in primary neurons." Redox Biol **11**: 73-81.

Roskoski, R., Jr. (2012). "ERK1/2 MAP kinases: structure, function, and regulation." Pharmacol Res **66**(2): 105-143.

Sabzevari, O., G. Galati, M. Y. Moridani, A. Siraki and P. J. O'Brien (2004). "Molecular cytotoxic mechanisms of anticancer hydroxychalcones." Chemico-Biological Interactions **148**(1): 57-67.

Sabzevari, O., G. Galati, M. Y. Moridani, A. Siraki and P. J. O'Brien (2004). "Molecular cytotoxic mechanisms of anticancer hydroxychalcones." Chemico-Biological Interactions **148**(1–2): 57-67.

Sano, R. and J. C. Reed (2013). "ER stress-induced cell death mechanisms." Biochimica et Biophysica Acta (BBA) - Molecular Cell Research **1833**(12): 3460-3470.

Saydam, G., H. H. Aydin, F. Sahin, O. Kucukoglu, E. Erciyas, E. Terzioglu, F. Buyukkececi and S. B. Omay (2003). "Cytotoxic and inhibitory effects of 4,4'-dihydroxy chalcone (RVC-588) on proliferation of human leukemic HL-60 cells." Leuk Res **27**(1): 57-64.

Schwarz, D. S. and M. D. Blower (2016). "The endoplasmic reticulum: structure, function and response to cellular signaling." Cell Mol Life Sci **73**: 79-94.

Sharma, R., R. Kumar, R. Kodwani, S. Kapoor, A. Khare, R. Bansal, S. Khurana, S. Singh, J. Thomas, B. Roy, R. Phartyal, S. Saluja and S. Kumar (2015). "A Review on Mechanisms of Anti Tumor Activity of Chalcones." Anticancer Agents Med Chem **16**(2): 200-211.

Shin, S. Y., J. H. Kim, H. Yoon, Y. K. Choi, D. Koh, Y. Lim and Y. H. Lee (2013). "Novel antimitotic activity of 2-hydroxy-4-methoxy-2',3'-benzochalcone (HymnPro) through the inhibition of tubulin polymerization." J Agric Food Chem **61**(51): 12588-12597.

Sikander, M., S. Malik, D. Yadav, S. Biswas, D. P. Katare and S. K. Jain (2011). "Cytoprotective activity of a trans-chalcone against hydrogen peroxide induced toxicity in hepatocellular carcinoma (HepG2) cells." Asian Pac J Cancer Prev **12**(10): 2513-2516.

Silke, J., J. A. Rickard and M. Gerlic (2015). "The diverse role of RIP kinases in necroptosis and inflammation." Nat Immunol **16**(7): 689-697.

Singh, S. S., S. Vats, A. Y. Chia, T. Z. Tan, S. Deng, M. S. Ong, F. Arfuso, C. T. Yap, B. C. Goh, G. Sethi, R. Y. Huang, H. M. Shen, R. Manjithaya and A. P. Kumar (2018). "Dual role of autophagy in hallmarks of cancer." Oncogene **37**(9): 1142-1158.

Stevens, J. F., J. S. Revel and C. S. Maier (2017). "Mitochondria-Centric Review of Polyphenol Bioactivity in Cancer Models." Antioxid Redox Signal.

Sun, C., H. Zhang, X. F. Ma, X. Zhou, L. Gan, Y. Y. Liu and Z. H. Wang (2013). "Isoliquiritigenin Enhances Radiosensitivity of HepG2 Cells via Disturbance of Redox Status." Cell Biochemistry and Biophysics **65**(3): 433-444.

Susin, S. A., E. Daugas, L. Ravagnan, K. Samejima, N. Zamzami, M. Loeffler, P. Costantini, K. F. Ferri, T. Irinopoulou, M. C. Prevost, G. Brothers, T. W. Mak, J. Penninger, W. C. Earnshaw and G. Kroemer (2000). "Two distinct pathways leading to nuclear apoptosis." J Exp Med **192**(4): 571-580.

Szegezdi, E., S. E. Logue, A. M. Gorman and A. Samali (2006). "Mediators of endoplasmic reticulum stress-induced apoptosis." EMBO Rep **7**(9): 880-885.

Tabas, I. and D. Ron (2011). "Integrating the mechanisms of apoptosis induced by endoplasmic reticulum stress." Nature Cell Biology **13**: 184.

Thornton, T. M. and M. Rincon (2009). "Non-Classical P38 Map Kinase Functions: Cell Cycle Checkpoints and Survival." Int J Biol Sci **5**(1): 44-52.

Tibullo, D., C. Giallongo, F. Puglisi, D. Tomassoni, G. Camiolo, M. Cristaldi, M. V. Brundo, C. D. Anfuso, G. Lupo, T. Stampone, G. Li Volti, F. Amenta, R. Avola and V. Bramanti (2017). "Effect of Lipoic Acid on the Biochemical Mechanisms of Resistance to Bortezomib in SH-SY5Y Neuroblastoma Cells." Molecular Neurobiology: 1-7.

van Vliet, A. R. and P. Agostinis (2018). "Mitochondria-Associated Membranes and ER Stress." Curr Top Microbiol Immunol **414**: 73-102.

Venu Venkatarame Gowda Saralamma, E. H. K. H. J. L. S. R. W. S. L. J. D. H. S. J. L. C.-K. W. G.-S. K. (2017). "Flavonoids: A new generation molecule to stimulate programmed cell deaths in cancer cells." Journal of Biomedical and Translational Research **18**(1): 30-37.

Wallace, K. B. and A. A. Starkov (2000). "Mitochondrial targets of drug toxicity." Annu Rev Pharmacol Toxicol **40**: 353-388.

Wang, C. and R. J. Youle (2009). "The Role of Mitochondria in Apoptosis()." Annu Rev Genet **43**: 95-118.

Wen, S., D. Zhu and P. Huang (2013). "Targeting cancer cell mitochondria as a therapeutic approach." Future Med Chem **5**(1): 53-67.

Wu, C. H., H. Y. Chen, C. W. Wang, T. M. Shieh, T. C. Huang, L. C. Lin, K. L. Wang and S. M. Hsia (2016). "Isoliquiritigenin induces apoptosis and autophagy and inhibits endometrial cancer growth in mice." Oncotarget **7**(45): 73432-73447.

Yang, H. H., C. Zhang, S. H. Lai, C. C. Zeng, Y. J. Liu and X. Z. Wang (2017). "Isoliquiritigenin Induces Cytotoxicity in PC-12 Cells In Vitro." Appl Biochem Biotechnol **183**(4): 1173-1190.

Yang, P. Y., D. N. Hu, I. C. Lin and F. S. Liu (2015). "Butein Shows Cytotoxic Effects and Induces Apoptosis in Human Ovarian Cancer Cells." Am J Chin Med **43**(4): 769-782.
Yang, S., X. Zhao, H. Xu, F. Chen, Y. Xu, Z. Li, D. Sanchis, L. Jin, Y. Zhang and J. Ye (2017). "AKT2 Blocks Nucleus Translocation of Apoptosis-Inducing Factor (AIF) and Endonuclease G (EndoG) While Promoting Caspase Activation during Cardiac Ischemia." Int J Mol Sci **18**(3).

Yoshii, S. R. and N. Mizushima (2017). "Monitoring and Measuring Autophagy." Int J Mol Sci **18**(9).

Zhang, B., W. Chu, P. Wei, Y. Liu and T. Wei (2015). "Xanthohumol induces generation of reactive oxygen species and triggers apoptosis through inhibition of mitochondrial electron transfer chain complex I." Free Radical Biology and Medicine **89**: 486-497.

Zhang, X., E. D. Yeung, J. Wang, E. E. Panzhinskiy, C. Tong, W. Li and J. Li (2010). "Isoliquiritigenin, a natural anti-oxidant, selectively inhibits the proliferation of prostate cancer cells." Clin Exp Pharmacol Physiol **37**(8): 841-847.

Zhang, X., P. Zhu, X. Zhang, Y. Ma, W. Li, J. M. Chen, H. M. Guo, R. Bucala, J. Zhuang and J. Li (2013). "Natural antioxidant-isoliquiritigenin ameliorates contractile dysfunction of hypoxic cardiomyocytes via AMPK signaling pathway." Mediators Inflamm **2013**: 390890.
Zhao, S., H. Chang, P. Ma, G. Gao, C. Jin, X. Zhao, W. Zhou and B. Jin (2015). "Inhibitory effect of DNA topoisomerase inhibitor isoliquiritigenin on the growth of glioma cells." Int J Clin Exp Pathol **8**(10): 12577-12582.

Zhou, G. S., L. J. Song and B. Yang (2013). "Isoliquiritigenin inhibits proliferation and induces apoptosis of U87 human glioma cells in vitro." Mol Med Rep **7**(2): 531-536.